PENETRATIVE CONVECTION IN SEDIMENTS

RECOMMENDED:

W. O. Harrison

D B Hawkins

J J Goerick

N. J. Gilbaum

Chairman, Advisory Committee

John J Goerick

Program Head, Marine Science Program

Director, Institute of Marine Science

APPROVED:

Vice Chancellor for Research and Advanced Study

3 May 1983

Date

PENETRATIVE CONVECTION IN SEDIMENTS

A

THESIS

[redacted] Science

Presented to the Faculty of the University of Alaska

in Partial Fulfillment of the Requirements

for the Degree of

DOCTOR OF PHILOSOPHY

By

David L. Musgrave, M.S.

Fairbanks, Alaska

May, 1983

ABSTRACT

Modelers of early diagenesis in sediments have, in general, ignored the possibility and consequences of penetrative convection due to increases in the density of bottom water. Some common assumptions made by modelers, e.g. steady-state diagenesis and lateral homogeneity, do not hold when penetrative convection occurs, and conclusions about chemical fluxes and diagenetic reactions may be wrong. This thesis describes observations of penetrative convection in the sediments of a fresh-water lake undergoing fall cooling. To that end, three probes with thermistors spaced at 1.0 to 7.5 cm measured temperature in the sediments every 5 minutes. In anticipation of fall cooling, the probes were in place for the last two weeks of October, 1979, in Lake 227 of the Experimental Lakes Area, northwestern Ontario. I attempted to estimate the average or "global" velocity of pore waters by matching the observed time series of temperature to time series generated by a heat transport model that included advective transport of heat. The nonlinear regression did not give any global velocities greater than 5×10^{-6} m s^{-1}, which was not significantly different from zero. However, periodic fluctuations of temperature in the upper 8 centimeters at the shallow probe site (0.75 m water depth) indicated that high frequency velocity fluctuations had amplitudes as large as 7×10^{-5} m s^{-1}.

Calculations of the time-dependent Rayleigh number indicated

that the pore waters were marginally unstable with respect to convection.

A short discussion of the theory of penetrative convection in sediments indicates when and where this process might be important in the oceans. Temperature changes of 10 deg or salinity changes of 1.0 g/kg could cause penetrative convection in sediments that are very permeable (e.g., coarse sands).

TABLE OF CONTENTS

TABLE OF CONTENTS (CONTINUED)

LIST OF TABLES

ACKNOWLEDGMENTS

It is fitting that a doctoral dissertation, which represents a major portion of one's career and life, should provide an opportunity to acknowledge and thank those people who have had great and positive impact upon my career and life.

Bill Reeburgh provided support through my tenure as a Ph.D. candidate. This support came in all forms: scientific, academic, financial, emotional and spiritual (if not in the religious sense, then certainly in the alcoholic sense). He and his wife, Carelyn, made me a part of their family and shared their home and lives with me. In these few words, I cannot express the respect and affection that I have for both of them.

Tom Royer fed my increasing interest in physical oceanography through long discussions about his research, specifically, and about physical oceanography, in general. Beyond that his friendship was most appreciated throughout my tenure as a graduate student. Through his friendship and research he has provided an excellent role model for me.

Will Harrison spent many hours in discussions concerning data interpretation and the theory of convection. I appreciate the time and energy that he spent on my behalf. Dan Swift furthered my interest and understanding of the physics of fluids and numerical modeling.

I spent many hours (days, years?) with Tom Weingartner, Karl Haflinger and Grant Matheke in maundering discussions about life, science, research and computer-mind links. I developed greater appreciation for chemical oceanography through discussions with Marc Alperin and Dave Glover.

Dave Schindler and Ray Hesslein were extremely helpful at the ELA. Gil Mimken was my mentor in all things electronic.

Thanks to my wife, Nancy Murphy, for her support and love during the past 4 years.

This research was supported by the National Science Foundation under Grants OCE 78-20896 and OCE 80-26046. I also gratefully acknowledge support for a fellowship from the Jesse Smith Noyes Foundation.

I. INTRODUCTION

Chemical oceanography is the study of the ocean as a chemical system. Broecker and Peng (1982) liken chemical oceanographers to "inverse" chemical engineers: we try to reconstruct the operational blueprint of the chemical plant (i.e. the ocean) by quantifying inputs, outputs and internal concentrations of chemical substances. The major sources (inputs) of most dissolved substances are river water and to a lesser extent the atmosphere. The sediments are the largest sink (output) for most sea salt constituents but they are a source for other constituents such as nutrients. Therefore, the study of the fluxes of dissolved and particulate forms of chemical substances at the sediment surface is one of the central themes of chemical oceanography. The diagenesis of particulate matter that falls to the sediments determines the fluxes. Sediment geochemists measure profiles of dissolved and particulate substances in sediments in order to make conclusions about fluxes and diagenetic reactions. The conclusions are based on the profiles and some assumed model of how the sediment works as a chemical system.

Most modelers of concentration profiles in sediments assume that the pore waters are quiescent and that molecular diffusion is the only significant transport mechanism for dissolved components. This may be a result of the lack of time-series data of measured profiles. However, studies have shown that transport by steady advection of pore waters can be greater than diffusive transport. Therefore, the possibility of nonsteady advection which leads to significant

transport is not so remote. Indeed, studies of time-dependent concentration profiles suggest that penetrative convection occurs in the upper sediments due to temporary increases in the density of bottom water. The dynamic theory of penetrative convection has not been applied to the possibility of penetrative convection in sediments or to the increased transport of solutes when penetrative convection occurs. In an attempt to illustrate the process of penetrative convection, I measured time-dependent profiles of temperatures in fresh-water sediments. I found that nonsteady advective transport was sometimes significant when the density gradient was unstable. I relate the observations to a previously developed theory of penetrative convection in porous media.

The following section titled "Background" describes the models used to interpret fluxes at the sediment surface and early diagenesis within the sediments. I discuss the assumptions that are made in using these models. If the assumptions do no apply, improper conclusions about fluxes and diagenetic reactions are made. I then discuss studies of steady convection in sediments. Two chemical studies provide observations which suggest that penetrative convection can occur in sediments. When steady or penetrative convection occurs, several common assumptions made in modeling do not apply. These assumptions lead to qualitatively inaccurate conclusions. I conclude this introduction with a discussion of my approach to studying penetrative convection in a fresh-water lake.

Background

Interstitial Solute Fluxes

Diffusion and advection are the two processes that contribute to the flux of any sediment property. The expression for the flux, J, of a dissolved component, C, across a horizontal plane in the sediment is:

$$J = -(D_B + D_{wc}) \frac{\partial(\phi C)}{\partial z} + \phi(D_I + D_S) \frac{\partial C}{\partial z} + \phi w C \qquad 1$$

where J is the vertical flux; C is the mass of dissolved component per unit volume of pore water; D_B, D_{wc}, D_S and D_I are the biodiffusion, wave and current mixing, molecular diffusion and bioirrigation coefficients, respectively; ϕ is the porosity; w is the vertical water flow velocity relative to sediment solid particles; and z is the vertical distance measured from the sediment-water interface. (I have used the notation from Berner [1980], which should be consulted for a comprehensive discussion of the equations for flux and diagenesis.) When the terms are evaluated at the sediment-water interface, this equation gives the interfacial flux, which can contribute significantly to the budgets of dissolved chemical components in the overlying water (e.g., Sayles, 1979). The "D" terms represent fluxes due to mixing or molecular diffusion. D_S is the molecular diffusion coefficient of the dissolved component in water corrected for tortuosity and ionic effects. The other mixing terms are significant only in the upper sediments (tens of centimeters) in shallow waters where macrofauna abound and strong bottom currents exist. The biodif-

fusion, wave and current mixing, and bioirrigation terms parameterize, respectively: pore water mixing caused by macrofaunal reworking of sediments, sediment stirring due to shear stresses exerted by high bottom-water velocities, and macrofaunal flushing through burrows open to the overlying seawater. These mixing processes are formulated similarly to molecular diffusion for mathematical expediency and because they realistically model observed concentration profiles.

The last term in equation 1 is the advective term. The relative magnitude of the advective term compared to the diffusion term is estimated by the dimensionless Peclet number LW/D_s, where L is the scale length for the process under consideration and W is the velocity of the pore water. When the Peclet number is $<<1$ diffusion dominates the flux and when the Peclet number is $>>1$ advection dominates. (Note that Berner [1980] defines the Peclet number as D_s/LW which is the inverse of the above expression. The definition that I have used is that used in fluid mechanics.) For values close to 1, both processes are significant. Most workers in sediment geochemistry have assumed that the main contribution to the velocity is the relative motion of the pore water when the sediment-water interface is taken as the origin (instead of a fixed layer that is buried as more material accumulates at the sediment-water interface). This component of the velocity is proportional to the rate of sedimentation. In most cases the Peclet number is small, which indicates that the

advective term may be unimportant. One notable exception is the advective transport of Na^+, due to burial, which is 25-30% of the diffusive flux from deep-sea sediments and opposes the diffusive flux (Sayles, 1979).

The Diagenetic Equation

The diagenetic equation for dissolved substances (2) equates the

$$\frac{\partial(\phi C)}{\partial t} = - \frac{\partial J}{\partial z} + \phi \Sigma R \qquad 2$$

time rate of change of solute concentration to reaction terms involving the solute and to the gradient of the vertical flux (ΣR is the sum of all diagenetic reactions involving C). This equation is really a conservation equation for the solute. It describes mathematically the concentration of a solute in time and space, and oro-vides a rigorous formulation of early diagenesis for analyzing and understanding the solute distributions in the sediments. The form of this equation implies that the solute concentration is not a function of the horizontal dimensions. This is usually a good assumption because lateral gradients are neglible over horizontal scales equivalent to the depth of interest. This assumption may be invalid if convection is occurring.

When obtaining values for parameters (e.g., diffusion coefficient, vertical velocity, rate constants for reaction) from measured profiles, the assumed form of the diagenetic equation is very important because reasonable profiles are obtained from disparate models.

Lerman (1975) models the distributions of Mg^{+2} and Ca^{+2} in pore waters from the deep sea assuming depth-independent molecular diffusivities. From measured concentrations he obtains rate constants for mineral reactions involving Ca^{+2} and Mg^{+2}. In contrast, McDuff and Gieskes (1976) model the same measured distributions assuming variable diffusivities and show that reaction terms are not necessary. Sayles and Jenkins (1982) attribute curvature of Ca^{+2} profiles to advection of pore waters in the eastern equatorial Pacific. The exponential distributions of $^4He/^3He$ in pore waters provide the evidence for the advection of pore waters. However, linear distributions describe the helium data if the errors in the measured isotopic ratio of helium are considered. In this case the curvature in the Ca^{+2} profiles would be entirely due to reaction. (Sayles and Jenkins confirm the absence of reaction using mass balance constraints.) Lerman (1975) shows that the zero-order dissolution term and the first-order rate constant for Ca^{+2} and Mg^{+2} in deep-sea sediments obtained from observed profiles are significantly different when his model includes advection due to burial of pore water.

The most ubiquitous assumption in modeling the chemistry of pore waters is steady-state diagenesis. Curvature in solute profiles due to time-dependent concentrations in the overlying water (Matisoff, 1980) can be misinterpreted as due to reaction if the distribution is only sampled once and one assumes steady-state diagenesis.

I have documented the importance of the assumed form of the

diagenetic equation and have presented two common assumptions that affect the form: negligible advection of pore waters and steady state. Implicit in the form of equation (2) is a third assumption of negligible lateral gradients. I now address evidence for the nonapplicability of these assumptions. In the next subsection I cite several examples of steady-state processes that do not permit the last two assumptions.

Steady Convection

The discrepancy between the use of the word convection by oceanographers and fluid dynamicists requires definition of several terms to avoid ambiguity. I will use convection to mean motion caused by arbitrary forces; free convection, motion caused by buoyancy forces; and forced convection, motion caused by gradients in pressure and elevation head. Penetrative convection describes the time-dependent penetration of a freely convecting layer into a stable, quiescent layer.

In most sediments, advection due to burial is not significant compared to diffusion, but advection due to steady free or forced convection can lead to a large Peclet number (>1). Riedl *et al* (1972) measured velocities of pore waters in subtidal sediments (water depths 0.15-1.0 m) and show that a fluctuating component had the same frequency as the surface waves. (I discuss wave-induced motion in this section on steady convection because a steady state is obtained after averaging the diagenetic equation over one wave

period.) The observed attentuation of the vertical component with sediment depth confirms theory of the wave influence on water exchange in sediments (Putnam, 1949). Riedl *et al* (1972) use a theory similar to Putnam's to calculate the amount of water filtered through the sediments due to wave action. They estimate that the amount of water filtered, which is mostly confined to the shallow shelves, is one-third the seawater evaporated from the world's oceans. Harrison *et al* (1983) present a formulation for the diagenetic equation which includes reaction terms and mechanical dispersion effects due to wave-induced velocities of pore waters. Under certain circumstances the effect of wave-induced motion enters the diagenetic equation as an effective diffusivity which is a function of sediment properties, wave state and water depth. This effective diffusivity is similar to D_{wc} in equation (1), but it is a tensor quantity. They estimate that the increase in unidirectional transport on the eastern shelf of the United States is greater than one. Vanderborght *et al* (1977) present evidence for wave-induced motion from profiles of dissolved silica, nitrate, ammonium and sulfate in muddy, shallow (20 m) sediments, but the possibility of stirring of the whole sediment weakens their argument.

Forced convection due to submarine ground-water discharge occurs in coastal areas where fresh-water aquifers intersect the sea through permeable sediments and the head is above sea level (Johannes, 1980). Homogeneous unconfined aquifers discharge in a narrow near-shore zone; Bokuniewicz (1980) reports that 40% to 98% of the discharge

occurs within 100 m of shore in the Great South Bay, New York. However, confined (artesian) aquifers can connect with the sea-floor at any distance from the shore; Manheim and Sayles (1974) report brackish aquifers 120 km offshore.

Steady, free convection occurs near spreading centers in the deep sea and above subsea permafrost on the Arctic coast due to deep sources of heat and fresh water, respectively. Profiles of $^4He/^3He$ and of Ca^{+2} yield velocities of $6.4X10^{-9}$ m s^{-1} (.20 m yr-1) in the equatorial East Pacific (Sayles and Jenkins, 1982). Harrison and Osterkamp (1978) show that free convection must be occuring between the sediment-water interface and the top of the subsea permafrost (40 m) because diffusion of salt from the overlying bottom waters to the permafrost is too slow to account for the permafrost thawing rate. The free convection is driven by buoyancy created by melting of the permafrost which releases fresh water into the saltier, heavier pore water.

Clearly, advective transport of solutes can be significant in some sediments. Steady, linear, free convection imparts horizontal heterogeneity on length scales of the order of the depth of unconsolidated sediment. Lateral gradients in vertical velocities near areas of ground-water discharge also impart horizontal heterogeneity in concentration profiles. The form of the diagenetic equation must reflect the added dimensionality when modeling solute distributions over the whole sediment depth. When considering concentration pro-

files in the upper sediments, one can usually assume local absence of horizontal gradients if the depth of interest is much less than the width of a convection cell. Sayles and Jenkins (1982) make this assumption implicitly. They report profiles to 1 m whereas the width of convective cells are probably the same order of magnitude as the depth of the cells. These cells should extend to the basalt basement at 600 m (Poldervaart, 1955).

Solution of the equations for the dynamics of steady convection yields the time-independent velocity field. Once the velocity field is known, one solves the diagenetic equation to obtain the solute distribution, from which fluxes are computed. However, the velocities are time-dependent in a convecting layer that penetrates a stable layer and no studies have addressed this time-dependent velocity field and its effect on the diagenetic equation. The examples in the next section show that penetrative convection may occur and indicate the space and time scales of the process.

Chemical Evidence for Penetrative Convection

Two studies of concentration profiles suggest that penetrative convection due to increases in bottom-water density cause temporal changes in solute profiles. Thorstenson and Mackenzie (1974) report summer and winter profiles of pore-water ammonium, sulfide, pH and titration alkalinity from Devil's Hole, Harrington Sound, Bermuda. They cannot explain the striking homogeneity in the upper 60 cm of the winter profiles with the processes of diffusion, reaction, bio-

turbation or variations in ground-water discharge. Citing a study by Clark (1973), they suggest that convection and wind mixing in the fall caused the summer thermocline in the water column to deepen and then intersect the bottom. This induced the subsequent motion of pore waters in the sediments.

Hesslein (1980) presents similar evidence of increased transport of solutes in the upper sediments due to buoyancy-induced motion of pore water. His observations are so definitive of the process that I designed an experimental system to return to the same sediments to address the dynamics of the process and increase the temporal resolution of observations. He reports profiles of tritiated water in the sediments of Lake 227, Experimental Lakes Area (ELA), Ontario, Canada, during the summer and fall, 1975, at water depths above, in and below (water depths 0.75, 3.85 and 8.75 m, respectively) the summer thermocline (3-4 m). Tritiated water that had been injected into the water column of Lake 227 moved into the sediments during the summer. He estimates the diffusion coefficient by matching calculated with measured tritium profiles. He obtains the calculated profiles by integrating the diagenetic equation (2). He faithfully reproduces the September tritium profiles above the thermocline using a diffusivity of $1\text{-}2\times10^{-9}$ m^2s^{-1} (compare to the self-diffusion coefficient of water, 2.1×10^{-9} m^2s^{-1}). In October, the tritium activity was near-constant in the upper 10 cm of the measured profiles from above and in the summer thermocline. The October profile from below the thermocline did not show this behavior (he does not report pre-

October profiles below the thermocline). A reasonable fit to the measured activity in the profile at 0.75 m is not obtained using a constant diffusivity equal to the summer value. He presents a two-layer model with a different diffusivity in the upper 10 cm than the summer diffusivity in the rest of the sediment. The time interval for increased tritium transport is not known, because his last sampling of the tritium profile before October was one month prior. As limiting cases, he assumes the increase occurred 3 and 27 days before sampling and obtains profiles that matched the data using diffusivities of 50×10^{-9} $m^2 s^{-1}$ and 5×10^{-9} $m^2 s^{-1}$, respectively. Furthermore, measured activities of ^{137}Cs on the solid phase shows that reworking of whole sediment by organisms or by mechanical mixing has not occurred since deposition. Hesslein's conclusion is that sediments above and in the thermocline were exposed to increased temperatures in the summer and warmed to the extent that fall cooling decreased the temperature at the sediment-water interface. The decreased temperature caused penetrative convection to initiate and this increased the transport of tritium in the upper sediments.

Approach

Although these two studies give convincing arguments for the occurence of penetrative convection, they lack enough temporal resolution to examine qualitatively the penetration of the unstable layer into the quiescent layer below. Furthermore, the studies did not address the dynamics of the increased transport, theoretically or

observationally, and one cannot use their observations to estimate quantitatively the increased transport in other sediment systems that experience temporary increases in bottom-water density. I planned to monitor the penetration of a convecting layer into the sediments on time scales that would provide a better qualitative description of the process and to measure the density gradient of the pore waters so that the observations could be reconciled with the dynamics. Therefore, I used *in situ* probes to measure temperature every few centimeters into fresh-water sediments and sampled the temperature over intervals less than one hour. The temporal change in temperature is due only to transport processes since there are no appreciable heat sinks or sources in the sediments, and temperature is a measure of density in fresh water. I returned to Lake 227 for field studies because Hesslein's study defined the time of year (October) and the depth range (about 10 cm) of the process. I assumed that a sampling interval of less than an hour would suffice to evidence the process. Chemical or radiotracers are more sensitive than heat to motion of pore waters because diffusive transport of solutes is so much less than diffusive transport of heat. However, I used heat as a tracer because the data obtained was easily processed by computer whereas chemical or radiotracers would involve processing by extraction of pore waters followed by chemical analysis, a prohibitively lengthy and laborius procedure when the sampling rate is high. Furthermore, using an *in situ* probe obviated the problem of disturbing the sedi-

ments by repeated core sampling.

II. INSTRUMENTATION AND DEPLOYMENT

In this chapter I discuss the technical aspects of the probe construction and calibration. I then discuss the field site and the deployment of the probes.

Intrumentation

I used a thermistor in one arm of a bridge circuit to measure temperature. The bridge design was a compromise of the following criteria: maximum response to temperature changes in the range from 0 to 20 deg C, low power consumption, negligible self-heating of the thermistors, and near-linear response to temperature. The thermistors protruded through the wall of a 2.54 cm PVC pipe (Figure 1). The output voltages from the bridges were recorded on cassette tape by a data logger. I used Fenwal GB32J3 glass bead and GB32P62 glass probe thermistors each with resistance of 3.7 kohm at the mid-point temperature (10 deg C). The product specifications indicate that the time constants of the thermistors are 4 and 22 s, respectively. The fixed resistors were 3.74 kohm (Corning RN55D 3741F) which were chosen for the low temperature coefficient (100 ppm deg^{-1}). I calculated the maximum temperature offset due to self-heating of the thermistors to be 0.015 deg C. This offset did not present any problems, since most analyses used temperature differences. The effective voltage output of the bridges over the 0 to 25 deg C was -300 to 300 mV when using the power supply of 2 V. The thermistor leads were soldered to 25 AWG plastic coated wire which were soldered

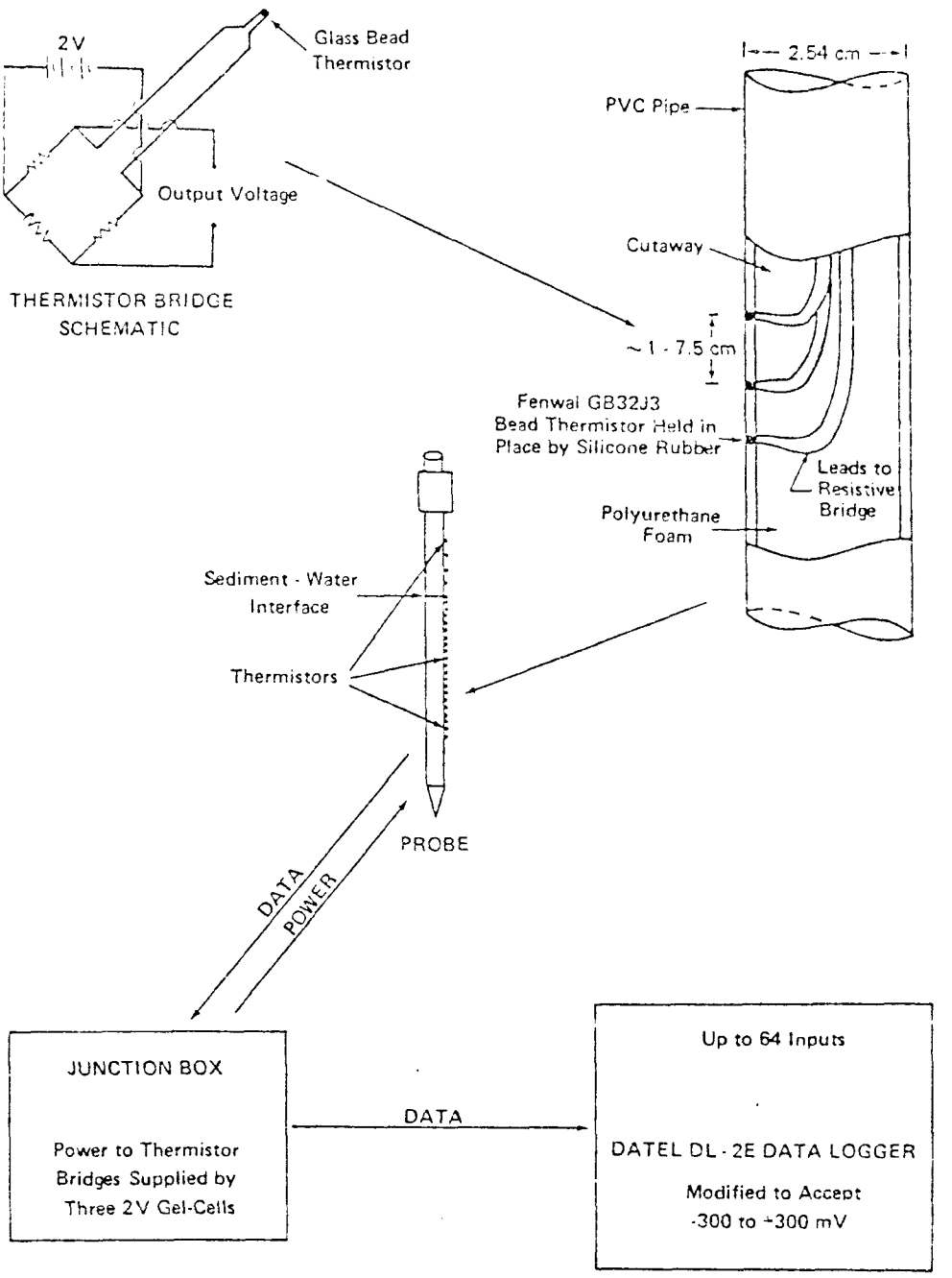

Figure 1. *In situ* data aquisition system. Thermistor beads were potted in drilled holes in PVC pipe and the leads were wired to resistance bridges at the top of the pipe. The polyurethane foam prevented the probe from acting as a cold finger.

to the resistance bridges. A compact configuration of the three resistors in the resistance bridges facilitated their placement just above the PVC pipe. The bare portions of the thermistor leads and the resistance bridges were painted with several coats of Scotchkote Electrical Coating and then covered with Dow Corning 3145 RTV adhesive-sealant.

I built the probe by cutting the PVC pipe (0.40 m) in half along the axial dimension and drilling seventeen 3 mm holes at 1.0 to 7.5 cm intervals along a line down the center of one of the halves. The Dow Corning adhesive held the thermistors in the holes so that at least 1 mm of the sensing element protruded beyond the exterior wall of the pipe. The connecting wires to the bridge ran to the top of the pipe through the interior. After the thermistors were secured in one half of the pipe, I filled the interior with polyurethane foam and quickly mated the other half to the first thereby trapping the foam in the interior. The foam effectively prevented water from entering the probe and convecting and it also reduced the heat transport along the probe. (Appendix B discusses spurious results obtained from a probe that was not filled with foam.) Plastic cable ties held the two halves together. Strain gauge cable (20 m of Belden 8438-1000 25 AWG, 4 conductor, 2 pair each shielded, plastic jacketed) connected each resistance bridge to a junction box at the water surface. The junction box contained three Gel Cell GC 280 2 V, 8 amp-hr batteries connected in parallel which provided the power to the resistance bridges. A constant voltage source powered by the

batteries and stepped down to 300 mV provided a constant voltage that could be monitored by one channel of the data logger for changes in the gain of the data logger's A/D converter. Another channel monitored the supply voltage for the resistance bridges. The temperature conversion software used the changes in these channels to compute correction factors. Terminal strips in the junction box connected the power to the cables leading to the resistance bridges and connected the output voltage from the resistance bridges to the data logger leads.

A Datel D2 Data Logger, modified to accept from -300 to +300 mV full range, recorded the output voltages from all bridge circuits on each of three probes every 5 minutes. The logger could accept up to 64 differential inputs at intervals as short as 11 s. The cassette tapes were read by a Datel DL 2R Cassette Reader and the data was transferred by a HP-85 to the UACN HIS 66/20 computer for processing and analysis.

Calibration

I calibrated the entire data acquisition system in a reversing thermometer calibration bath at the Northwest Regional Calibration Center, Bellevue, Washington. A calibrated platinum resistance thermometer measured the bath temperature accurately to 0.001 deg C. The readings of the bath temperatures at 2 deg intervals from 0 to 20 deg C fitted to third and fourth order polynomials indicated that no additional variance was removed by using a quartic term in the re-

gression. The 12 bit data logger limited the precision of the temperature measurement to 1 part in 4096 which is equivalent to 0.006 deg over the 25 deg range of the data acquisition system. I calculated the mean square of the residuals (Draper and Smith, 1981) for the calibration for each thermistor. The average mean square was 4×10^{-5} deg^2 (std. dev.= 2×10^{-5} deg^2) which can be compared to the square of the precision of the data logger (i.e. $0.006^2 \cong 4 \times 10^{-5}$). This indicates that all the error in temperature measurements was due to error of truncation during analog to digital conversion. I consider this to be an indication of the precision of the system over periods less than a few days. The maximum drift in temperature measurement, as indicated by recalibration after 6 months at the freezing point of water, was ± 0.01 deg. A further test of the time response of the of the probe indicated that it took less than 60 s for the temperature of the thermistors to change their own temperatures 98% of the way from their original value to the value impressed upon them in a step change. The *in situ* temperature distributions were disturbed by the initial insertion of the probe for less than 4 hrs but Figures A.4, A.10 and A.12 show that after this period *in situ* temperatures were faithfully measured.

Deployment

I placed three probes in the sediments of the southwest corner of Lake 227. Brunskill and Schindler (1971) describe the bathymetry of several of the ELA lakes, including Lake 227 (shown in Figure 2),

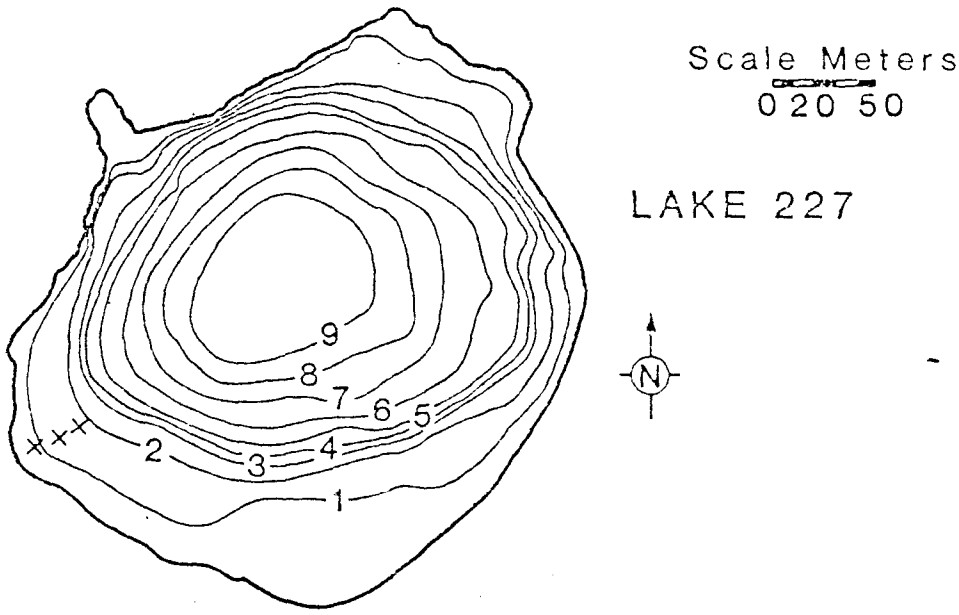

Figure 2. Bathymetric chart of Lake 227. The crosses (X) show where the probes were placed in the sediments.

and the geology of the ELA. Precambrian acid granites underlie the area, which in some places is overlain by glacial drift composed mainly of sand and gravel. Hilltops and hill slopes (relief is usually less than 80 m) have little or no soils. Lake 227 is circular with a radius at the surface of 150 m; the maximum depth is 10 m. The sediments of Lake 227 have high, nearly constant porosity (0.96) and organic content (48% dry weight measured by loss of weight on ignition at 900 deg C) (Hesslein, 1980; Brunskill *et al*, 1971). The particle size distribution for two nearby lakes with similar sediment characteristics is: sand (>50μm) 13%; silt (2-50μm) 75%; clay (<2 μm) (Brunskill *et al*, 1971). No particle size data are available for Lake 227.

The summer thermocline is 3-4 m deep and is established in early May (Schindler, 1971; Schindler *et al*, 1973). The average temperature from June to early September in the upper meter is 20 deg C, and the average temperature in the hypolimnion is 5 deg. The temperature of the epilimnion decreases linearly with time from late August to late October when the lake is isothermal at 4 deg.

The probes were at water depths of 0.75, 1.25 and 1.75 m, respectively, in line perpendicular to the shore (Figure 2). The first probe was 15 m from shore and the distance between the probes was 15 m. The sediments were so flocculent and unconsolidated that the probes would not stay vertical without some supporting structure. I built frames to keep the probes perpendicular to the plane of the sediment surface and placed the probes in the sediments by diving.

The cables from each probe trailed along the bottom to a floating, covered dock which housed the data logger and junction box.

III. RESULTS AND ANALYSIS

Plots of temperature time series for each thermistor depth are in Appendix A (Figures A.1-A.27). Each plot shows up to 24 hrs of temperatures for all functioning thermistors in one probe. Several thermistors failed, presumably due to shorting, as indicated by erratic temperatures, and the recorded temperatures from these thermistors are not shown (e.g., the temperature at depths of 0.10, 0.13 and 0.16 m in probe 2 on 17 Oct. are all missing in Figure A.1). The plots which have less than 24 hrs of data reflect discontinuities due to cassette changes. The temperature range in each plot is 5 deg C.

Figure 3 shows the dates and times covered by each figure. Beginning about 1110, 20 Oct., all time series were very erratic because the floating dock broke loose from its mooring and pulled the probes out of the sediments. I replaced the probes in the sediment at different times as indicated in Figure 3.

On 17 October, when the probes were first deployed, the temperature at the shallow probe ranged from 7 deg at the sediment surface to 10 deg at 0.35 m (Figure 4). The temperatures at the two deeper probe sites were uniformly 0.5 deg less at each thermistor depth, which resulted in a near-constant temperature gradient of 10 deg m^{-1} at all probe sites. The temperatures decreased with time as the bottom water continued cooling and by the last day that temperatures were recorded (30 October) the temperature at the sediment surface at all probes was about 4.5 deg. The temperature gradients remained approximately constant during this time at 10 deg m^{-1}.

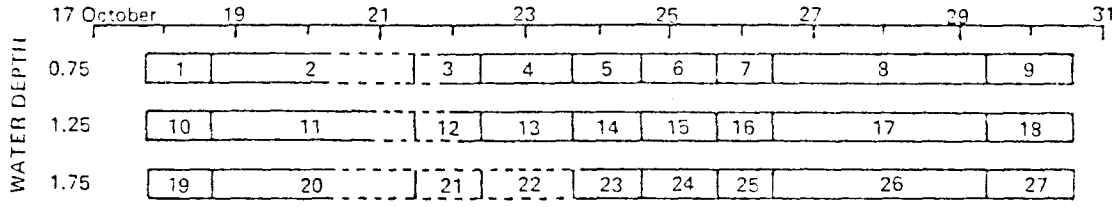

Figure 3. Dates and times covered by each figure (number in the box) in Appendix A. The dashed sections indicate when the temperatures are unreliable due to the probes moving in and out of the sediment.

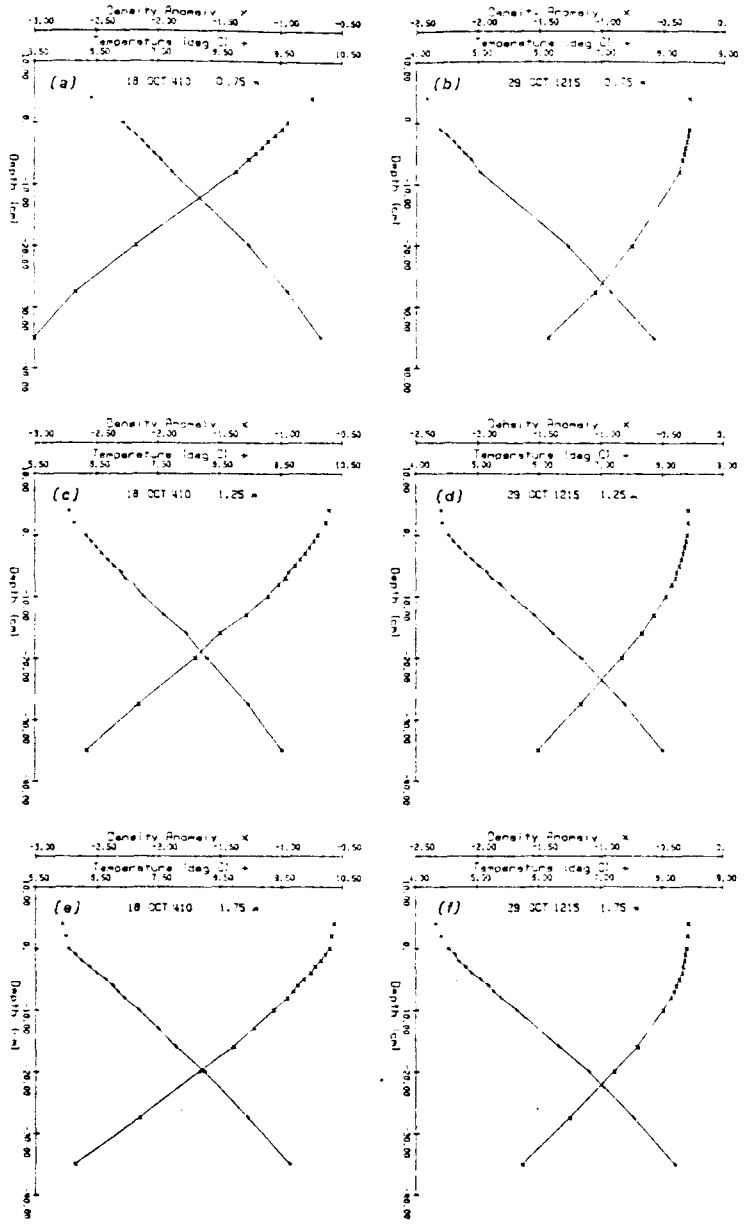

Figure 4. Temperature and density anomaly profiles. (Density anomaly is $(\rho-1)\times10^7$ kg m^{-3}, where ρ is the density.) The time, date and water depth for each profile are indicated in the upper center of each plot. The two dates are close the beginning and the end of the two weeks that I measured temperatures.

The density decreased into the sediments. I calculated density from temperature (Kell, 1967) which ignores the contribution of solutes to the density. Quay (1977) shows that dissolved solids can significantly affect water density in Lake 227; the main effect in this context would be an offset in the density since all solute gradients are above depths of 0.10 m (Hesslein, 1976). The density gradients would not be affected below this depth.

Diffusive Transport of Heat

Usually, the temperature time series behaved in accordance with diffusive transport of heat. Temperature variations at depth progressively decreased in magnitude and lagged the variations in the upper sediments. The attentuation was frequency dependent so that the higher frequencies were attenuated very rapidly with depth. This behavior is consistent with diffusive transport of heat (Carslaw and Jaeger, 1959) and I attempted to use spectral analysis to obtain an estimate of the frequency response function (Jenkins and Watts, 1968). The frequency response function between two time series is a function of the distance between the depths of the time series, the diffusivity and the velocity of the pore water (assuming a one dimensional system). In theory, the velocity and the thermal diffusivity can be estimated by inverting the estimated frequency response function (Cairns, 1973; Farmer, 1975). However, the temperature variation at the surface was neither large enough nor long enough to obtain meaningful estimates of the frequency response function for

depths below a few centimeters. Other approaches to estimating the velocities and diffusivity will be described.

Departures from Purely Diffusive Heat Transport

The time series of temperature were the only evidence that I could use to look for departures from diffusive heat transport. Visual inspection of the time series did not reveal any obvious departures from purely diffusive heat transport in most of the time series. A more sophisticated approach was needed to find advective transport of heat through the upper 35 cm for which I had time series of temperature. This approach will be described later. Visual inspection of the time series in the upper 8 cm of the shallow probe site revealed high frequency (periods of 600 to 7.2×10^3 s) temperature fluctuations that could not be due to diffusive heat transport. These fluctuations were superimposed on the slowly varying, quasi-diurnal fluctuations that I will refer to as the low frequency fluctuations. The next section describes and analyzes the high frequency fluctuations in detail. The section titled "Global Advection of Heat" describes the more sophisticated approach for finding advective transport of heat through the upper 35 cm which I will call global advection of heat.

High Frequency Temperature Fluctuations

Description

Close examination of the time series revealed high frequency temperature fluctuations that were obviously nondiffusive in origin.

The low frequency temperature fluctuations that were of diffusive origin were all derived from fluctuations at the sediment surface and they propagated into the sediments with concomitant attentuation and time lag. The clue to the convective nature of the nondiffusive fluctuations was that they occurred only below the upper few centimeters of the sediment. That is, there were no fluctuations in the upper few centimeters of the sediments from which the nondiffusive fluctuations could be derived. The high frequency fluctuations occurred only at the shallow probe site. There was a definite temporal sequence to the fluctuations at the shallow probe site. Figures 5a-*h* show this sequence for the upper 8 centimeters at the shallow probe site. The smoothness of the time series at depths below the upper 2 centimeters of the sediments is apparent in Figures 5a and *b*. The maximum temperature change between any two sampling intervals at 5-8 cm was just the least significant bit of the data logger (0.006 deg). At about 1600, 24 October, (Figure 5c) a qualitative difference in the time series became apparent. The maximum change in temperature between sampling intervals was 3 significant bits (0.018 deg) and periodic fluctuations occurred with periods of 600 to 3.6×10^3 s (10 minutes to 1 hour). This was in contrast to the monotonically varying (monotonically over periods of 4×10^4 s [$\simeq$ 12 hours]) temperatures prior to this time. Some of the fluctuations occurred at all depths between 4 and 8 cm with little of no attentuation or time lag (e.g., those indicated by a bracket in Figure 5c).

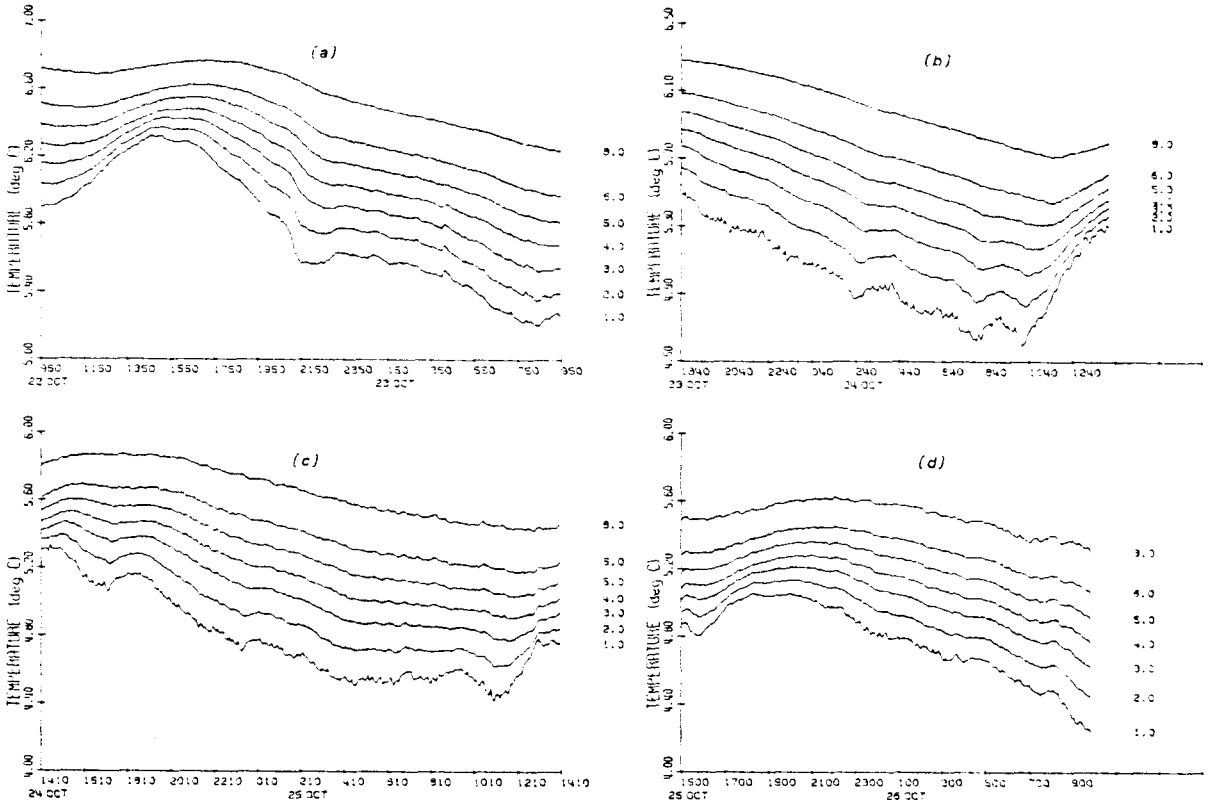

Figure 5a-h. Time series of temperature in the upper 8 centimeters at the shallow probe site. *a* and *b*. The smoothness of the time series at 3 to 8 centimeters was characteristic of diffusive transport of heat. *c* and *d*. Intermittent temperature fluctuations occurred during this time at depths from 4 to 8 centimeters. The bracket in *c* indicates an example of coherent fluctuations at all depths from 4 to 8 centimeters. At 700, 26 October, regular fluctuations began to occur.

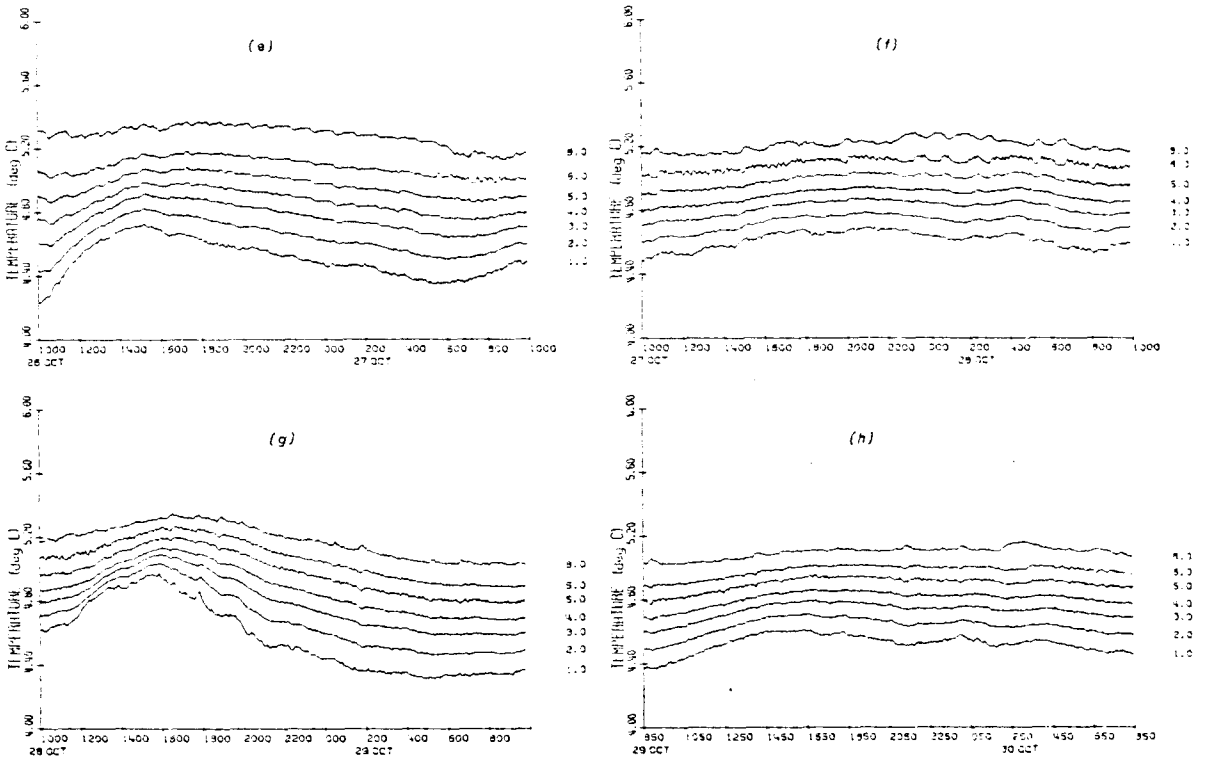

Figure 5a-h continued. e-h. At 600, 27 October, a high frequency fluctuation began at depths from 3 to 6 centimeters. Fluctuations at 8 cm were sometimes coherent with those at 6 cm, but were 180° out of phase at other times (e.g., at 2300, 28 October, f).

This type of fluctuation occurred intermittently until about 700, 26 October, (Figure 5*d*) when more regular fluctuations began to occur with periods of 5.4×10^3 s to 7.2×10^3 s (1.5 to 2 hours) and maximum amplitudes of $\simeq$ 0.07 deg. The largest amplitudes occurred in the time series at 8 cm. The amplitudes at depths between 4 and 6 are less than at 8 cm, but there was no apparent time lag. This type of fluctuations continued with reduced amplitude from 1800, 26 October, to 600, 27 October (Figure 5*e*).

A new kind of fluctuation then began which was characterized by high frequency at 3-6 cm (Figure 5*e*). The period of the fluctuations at these depths was as short as 600 s (10 minutes) and the sampling could have aliased fluctuations with periods less than this. The fluctuations occurred with reduced amplitudes but no time lag at depths between 3-5 cm. There seemed to be some coherence between the time series at 6 and 8 cm but not at all like that between 3-8 cm. Indeed, at 2300, 28 October, (Figure 5*f*) the temperature anomalies at 6 and 8 cm were of the same magnitude but opposite sign. The largest amplitude during this kind of fluctuation was 0.07 deg and the maximum temperature change between sampling intervals was 0.044 deg (6 significant bits of the data logger).

Analysis of High Frequency Vertical Velocity Fluctuations

If the temperature fluctuations are assumed to be due to vertical velocity fluctuations of the pore waters, then the following approach can estimate the magnitude of the velocity.

The amplitude of a periodically varying vertical velocity is related to the amplitude of the periodic temperature fluctuation through the heat conservation equation for a porous medium (3).

$$(\rho c)^* \frac{\partial T}{\partial t} = \nabla\cdot(\lambda_B \nabla T) - (\rho c)_f \vec{v}\nabla T \qquad 3$$

Here, $(\rho c)^*$ is the heat capacity of the saturated porous medium, T is the temperature, λ_B is the thermal conductivity of the saturated medium, $(\rho c)_f$ is the heat capacity of the pore water and $\vec{v}$ is the filtration velocity vector (discharge per unit area). (See Cheng [1978] for the assumptions on which this equation, and other equations applicable to convection in porous media, are based.) Since the gradients and curvature of temperature in the lateral dimensions are negligible, this equation simplifies to the one dimensional

$$\frac{\partial T}{\partial t} = K \frac{\partial^2 T}{\partial z^2} - v_z \frac{\partial T}{\partial z} \qquad 4$$

heat transport equation (4). Equation 4 assumes that λ_B does not vary with depth, that K $(=\lambda_B/(\rho c)^*)$ can be approximated by the thermal diffusivity of water and that $(\rho c)_f=(\rho c)^*$. These are valid assumptions since the porosity is 0.96 and constant to at least 0.45 m (Hesslein, 1980). If the fluctuations are treated as perturbations on some steady state, then T and v_z can be expanded in a perturbation series, i.e. $T=T_0+T_1+\ldots$ and similarly for v_z, where $T_0=\langle T\rangle$, $v_{z0}=0$, and $\langle\ \rangle$ indicates an average over one period. The time series indicates that the change in the average temperature is negligible so that $\partial\langle T\rangle/\partial t\cong 0$ and, therefore, the solution to equation 4 to order

zero is $T=mz+C$, where C is a constant. Now $v_{z1}=A\sin(\omega t)$ and equation 4 to first order is:

$$\frac{\partial T_1}{\partial t} = K\frac{\partial^2 T_1}{\partial z^2} - Am\sin(\omega t) \qquad 5$$

If v_{z1} is constant over a scale depth, H, such that the dimensionless number AH/K (which is a perturbation Peclet number) is >>1, then the diffusive term can be neglected and the solution is:

$$T_1 = \frac{Am}{\omega}\cos(\omega t) \qquad 6$$

and the amplitude of the temperature fluctuation is therefore Am/ω. The time series showed that the period of the fluctuations varies from 600 s to 3.6×10^3 s. Assuming the maximum amplitude of 0.07 deg for the temperature fluctuations and the temperature gradient of 10 deg m^{-1}, this gives a range of velocity amplitudes of $1\text{-}7\times10^{-5}$ m s^{-1}.

Using the larger value for the velocity amplitude, the criterion for neglecting the diffusive term is satisfied marginally. The value of AH/K is about 1 if the scale depth is taken as 0.01 m. (The thermal diffusivity of water is 1.4×10^{-7} m^2 s^{-1} [1.4×10^{-3} cm^2 s^{-1}].) I used 0.01 m as the scale depth because the amplitudes of the temperature fluctuations are slightly attenuated over this distance. Since the perturbation Peclet number is about 5, diffusion of heat cannot be ignored. However, the above estimates of the velocity fluctuations should hold over as an order of magnitude estimate because the perturbation Peclet number was at least greater than 1.

Global Advection of Heat

The vertical velocities in a convection cell are into or out of the sediment in areas of recharge or discharge, respectively. Between the areas of discharge and recharge, only horizontal motion occurs. The unidirectional vertical velocities in the areas of recharge and discharge approach zero at the bottom of the convective cell. After the data was collected, I realized that the depth of the convection cells should be greater than the depth of the probes. (The appropriate theory and calculations are in the next chapter in the section titled, "Estimation of the Time-dependent Rayleigh Number".) Therefore, I wanted to estimate the unidirectional vertical velocities and their depth distribution from the time series of temperature at each probe site. I call these velocities "global" to distinguish them from the high frequency velocity fluctuations which were discussed in the previous section and were limited to a narrow range of depths.

Curvature of temperature profiles in sediments is taken as indication of pore water motion in deep sea sediments (Anderson *et al*, 1979). This interpretation assumes steady state so that the time derivative in equation 4 is 0 and the curvature is balanced by the temperature gradient. Temperature profiles from all probes showed some curvature at some times, but some, if not all, of this curvature is balanced by the time derivative as well as the advective term. The proper approach to evaluate subtle departures from diffusive

transport is to evaluate the terms in the heat transport equation (4) and solve for v_z.

One way to evaluate the derivatives in equation 4 is to use the observed data in finite difference approximations of the derivatives. Beck (1963) points out that this method requires very precise temperature measurements since errors in measurement are magnified when differences are taken. This is particularly true for higher derivatives. He suggests an integration of the heat transport equation using observed measurements for the initial and boundary conditions. Calculated temperatures from the integration can then be compared to measured temperatures and the velocities (or diffusivity in Beck's study) can be adjusted to obtain a minimum in the mean sum of squares of the residuals.

I used this approach in the search for vertical velocities other than zero. I integrated numerically the heat transport equation using a fully implicit, centered space scheme. This method is unconditionally stable for any time step, is first order accurate in time and second order accurate in space (Roache, 1976). I evaluated the velocity at each depth for which I had a time series of temperature, and let the velocity vary linearly between those depths. I used conservative differencing for the convective term. The depth increment for the integration was 1 cm, because smaller increments did not improve the solution to a significant degree. The boundary conditions were taken from the temperature time series at the upper and lower depths of a data window and the initial condition was taken

from the initial temperature at each depth in the window (Figure 6). I used cubic spline interpolation to specify initial temperatures at depths between functioning thermistors. The time series at 1 cm and 35 cm defined the upper and lower limits of the data window. I used 1 cm as the upper limit since the thermistor at 0 cm could have been responding to temperatures in the water column if it was not situated directly at the sediment surface. The data window was 24 time increments long and the time increment varied from 300 to 4.8×10^3 s (5 to 80 minutes). The data window was moved over successive sections of measured temperatures.

I used the IMSL subroutine ZXSSQ to search for the minimum mean sum of squares of the residuals of the interior points of the data window. This subroutine uses the Levenberg-Marquardt algorithm (Draper and Smith, 1981).

The diffusivity of the saturated sediment should be very close to that for water (1.4×10^{-7} $m^2 s^{-1}$). I calculated the diffusivity assuming that the sediment solid phase was all inorganic or all organic according to the equation:

$$K = \frac{\lambda_f^{\phi} \cdot \lambda_s^{(1-\phi)}}{(\rho c)_f \phi + (\rho c)_s (1-\phi)} \qquad 8$$

where λ's and (ρc)'s denote thermal conductivities and heat capacities, respectively; the subscripts f and s represent the fluid phase and solid phase, respectively; ϕ is the porosity. Carslaw and Jaeger (1959) give values for the thermal diffusivities and heat capacities

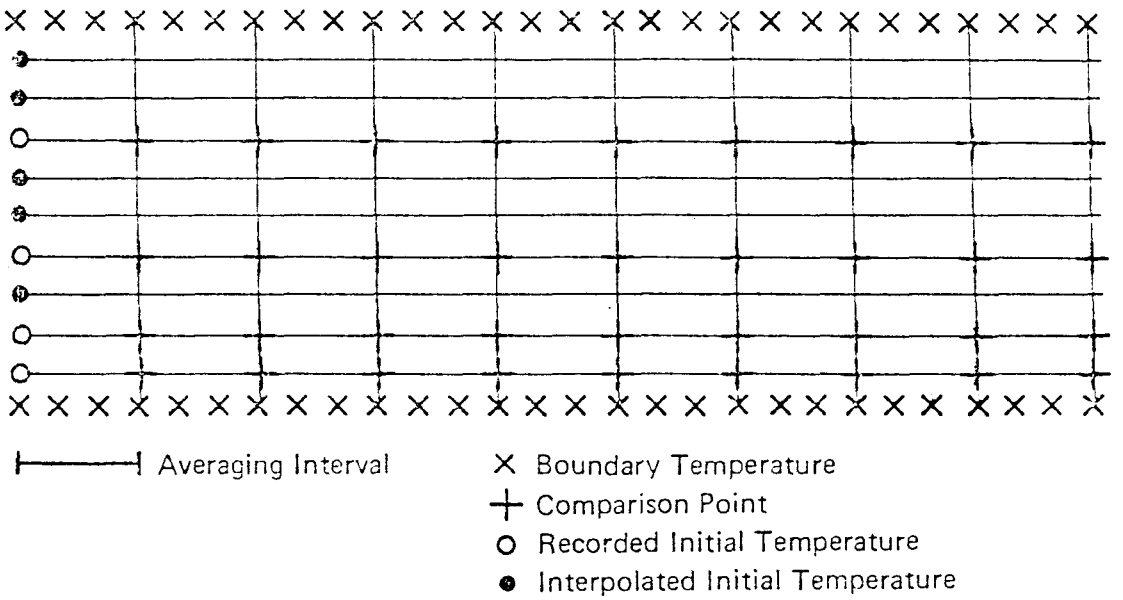

Figure 6. Grid for iterative calculation of diffusivity using finite difference, numerical model to evaluate temperatures at all grid points (intersection of vertical and horizontal lines). The data window was defined by the upper and lower boundary temperatures, the recorded initial temperatures and the number of time increments.

of granite and cork. I made the assumption that these two materials would serve as good analogs to the inorganic and organic phase of the sediment solids. The calculated diffusivities were 1.3×10^{-7} $m^2 s^{-1}$ (100% organic solid phase) and 1.5×10^{-7} $m^2 s^{-1}$ (100% inorganic solid phase). I used the porosity as given by Hesslein (1980) of 0.96. If the actual porosity was as low as 0.90 then the diffusivities are 1.2×10^{-7} $m^2 s^{-1}$ and 1.7×10^{-7} $m^2 s^{-1}$. In the numerical integration I used a value of 1.5×10^{-7} $m^2 s^{-1}$, which is a little higher than the self-diffusion coefficient of water, 1.4×10^{-7} $m^2 s^{-1}$.

This method of determining global velocities was not satisfactory. Most of the estimated velocities had confidence limits, typically $\pm 1 \times 10^{-7}$ m s^{-1}, that included zero. These confidence limits were calculated by the method given by Draper and Smith (1981) for nonlinear regression. The confidence intervals were based on a confidence level of approximately 95% (see Draper and Smith [1981] for a discussion of the application of statistics of linear regression to nonlinear regression.) Some estimated velocities were as high as 4×10^{-6} m s^{-1} with confidence intervals of $\pm 1 \times 10^{-6}$ m s^{-1}. The velocities for adjacent windows were zero. This led to some doubt as to whether these high velocities were real. Indeed, the mean sum of squares of residuals in one case with high velocities was 2.8×10^{-5} deg^2 and the mean sum of squares of the residuals when velocites were assumed to be zero was 3.4×10^{-5} deg^2. The standard deviations based on these mean sum of squares were 5.3×10^{-3} and 5.8×10^{-3} deg, which does not seem to be a significant difference.

Examination of the residuals from such regressions showed that the residuals are correlated (Figure 7). Schisler and Beck (1979) discuss the effect of correlated errors of the estimation of parameters and their confidence limits. They conclude that the estimated parameters are biased to a small degree but that the confidence level is significantly over estimated. I believe that the correlated residuals caused the confidence intervals to be underestimated and that any estimated velocities cannot be distinguised from zero.

The analysis does indicate that if there is pore water motion, then the global vertical velocities, averaged over the time of the data window, were not greater than the greatest estimated velocity of 5×10^{-6} m s^{-1}. The previous analysis of the high frequency velocity fluctuations gave an amplitude greater than this but the average velocity over the time of the data window was zero.

Although K is constrained by Hesslein's observations (1976) to a value close to that of water, I used this regression procedure to estimate the thermal diffusivity at the shallow probe site just to see how much variation would be in the estimate for different data windows. For ten different windows, the average was $2.0 \times 10^{-7} \pm 1.0 \times 10^{-7}$ m s^{-1} (standard deviation). Knowing that the actual value is close to 1.4×10^{-7} m s^{-1} any bias in the estimate was overwhelmed by the confidence interval for the estimate.

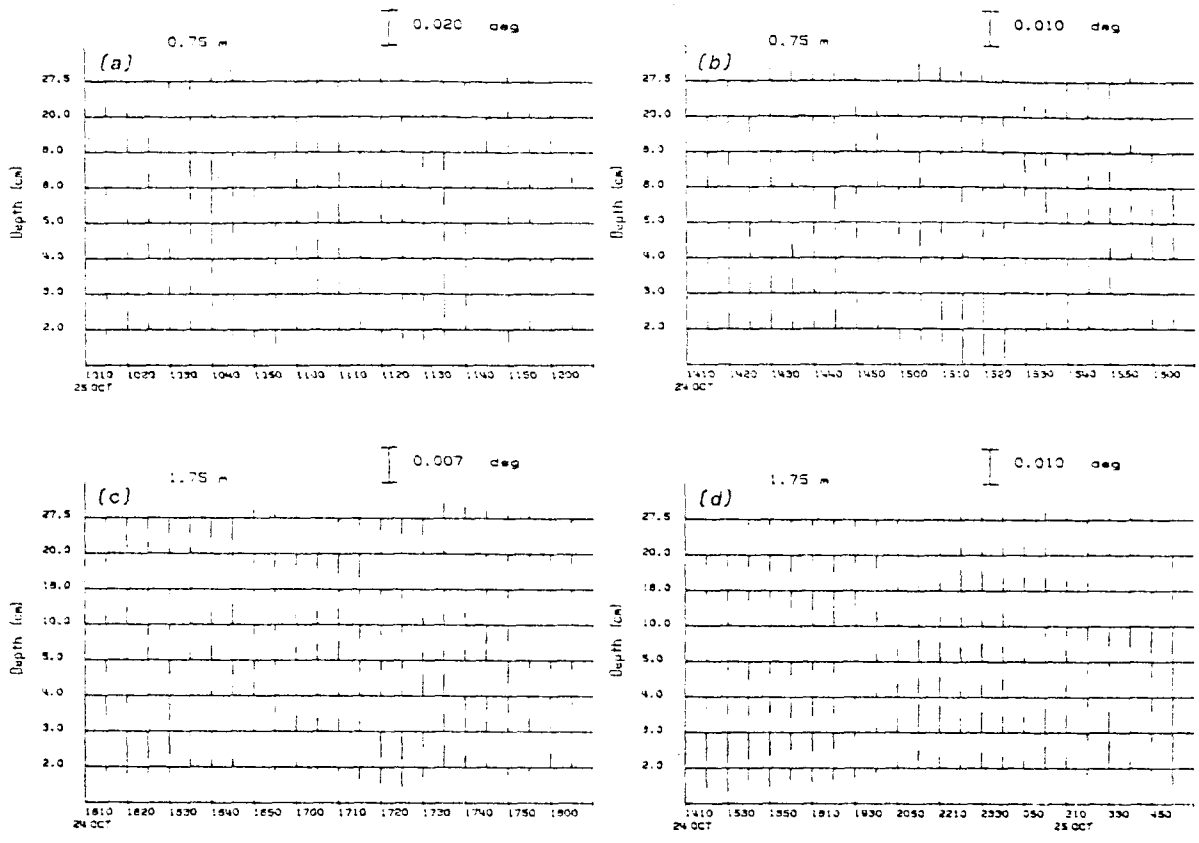

Figure 7a-d. Residuals of regression. a-c. Residuals of regression with no time averaging (time increment = 600 s [10 minutes]). The magnitudes of the residuals at each thermistor are represented by vertical sticks. The scales are in the upper right corner of the plots. The horizontal lines are the zero value at each thermistor; sticks above the line represent positive residuals. The water depths are in the upper left corner of the plots. There were correlations between successive times at any particular thermistor and between different thermistors at any particular time. d. The residuals were more correlated when the temperatures were averaged before regression (time increment = 4800 s [80 minutes]).

IV. DISCUSSION

From Hesslein's study (1980) of tritiated water transport in the upper sediments of Lake 227, I had expected the following sequence of events to occur. Summer heating above the thermocline would warm the bottom waters with which the sediments would be in thermal equilibrium. At the beginning of autumn cooling, the denser, cooler water at the sediment-water interface would begin to penetrate the sediments as an isothermal, convecting layer. This layer would continue to penetrate the deeper, quiescent sediments until there was no more density difference between the two. Hesslein observed that the depth of penetration was 0.1 m in late October. This process is qualitatively similar to the deepening of the mixed layer in oceans (e.g. Dodimead *et al*, 1962; Deardorff *et al*, 1969; Farmer, 1975). I had hoped to measure the rate of penetration and to relate the rate to the density difference in the two layers. Although Hesslein's study seemed fairly definitive in a qualitative sense, my observations did not follow the above sequence of events. The only indication that motion was occurring in the sediments were the appearance of temperature fluctuations that were not consistent with purely diffusive transport.

Density-driven Temperature Fluctuations

The density decreased into the sediments during all the time-series measurements (Figure 4). The observed temperature fluctuations are probably related to pore water motion due to buoyancy

forces. However, they may be caused by other mechanisms: (1) noise generated by the data acquisition system, and hence spurious; (2) pore water motion caused by biological processes such as bio-turbation and -irrigation; and (3) pore water motion due to physical forces other than buoyancy. I will discuss the possibility that these mechanisms caused the observed fluctuations before addressing free convection as having some relation to the fluctuations.

I relied on the calibration data and the long-term behavior of the data acquisition system, as indicated by the time series of temperature, to address questions of noise due to instabilities of the acquisition system. Any noise-like error due to electronic instabilities of the data logger should have appeared in all channels because all input signals were processed in serial mode and thus employed the same circuitry. The temperature fluctuations occurred simultaneously only over a few adjacent thermistors: the relative stability of thermistors at other depths proved that the electronics were introducing no sources of noise (and that the probe was not being physically moved into or out of the sediment). Two facts implied that the fluctuations were not caused by failure of electronics outside of the data logger: (1) before 24 October, fluctuations in the frequency range of the observed fluctuations did not occur in any channel; (2) the fluctuations in adjacent thermistors (5, 6 and 8 cm) were coherent. Therefore, I am confident that I observed *in situ* temperature fluctuations.

The fluctuations were not caused by bulk sediment redistribution

or irrigation by infauna. Infauna, if present, would disturb the sediment solid phase; yet these sediments have not been redistributed since deposition (Hesslein, 1980). The absence of temperature fluctuations before 25 October corroborated the absence of infauna. I eliminated the possibility of bubble ebullition for the same reasons.

Physical mechanisms that could cause pore water motion include ground water seepage, surface wave phenomena and buoyancy effects. Ground water flow was negligible (1-2% of the total water input to the lake) due to the low relief and the scant soil overburden (Kennedy [1976] as referenced in Newbury and Beatty [1980]). This was consistent with the absence of the fluctuations for long intervals of time. In any case, I would not expect fluctuations of ground-water flow with the regularity or high frequency of the observed fluctuations. Fluctuations of ground-water flow would have caused temperature fluctuations over the entire depth of the sediments, which was not observed. Forced convection in the sediments due to surface waves or seiches was precluded by the lack of coherent temperature fluctuations throughout the upper sediments.

The discrepancy between the anticipated and the observed sequence of events and the possibility that the temperature fluctuations were related to density-driven motion necessitate a discussion of previous work on free convection in porous media.

Estimation of the Rayleigh Number

The analysis of global velocities indicated that there were no

vertical velocities above 5×10^{-5} m s^{-1} in the upper 35 cm at any of the probe sites. Hesslein's observations led me to believe that penetrative convection should be occurring in these sediments. I examined the theory of convection in porous media to address this conundrum.

The possibility of free convection obliges a consideration of the Rayleigh number (Combarnous and Bories, 1974), Ra, defined by

$$Ra = \frac{\alpha \Delta T (\rho c)_f H K}{\lambda_B} \qquad 9$$

where K is the hydraulic conductivity, α is the thermal expansion coefficient ($=10^{-4}$ deg^{-1}), $(\rho c)_f$ is the heat capacity of the interstitial water, λ_B is the bulk thermal conductivity coefficient of the saturated porous medium, and H and ΔT are the scale depth and temperature difference, respectively. This dimensionless number is a measure of the ratio of the destabilizing buoyancy force to the stabilizing process of diffusion. According to theory and laboratory experiments, the thermal Rayleigh number must exceed a critical value before the motions induced by small horizontal temperature perturbations can maintain free convection. The critical value, Ra_c, is 27.1 , which Nield (1968) derives assuming a saturated, porous medium of depth H bounded above by permeable, isothermal and below by impermeable, isothermal boundaries across which a destabilizing temperature difference, ΔT, is imposed. The equation of state relating density to temperature is linear and the system is assumed to be time inde-

pendent. Periodic boundary conditions (Chhuon and Caltigirone, 1979), or nonhomogeneous (Green and Freehill, 1969) or anisotropic (Kvernvold and Tyvand, 1979) porous medium can all act to reduce the critical Rayleigh number, although probably not by a factor of 10, even if in combination. Near the maximum density of water at 4 deg C, the density is a quadratic function of temperature. Wu *et al* (1979) show that the critical Rayleigh number for systems near 4 deg is within 5% of the above critical value if the 4 deg isotherm is near the upper boundary. As Figure 4 shows, this was the case in late October. Therefore, the value of 27 is a good order of magnitude estimate for the critical Rayleigh number.

I estimated the Rayleigh number as follows. The high porosity permitted the use of the thermal diffusivity of water ($K=1.4\times10^{-7}$ m^2s^{-1}) for the quotient $\lambda_s/(\rho c)_f$. I tried to measure the *in situ* hydraulic conductivity using a self-made device based on a falling head permeameter, but the head moved too quickly to measure the rate of falling. I therefore had to estimate the hydraulic conductivity and I assumed it to be similar to the value in sands, 10^{-3} m s^{-1}. This is a high value but I think it is justified by the high porosity of Lake 227 sediments. The amplitude of the annual temperature cycle at the 1 m water depth is 20 deg C which I took for ΔT and the sediment depth, H, was 10 m (G. Kipphut, personal communication). Therefore, the maximum Rayleigh number was 143, which is realized only when the amplitude of the annual temperature cycle is expressed across the whole depth of the sediments. When this happens the pore

water is freely convecting over the entire sediment depth.

However, there is a period of time after autumn cooling begins when ΔT is not realized over the whole sediment depth. In transient systems, a time-dependent Rayleigh number can be calculated based on the product $H\Delta T$ where H and ΔT are scaled according to diffusion theory and both change with time (Elder, 1968). When this time-dependent Rayleigh number first exceeds the critical value at time t_c, convection ensues over the depth $H(t_c)$ (Elder, 1968). The convecting layer then erodes the stable layer below until the convecting layer reaches the sediment basement and ΔT is realized across the entire sediment depth.

Since I did not have temperatures below 35 cm, I estimated H and ΔT as functions of time as follows. The temperature of the bottom water in contact with the sediments at 1 m water depth is typically 22 deg C from 1 June to 1 September (Schindler *et al*, 1971; Schindler *et al* 1973). For this time interval, I calculated the diffusive scale length ($=2(Kt)^{1/2}$, where t is the time interval) to be 2.1 m, which is the depth to which summer heating occurs. This provided an initial condition, T_o, for the following analysis. I assumed, then, that on 1 September the sediments to 2.1 m are at about 22 deg, and the sediment surface begins cooling linearly with time to the observed temperature of 4.4 deg on 30 October. The temperature-depth distribution as a function of time, for a system undergoing surface cooling at a linear rate, is given by equation 10 (Carslaw and

Jaeger, 1959), where α, 3.5×10^{-6} deg s^{-1}, is the rate of cooling.

$$T(z,t) = -4\alpha t i^2 \mathrm{erfc} \frac{z}{2(Kt)^{1/2}} + T_o \qquad 10$$

(See Carslaw and Jaeger [1959] for the definition of the nth repeated integral of the complementary error function, $i^n \mathrm{erfc} x$.) For convenience, I took the diffusive scale depth, H, as $2(Kt)^{1/2}$, where t is the time after 1 September. This is the depth at which the argument of the repeated complimentary error function in equation 10 is 1, and is similar the e-folding depth for exponential distributions. At the time of the first appearance of the high frequency temperature fluctuations, the scale depth was 1.6 m. The temperature at the scale depth is $T = -0.0568 \alpha t + T_o$, which is just equation 10 when the argument is 1. The temperature difference between the scale depth and the sediment surface is $\Delta T = 0.95 \alpha t$. The product $H \Delta T = 1.9 \alpha (K t^3)^{1/2}$ increases as the 3/2 power of time and on 28 October was 25 m deg.

The Rayleigh number on this date was 19, assuming a hydraulic conductivity of 10^{-3} m s^{-1}, and is certainly within the range of the critical value, considering that this estimate is valid over an order of magnitude. The failure to detect any global velocities greater than 5×10^{-6} m s^{-1} indicated that the pore waters at the shallow probe site were marginally unstable. Therefore, the value that I have used for the hydraulic conductivity is probably an upper bound.

Although the pore waters were marginally unstable, I could not

easily account for the appearance of high frequency temperature fluctuations. I think the temperature fluctuations were related to the free convection that the above discussion indicated was occurring to about 1.6 m. But the fluctuations are not characteristic of linear, steady-state convection. Oscillatory convection occurs at Rayleigh numbers above 240 (Horne and O'Sullivan, 1974) which is more than ten-times greater than the estimated value. Furthermore, there were no temperature fluctuations below 8 cm. The oscillatory systems described by Horne and O'Sullivan show temperature fluctuations throughout the convecting layer.

The density, calculated from temperature, showed negligible gradients in the upper few centimeters because of the density maximum at 4 deg C (Figure 4). So at the time the fluctuations occurred, the unstable, convecting layer was bounded above by a stable, quiescent layer. Water near the density maximum at 4 deg C show large temperature fluctuations at the interface between the stable and convecting layers (Townsend, 1964). These fluctuations have been interpreted as internal waves propagating along the interface (Townsend, 1966). Townsend shows that these waves occur only when the inertial effects are greater than viscous effects. Usually, the dynamics of flow in porous media are described by Darcy's law (12) which assumes that the pressure gradient

$$\vec{v} = -K\nabla\left[\frac{p}{\rho g} + z\right] \qquad 11$$

is balanced by the frictional Darcy term. I considered the effect of adding allowing an inertial term as in equation 12. The ratio of the

$$\frac{K}{\phi g}\frac{\partial \vec{v}}{\partial t} + \vec{v} = -K\nabla\left[\frac{p}{\rho g} + z\right] \qquad 12$$

magnitude of the inertial term to the Darcy term is given by the dimensionless number $K/g\phi t^*$, where t^* is a is a characteristic time. I estimated this number to be 10^{-5} by using the assumed value of the hydraulic conductivity for K and using the smallest period of the observed temperature fluctuations for t^*. This shows the negligible effect of the inertial term for these fluctuations. However, I think that the convecting layer, beneath a shallow stable layer, causes the observed fluctuations in a manner whose details have yet to be examined theoretically .

Approach to Penetrative Convection, Fall, 1979

Based on the observations of temperatures at the shallow probe site and the above calculation of the time-dependent Rayleigh number, I believe the proper sequence of events in the fall, 1979, to be the following. Cold bottom water in contact with warm sediments began to cool the upper sediments in accordance with purely diffusive transport of heat. The temperature at the sediment surface decreased linearly with time and diffusive cooling continued until mid-October when the system became marginally unstable with respect to free convection. At that time, the unstable layer began to convect so slowly that the temperature profile was negligibly disturbed, as

indicated by the failure to find any global velocities greater that 5×10^{-6} m s^{-1}. The convecting cells extended from this upper boundary to about 1.6 m below the sediment surface and since the system was marginally unstable the aspect ratio of the cells (width:depth) was 2.73 (Lapwood, 1948). In late October, a stable layer was created by the cooling of the pore waters in the upper few centimeters to the temperature of the maximum density of water. I have suggested that the interaction of the convecting layer below this depth and the stable above caused the high frequency temperature fluctuations. The pore waters at the deeper probe sites were still quiescent since the bottom waters there did not reach as high a temperature during the summer as the bottom water at 0.75 m (Schindler *et al*, 1971; Schindler *et al*, 1973). Thus there were no temperature fluctuations at these probe sites.

The observations and calculations are hard to reconcile with observations by Hesslein (1980) that the depth of the layer of enhanced transport is 10 cm. Hesslein believes the increased transport is due to free convection; however, the depth of the convecting layer from the above calculations should be more than ten times the depth of Hesslein's layer of enhanced transport. The rate of cooling was probably much greater in 1975, the year of Hesslein's observations, because ice formed earlier on the lake. But this increase in cooling rate is not likely to account for such a shallow, convecting layer. The depth of the convection layer at the onset of convection, H_c,

varies as $z^{-1/3}$ which is derived by substituting the functional dependence for $H\Delta T(=-1.9z(Kt^3)^{1/2})$ into the expression for the Rayleigh number (9) and then equating the expression to the critical value and solving for H_c. Even if the cooling rate was twice as fast in 1975, the critical depth, H_c, would be $2^{-1/3}=(0.8)$ times the value calculated for 1979.

Implications for Penetrative Convection in Ocean Sediments

I have used the theory of penetrative convection in porous media to explain the failure to find global velocities in the time series of temperature. This theory can be applied to the possibility of penetrative convection in sediments other than Lake 227. This section discusses some theory of penetrative convection in porous media and the possibility of its occurrence in other environments.

Penetrative convection is not limited to fresh waters but occurs in coastal sediments also. Density is determined by salinity as well as temperature in these environments so that temporary increases in the salinity of bottom waters can also lead to penetrative convection. When and where this penetrative convection occurs is related to stability criteria based on the thermal Rayleigh number (9) and a similar solute Rayleigh number, Ra', defined as

$$Ra' = \frac{\alpha' \Delta S K H}{K'} \qquad 13$$

where α' is the salinity analog to the thermal expansion coefficient, ΔS is the scale salinity difference, and K' is the solute diffusivi-

ty. I made estimates of the depth of the convecting layer, H_c, at the time, t_c, that convection initiates (Table 1). I assumed the sediments are at some initial temperature or salinity (depending on whether the increase in bottom water density is caused by changes in temperature or salinity) and that at time zero the bottom water undergoes an increase in density, $\alpha\Delta T$ ($\alpha'\Delta S$). I used the diffusive scale depth, $H=2(Kt)^{1/2}$ ($H=2(K't)^{1/2}$), to solve for the critical time, t_c, where

$$t_c = \left[\frac{Ra_c}{2\alpha\Delta TK}\right]^2 K \qquad 14$$

and the critical depth, H_c, is

$$H_c = 2(Kt_c)^{1/2} = \frac{Ra_c K}{\alpha\Delta TK} . \qquad 15$$

H_c and t_c are proportional to the diffusivity; the thermal diffusivity is 1000 times as large as the solute diffusivity so that salt-driven convection initiates in one-thousandth the time that heat-driven convection initiates, given the same density difference, i.e. $\alpha\Delta T=\alpha'\Delta S$. H_c is, however, one-thousand times less for salt-driven than for heat-driven convection. Notice that H_c and t_c are proportional to the inverses of the density difference and the square of the density differences, respectively. Large salinity changes (ΔS=10 g/kg) in estuaries due to tides could lead to penetrative convection if the sediments were very permeable, e.g. coarse sand

($K=10^{-3}$ m s^{-1}). Smaller increases ($\Delta S=1$ g/kg) in salinity due to upwelling events could cause penetrative convection in shelf sediments where the permeability is as high as 10^{-3} m s^{-1} (Reidl *et al*, 1972). Double diffusive convection (Nield, 1968) is also possible in these two environments. Penetrative convection in deep-sea sediment is not likely to occur since the hydraulic conductivity is so low ($K<10^{-8}$ m s^{-1}, see Bryant *et al* [1981]). Convection would not ini-

Table 1. Critical times, t_c, and depths, H_c, are given for various values of ΔT and ΔS. The amplitudes of velocity, A, and of temperature (or salinity) perturbation, A_θ, are also given in the lower part of the table.

	Heat			
$\Delta T=$	10 deg	1.0 deg	0.1 deg	0.01 deg
$t_c(\propto\Delta T^{-2})$	212 days	6 yrs	6×10^{3} yrs	6×10^{6} yrs
$H_c(\propto\Delta T)=$	2.71 m	27.1 m	0.27 km	2.7 km
	Salt			
$\Delta S=$	10 g/kg	1.0 g/kg	0.1 g/kg	0.01 g/kg
$t_c(\propto\Delta S^{-2})=$	5.1 hrs	21 days	6 yrs	600 yrs
$H_c(\propto\Delta S)=$	0.3 cm	3 cm	27.1 cm	2.71 m
	Amplitude of Convection			
	(depends only on density difference)			
$A(\propto\Delta S$ or $\Delta T)=$ (m s^{-1})	3×10^{-7}	3×10^{-8}	3×10^{-9}	3×10^{-10}
$A_\theta=$ (deg or g/kg)	6	0.6	0.06	0.006

tiate for times less than the age of the earth (about 10^6 yrs) for salinity increases as large as 10 g/kg.

Streamlines and contours of the temperature perturbation for the convective motion, Figure 8, are based on Lapwood's (1948) solution (16) of the linearized, governing equations with an upper boundary

$$w = A\left[\frac{\sin\eta\xi}{\sin\eta} + \frac{\sinh\gamma\xi}{\sinh\gamma}\right]\sin lx\sin my$$

$$v = \frac{AHm}{a^2}\left[\frac{\eta\cos\eta\xi}{\sin\eta} + \frac{\gamma\cosh\gamma\xi}{\sinh\gamma}\right]\sin lx\cos my$$

$$u = \frac{AHl}{a^2}\left[\frac{\eta\cos\eta\xi}{\sin\eta} + \frac{\gamma\cosh\gamma\xi}{\sinh\gamma}\right]\cos lx\sin my$$

16

$$\theta = \frac{A(Ra_c)^{1/2}}{K\alpha a}\left[\frac{\sin\eta\xi}{\sin\eta} - \frac{\sinh\gamma\xi}{\sinh\gamma}\right]\sin lx\sin my$$

where

$$\gamma^2 = a((Ra_c)^{1/2} + a) \qquad \xi = z/H$$

$$\eta^2 = a((Ra_c)^{1/2} - a) \qquad Ra_c = 27.1$$

$$a^2 = H^2(l^2 + m^2) \qquad a = 2.3$$

in contact with a free fluid. The amplitude, A, of convection cannot be calculated from the linearized, governing equations. Combarnous and Bories (1974) outline a method based on energy conservation that yields the amplitude of convection. The amplitude of the vertical velocity, A, is given by

$$A^2 = \frac{-K^2a^2}{H^2}\,(Ra - Ra_c)\,\frac{\int_0^1 WF\,d\xi}{\int_0^1 W^2F^2\,d\xi + \left(\int_0^1 WF\,d\xi\right)^2} \qquad 17$$

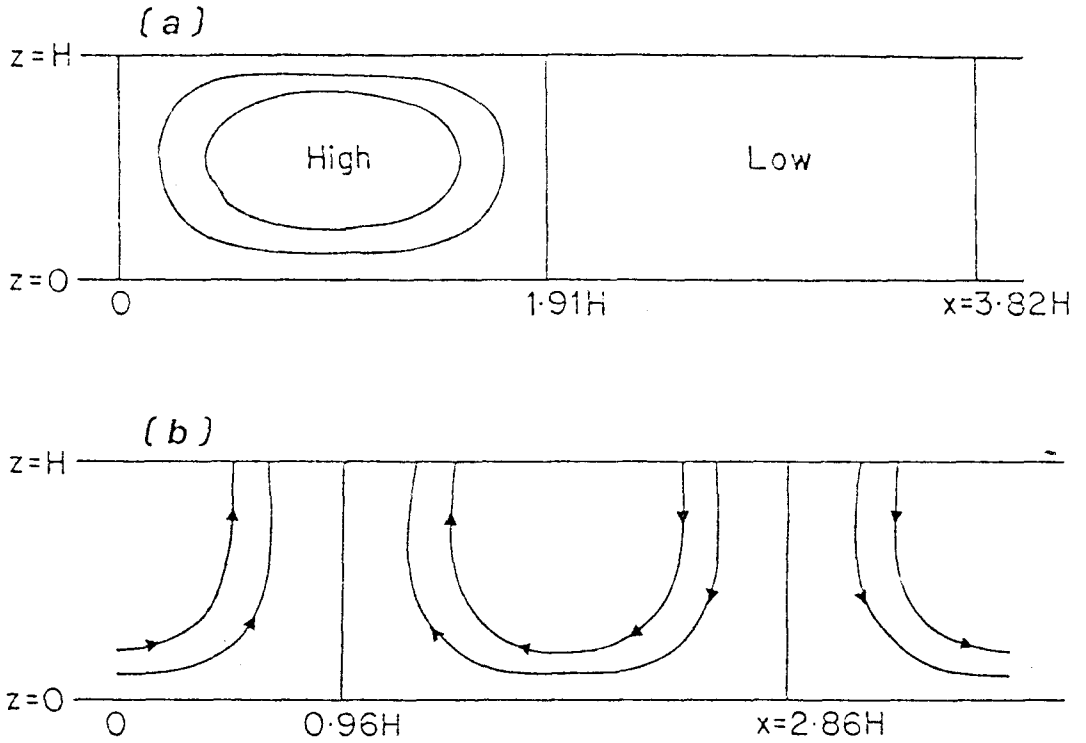

Figure 8. a. Isotherms of temperature perturbation and b. streamlines (Lapwood, 1948).

where $W = \frac{\sin\pi\xi}{\sin\pi} + \frac{\sinh\gamma\xi}{\sinh\gamma}$ and $F = \left[\frac{\partial^2}{\partial\xi^2} - a^2\right]W$

and where the quotient of intergrals evaluates to -1.35. Therefore, when convection first initiates and Ra is close to Ra_c, the amplitudes are negligible.

Initially, the depth of the convecting layer grows at a rate equal to the diffusive rate, i.e. $H=2(Kt)^{1/2}$. Numerical modeling of penetrative convection for times greater than $4t_c$ shows that linear theory breaks down and blobs of dense fluid begin to sink through the stable layer (Elder, 1968). Therefore equation 16, which is based on Lapwood's linear analysis (1948), is good only for times less than $4t_c$. It is instructive to calculate the amplitudes of the vertical velocity and temperature perturbation at $t=4t_c$ using equation (18).

$$A^2(4t_c) = \frac{1.35\ Ra_c k^2 a^2}{4H_c^2} \qquad A_\theta(4t_c) = \frac{A(4t_c)(Ra_c)^{1/2}}{K\alpha a} \qquad 18$$

I have included these values in Table 1. The growth of the velocity amplitude is given by

$$\left[\frac{A}{A(4t_c)}\right]^2 = 4\left[\left[\frac{t_c}{t}\right]^{1/2} - \frac{t_c}{t}\right] \qquad 20$$

which is plotted in Figure 9.

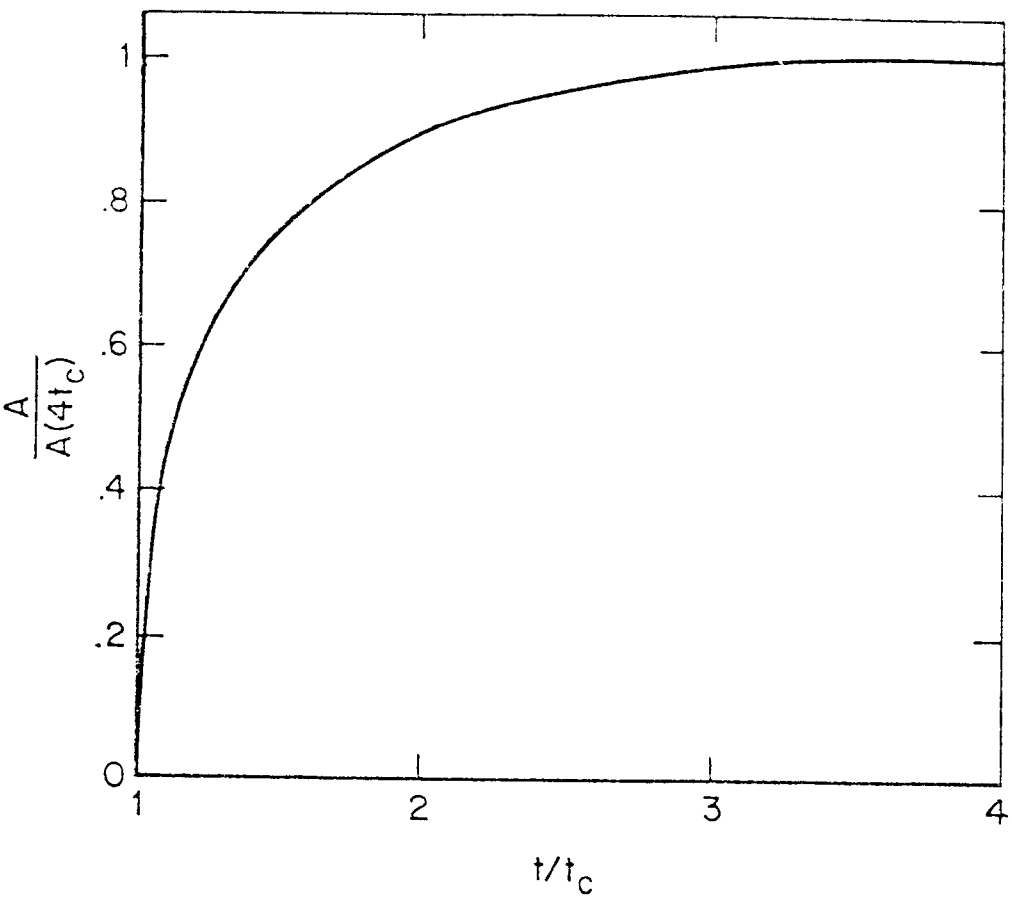

Figure 9. Time dependence of convective velocity amplitude (A) normalized to the amplitude at $t=4t_c$.

Implications for Increased Solute Transport

The increase in fluxes of solutes due to penetrative convection cannot be readily estimated. Convecting systems undergoing circular motion have no net water transport across any horizontal surface and net transport of solutes occurs only if vertical gradients in concentration exist. This implies that the increase in solute transport will depend on the strength of the solute sink (or source) in the sediments. To predict the increased transport of solutes across the sediment surface, the time-dependent diagenetic equation would have to be integrated numerically using the time-dependent velocity field. This calculation is beyond the scope of this dissertation. However, some generalizations about the effect of convection on solute distributions can be made:

1. Convection introduces periodic, lateral heterogeneity with length scales on the order of the depth of the convecting layer. Different vertical profiles would be obtained depending on whether the sampling was in an area of recharge or discharge (flow into or out of the sediments, respectively).

2. Penetrative convection is time-dependent and vertical profiles would change as the convecting layer penetrates the stable layer.

3. Although the net increase in solute flux cannot be easily estimated, note that solute diffusivities are typically 10^{-2}-10^{-3} time the thermal diffusivity and, therefore, they are more susceptible than heat to increased transport by convection.

APPENDIX A

The following figures are the recorded temperatures from Lake 227 from each probe. I have given the water depth at the top center of each figure. The horizontal axis is time which is labelled by date, hour and minute (CST), and the vertical axis is temperature in deg C. The temperature range in each figure is 5 deg. I have indicated the thermistor depth for each time series. I numbered the figures so that each time period that was not interrupted by a cassette change has the same figure number; I used lower case letters to indicate data which was uninterrupted for more than 24 hours.

I have not included tables of the time series of temperature because several volumes would be required to hold all of it. I have the time series available on tape for anyone interested in looking at the temperatures in detail.

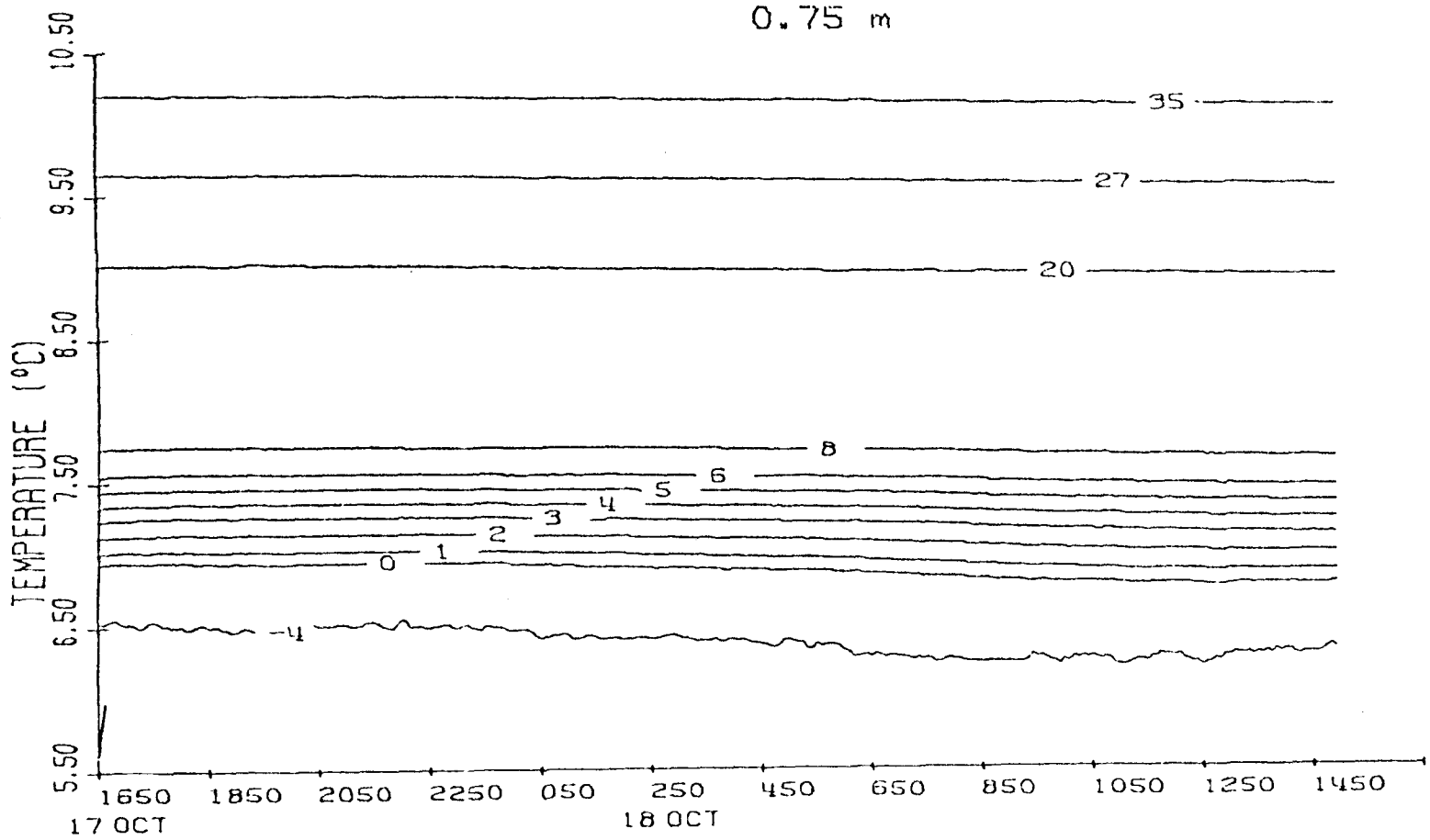
0.75 m
TEMPERATURE (°C)
10.50
9.50
8.50
7.50
6.50
5.50
35
27
20
8
6
5
4
3
2
1
0
-1
1650
1850
2050
2250
050
250
450
650
850
1050
1250
1450
17 OCT
18 OCT

Figure A.1

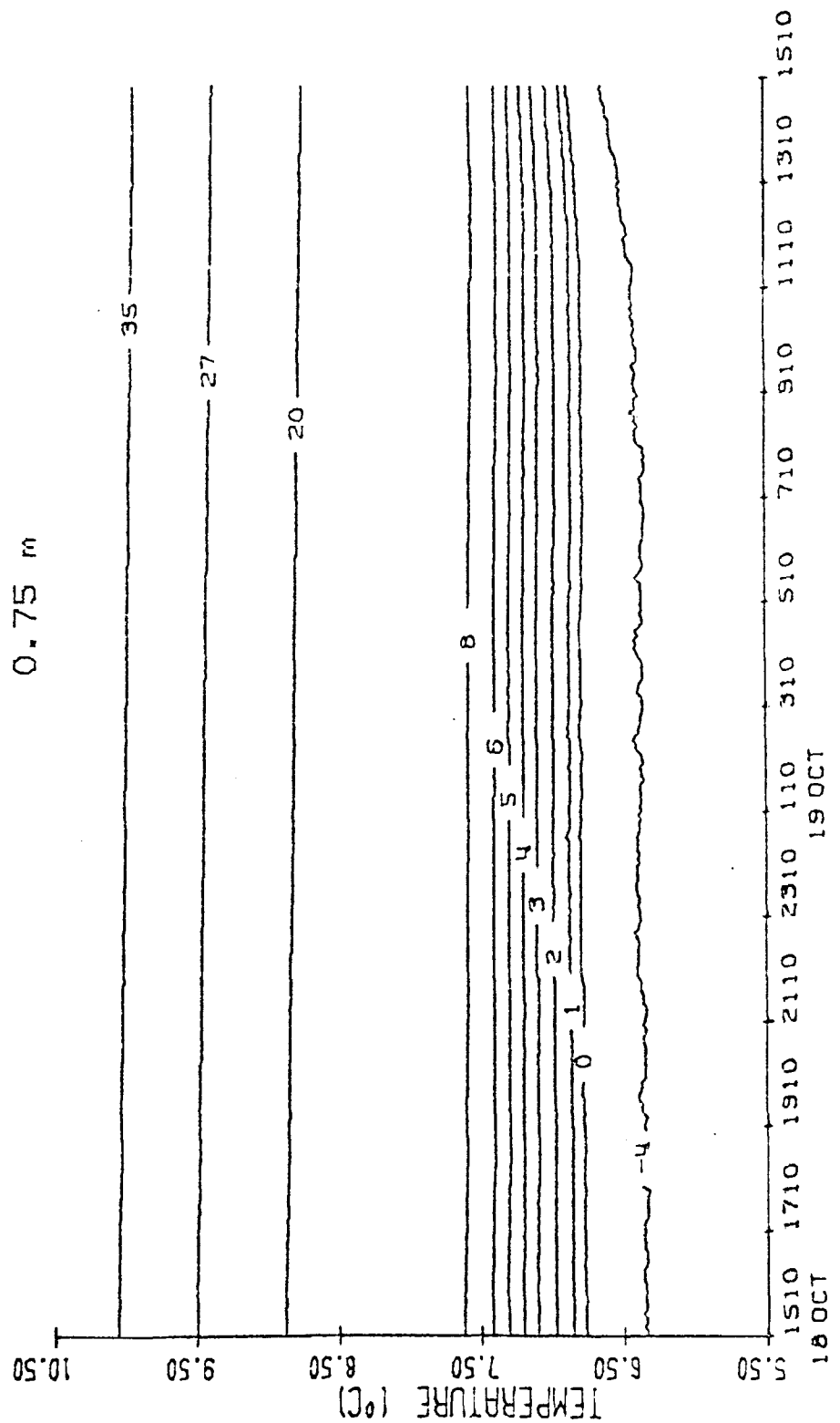
0.75 m
35
27
20
8
6
5
4
3
2
1
0
-4
TEMPERATURE (°C)
10.50
9.50
8.50
7.50
6.50
5.50
1510
1710
1910
2110
2310
110
310
510
710
910
1110
1310
1510
18 OCT
19 OCT

Figure A.2a

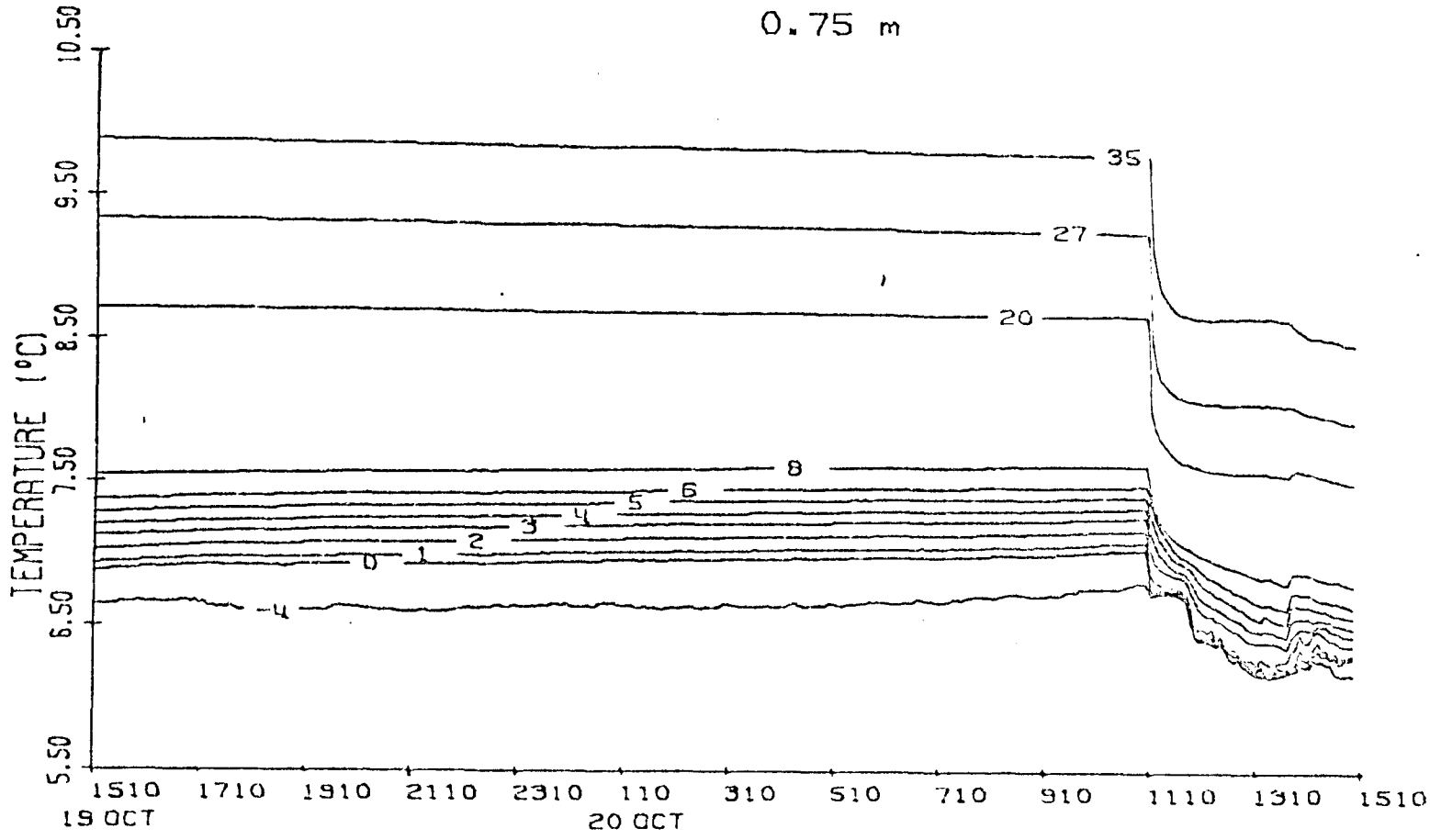
0.75 m
TEMPERATURE (°C)
10.50
9.50
8.50
7.50
6.50
5.50
35
27
20
8
6
5
4
3
2
1
0
-4
1510
1710
1910
2110
2310
110
310
510
710
910
1110
1310
1510
19 OCT
20 OCT

Figure A.26

TEMPERATURE (°C)
10.50
9.50
8.50
7.50
6.50
5.50
1510
1710
1910
2110
2310
110
20 OCT
21 OCT

Figure A.2c

0.75 m

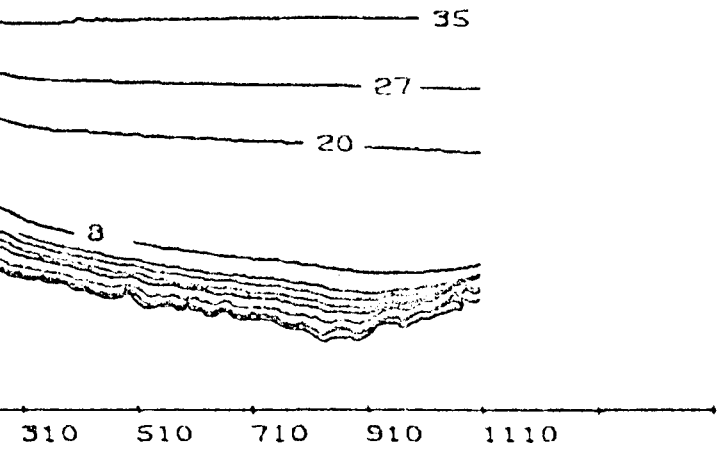

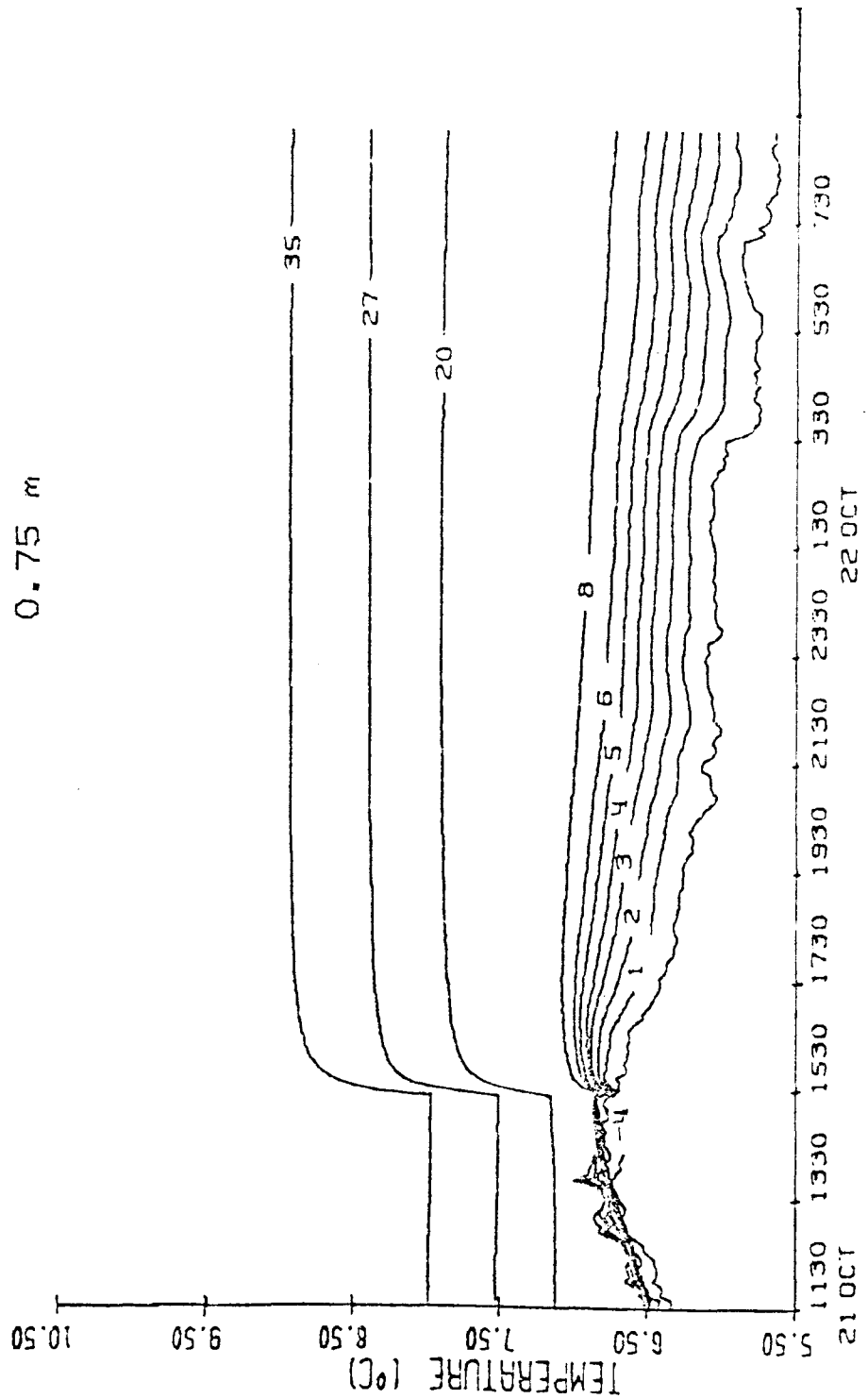
0.75 m
35
27
20
8
6
5
4
3
2
1
-1
TEMPERATURE (°C)
10.50
9.50
8.50
7.50
6.50
5.50
1130
1330
1530
1730
1930
2130
2330
130
330
530
730
21 OCT
22 OCT

Figure A.3

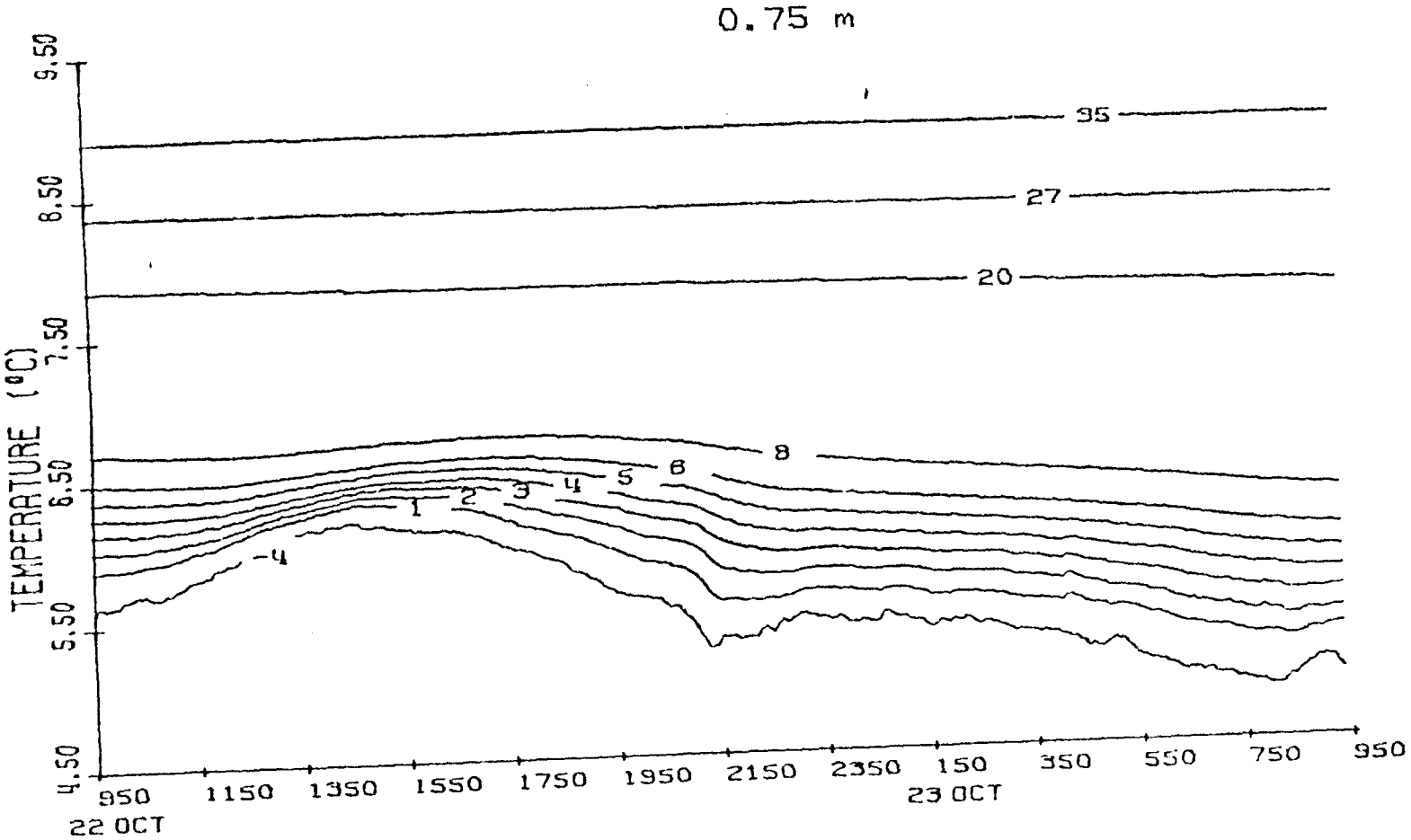
0.75 m
TEMPERATURE (°C)
9.50
8.50
7.50
6.50
5.50
4.50
95
27
20
8
6
5
4
3
2
1
-4
950
1150
1350
1550
1750
1950
2150
2350
150
350
550
750
950
22 OCT
23 OCT

Figure A.44

Figure A.45

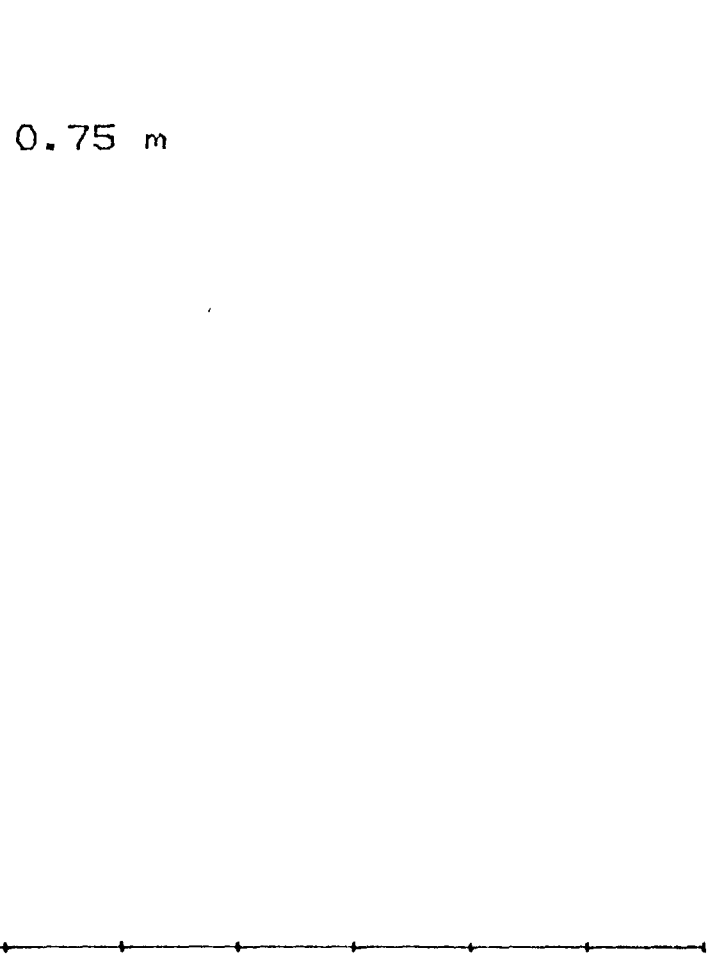
0.75 m

TEMPERATURE (°C)
4.00
5.00
6.00
7.00
8.00
9.00
23 OCT
15HS
17HS
19HS
21HS
23HS
24 OCT
1HS
3HS
5HS
7HS
9HS
11HS
13HS
1
2
3
4
5
6
8
20
27
35
0.75 m

Figure A.5

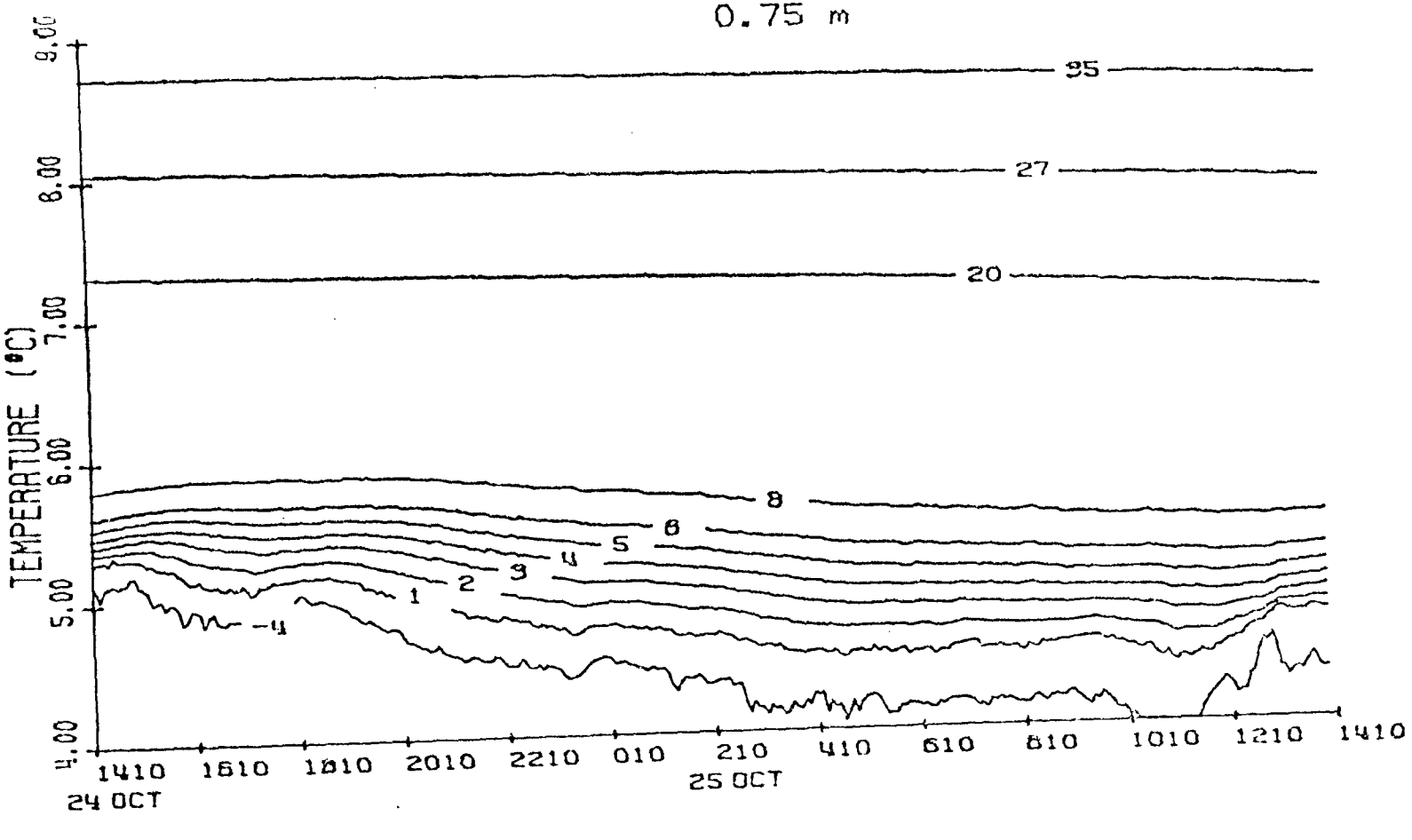
0.75 m
9.00
8.00
7.00
6.00
5.00
4.00
TEMPERATURE (°C)
95
27
20
8
6
5
4
3
2
1
-4
1410
1610
1810
2010
2210
010
210
410
610
810
1010
1210
1410
24 OCT
25 OCT

Figure A.5

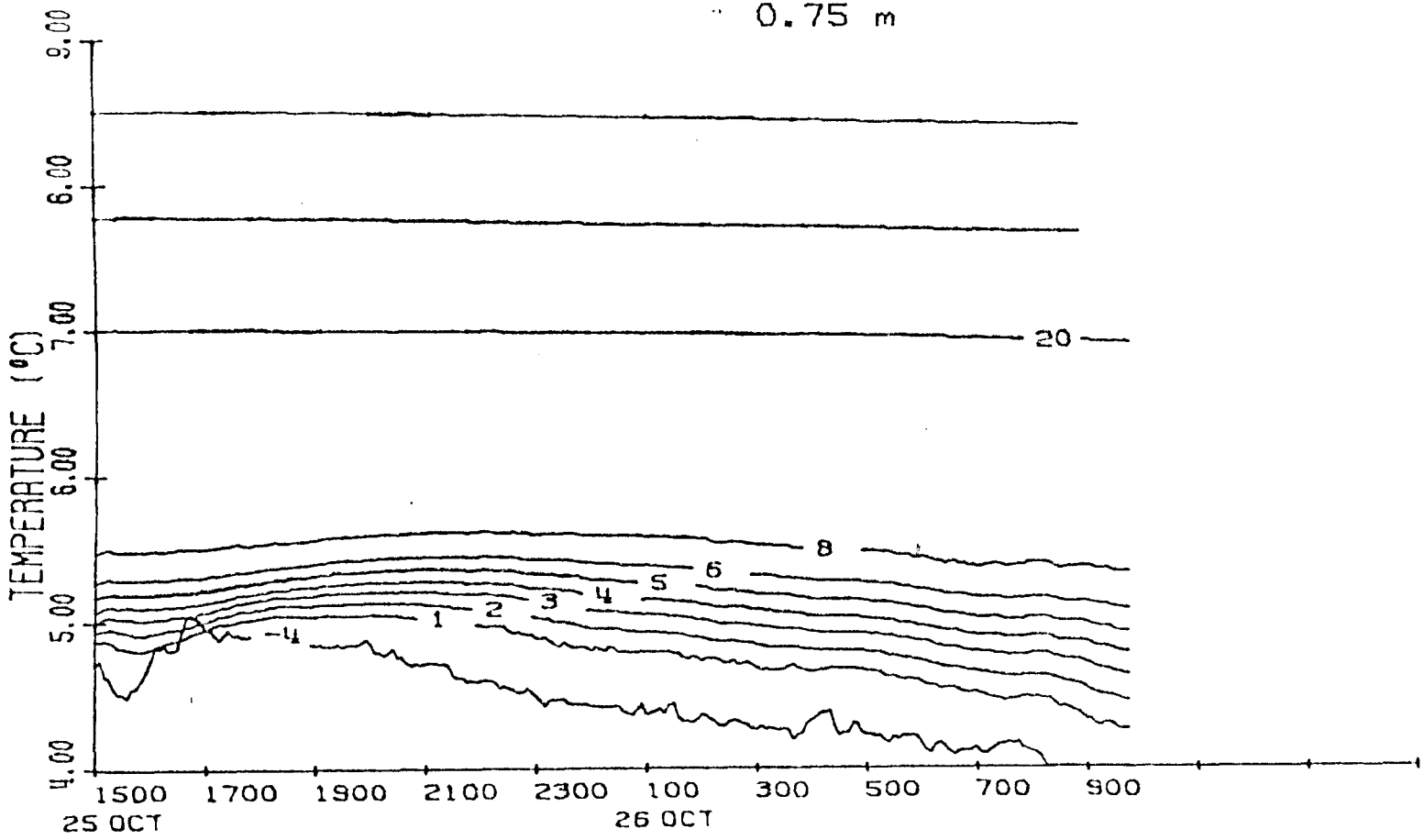
0.75 m
TEMPERATURE (°C)
9.00
8.00
7.00
6.00
5.00
4.00
20
8
6
5
4
3
2
1
-4
1500
1700
1900
2100
2300
100
300
500
700
900
25 OCT
26 OCT

Figure A.7

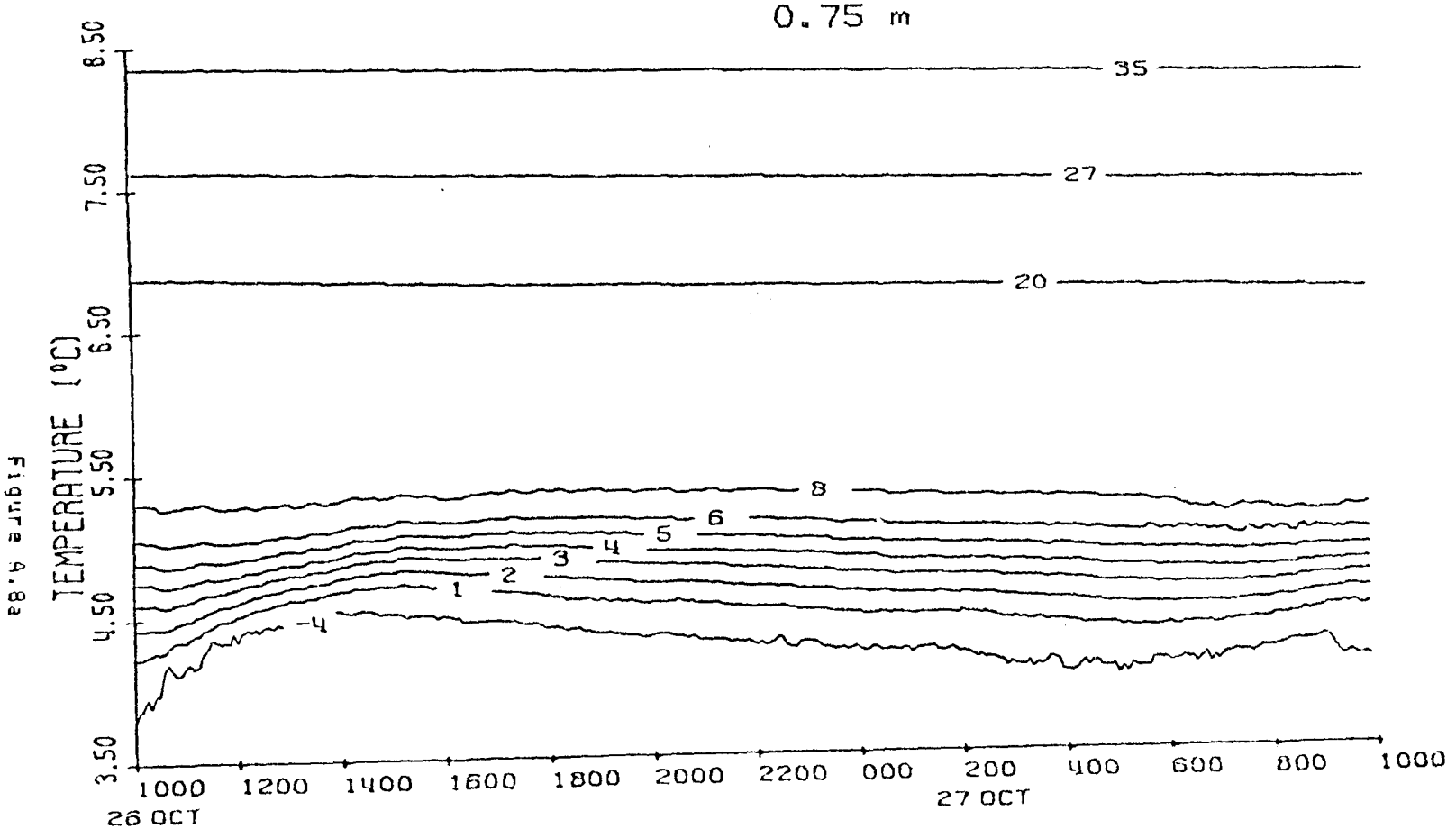
0.75 m
TEMPERATURE (°C)
8.50
7.50
6.50
5.50
4.50
3.50
35
27
20
8
6
5
4
3
2
1
-4
1000
1200
1400
1600
1800
2000
2200
000
200
400
600
800
1000
26 OCT
27 OCT

Figure 4.83

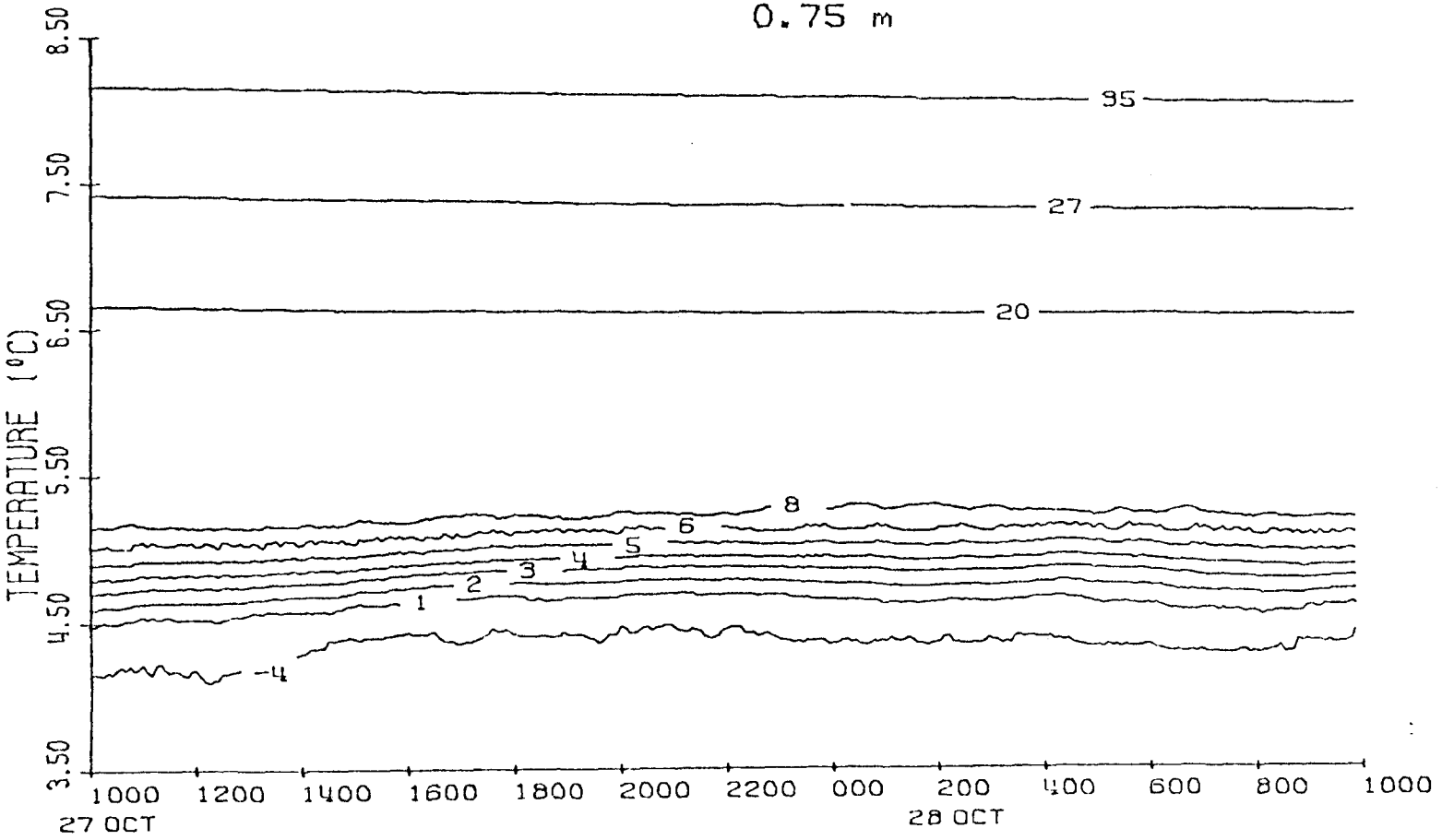
0.75 m
TEMPERATURE (°C)
8.50
7.50
6.50
5.50
4.50
3.50
95
27
20
8
6
5
4
3
2
1
-4
1000
1200
1400
1600
1800
2000
2200
000
200
400
600
800
1000
27 OCT
28 OCT

Figure A.8b

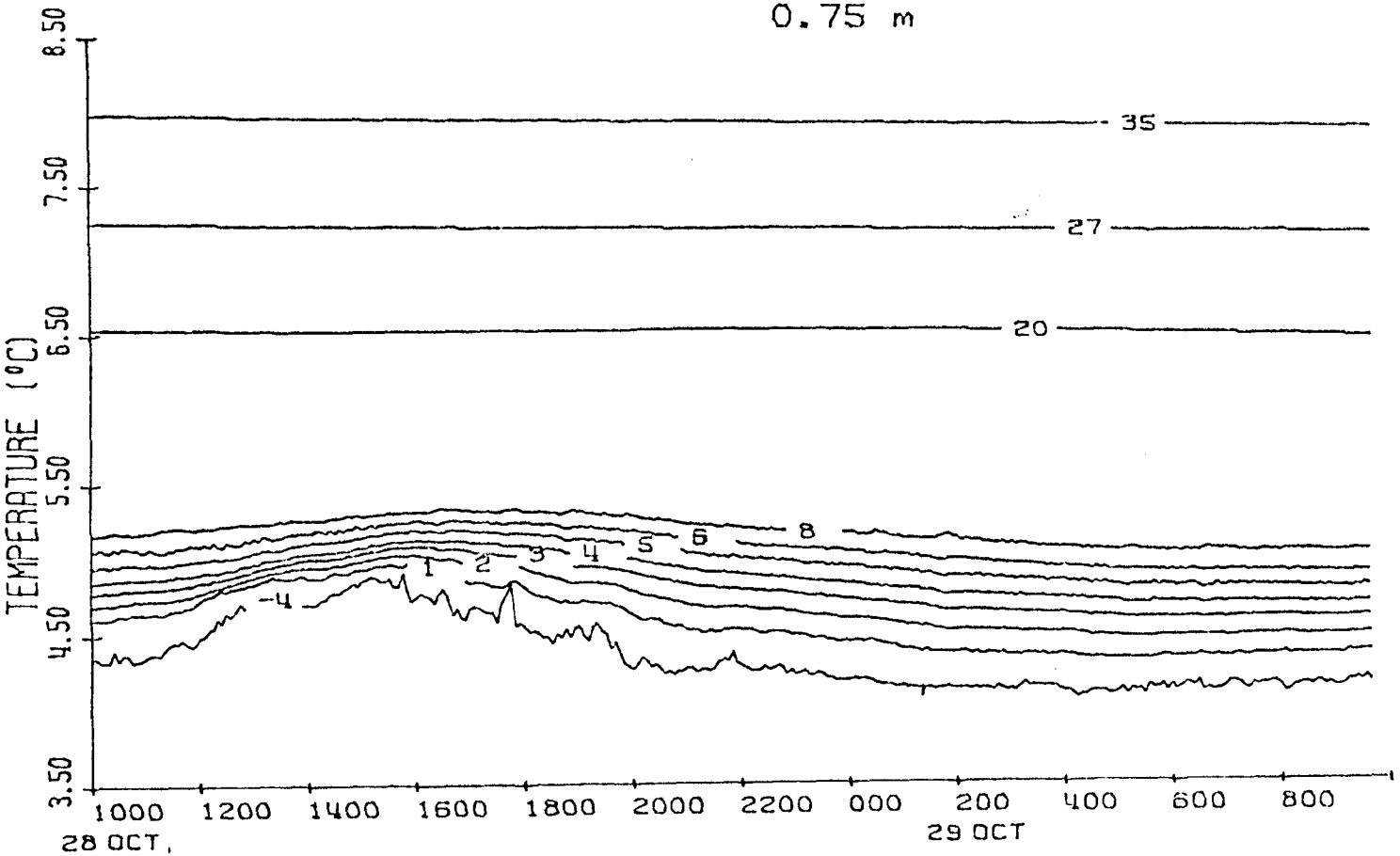
0.75 m
TEMPERATURE (°C)
8.50
7.50
6.50
5.50
4.50
3.50
35
27
20
8
6
5
4
3
2
1
-4
1000
1200
1400
1600
1800
2000
2200
000
200
400
600
800
28 OCT.
29 OCT

Figure A.8c

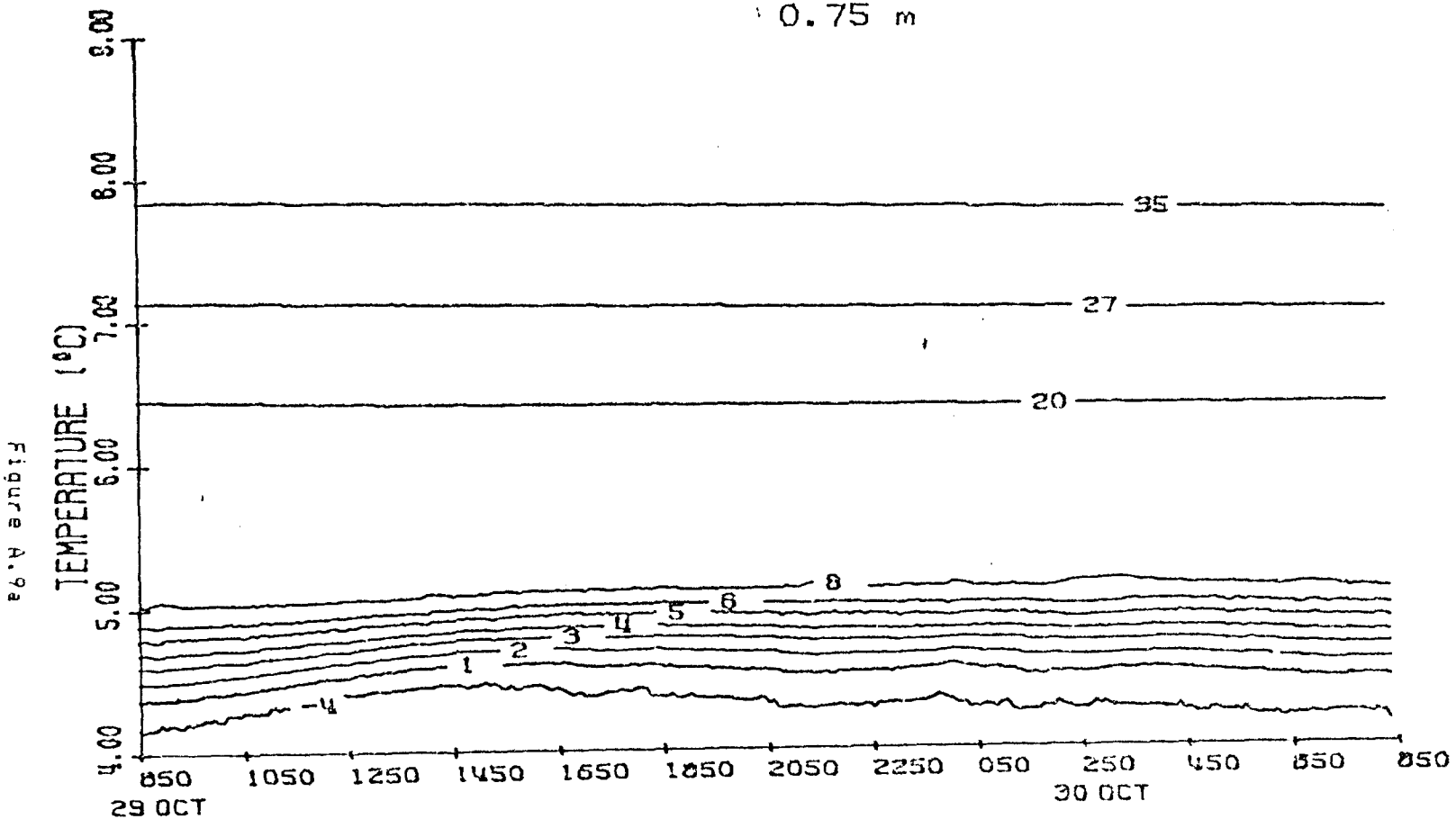
0.75 m
TEMPERATURE (°C)
9.00
8.00
7.00
6.00
5.00
4.00
35
27
20
8
6
5
4
3
2
1
-4
850
1050
1250
1450
1650
1850
2050
2250
050
250
450
650
850
29 OCT
30 OCT

Figure A.9a

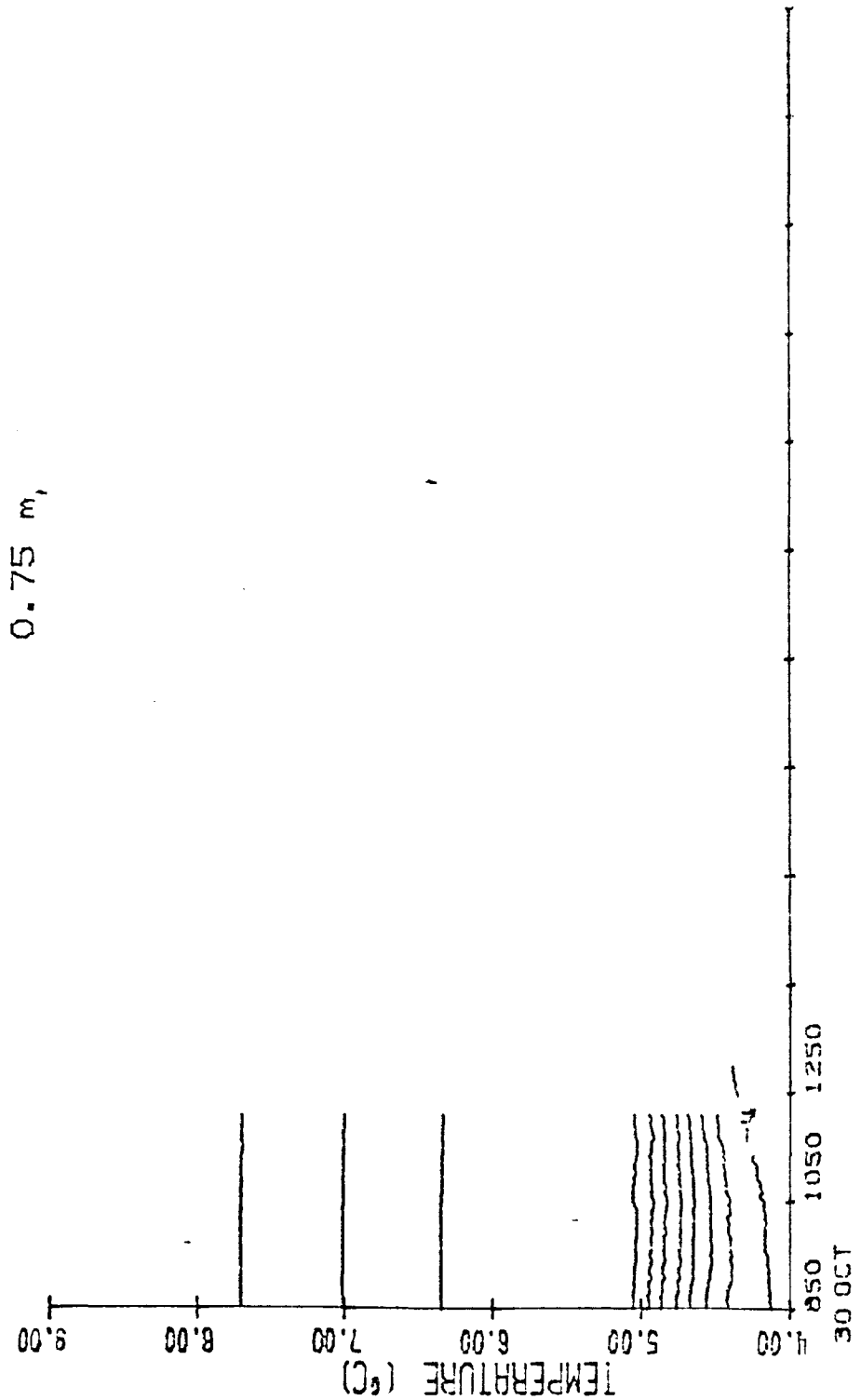
0.75 m
TEMPERATURE (°C)
4.00
5.00
6.00
7.00
8.00
9.00
850
1050
1250
30 OCT

Figure A.9b

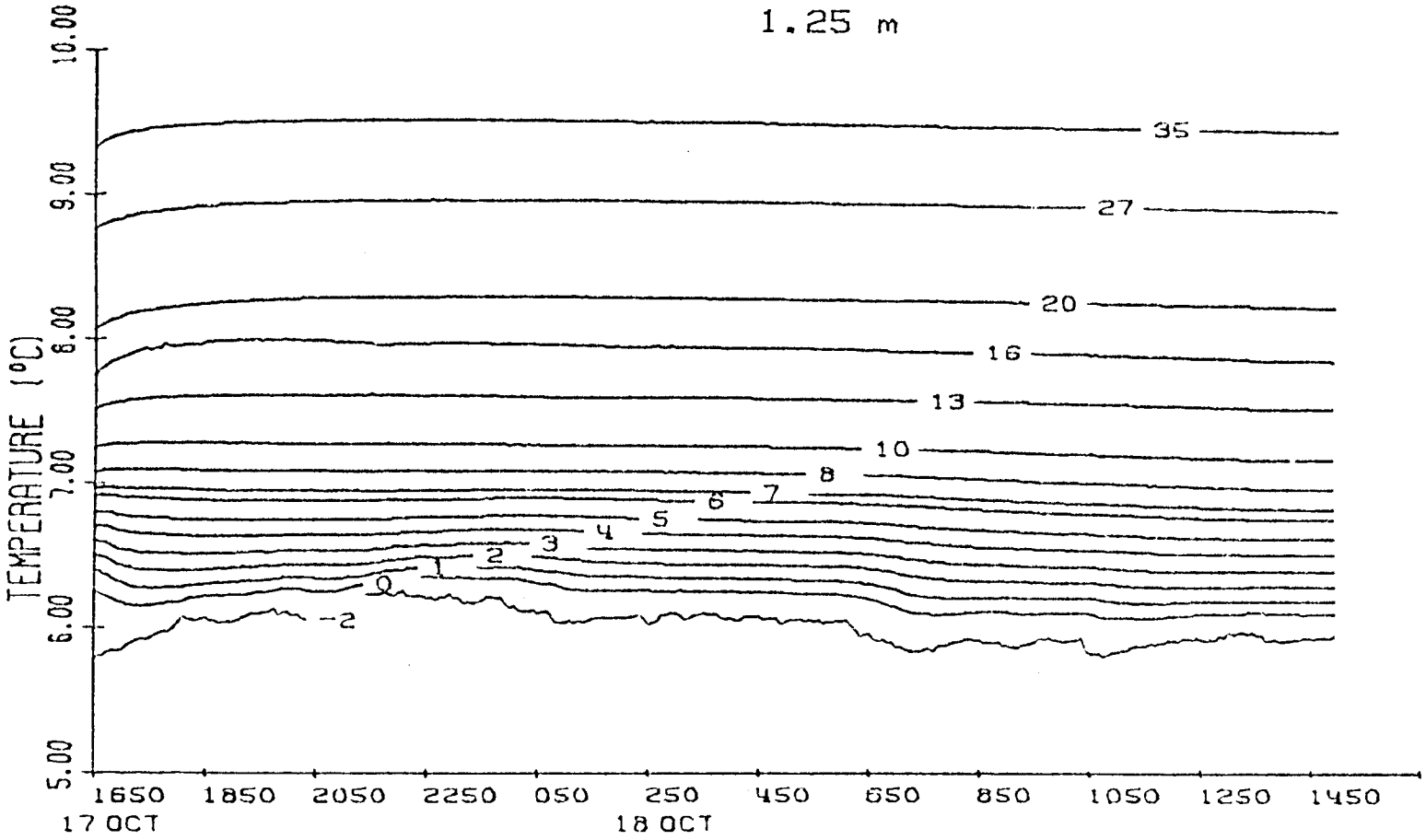
1.25 m
TEMPERATURE (°C)
10.00
9.00
8.00
7.00
6.00
5.00
35
27
20
16
13
10
8
7
6
5
4
3
2
1
0
-2
1650
1850
2050
2250
050
250
450
650
850
1050
1250
1450
17 OCT
18 OCT

Figure A.10

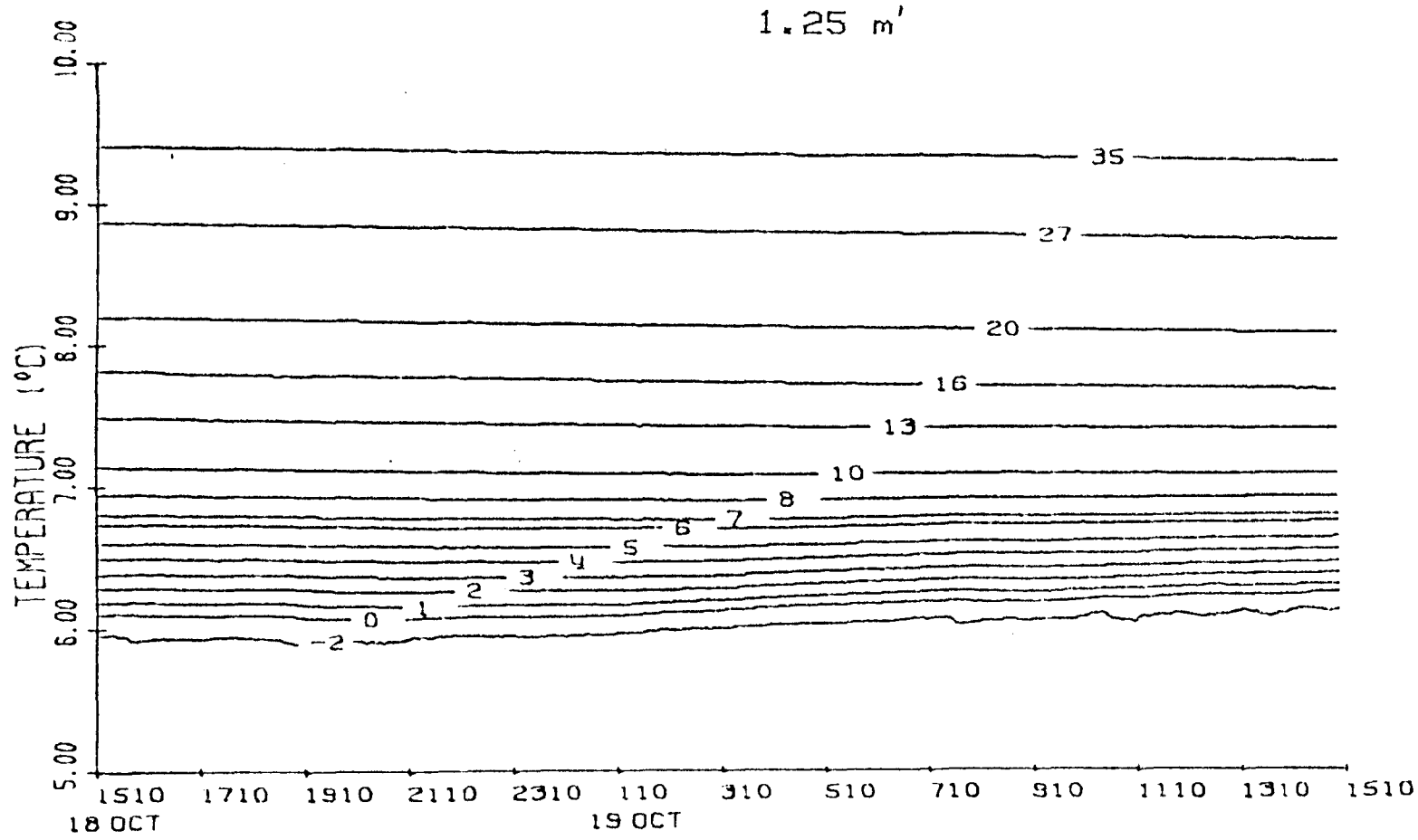
1.25 m'
TEMPERATURE (°C)
10.00
9.00
8.00
7.00
6.00
5.00
35
27
20
16
13
10
8
7
6
5
4
3
2
1
0
-2
1510
1710
1910
2110
2310
110
310
510
710
910
1110
1310
1510
18 OCT
19 OCT

Figure A.11a

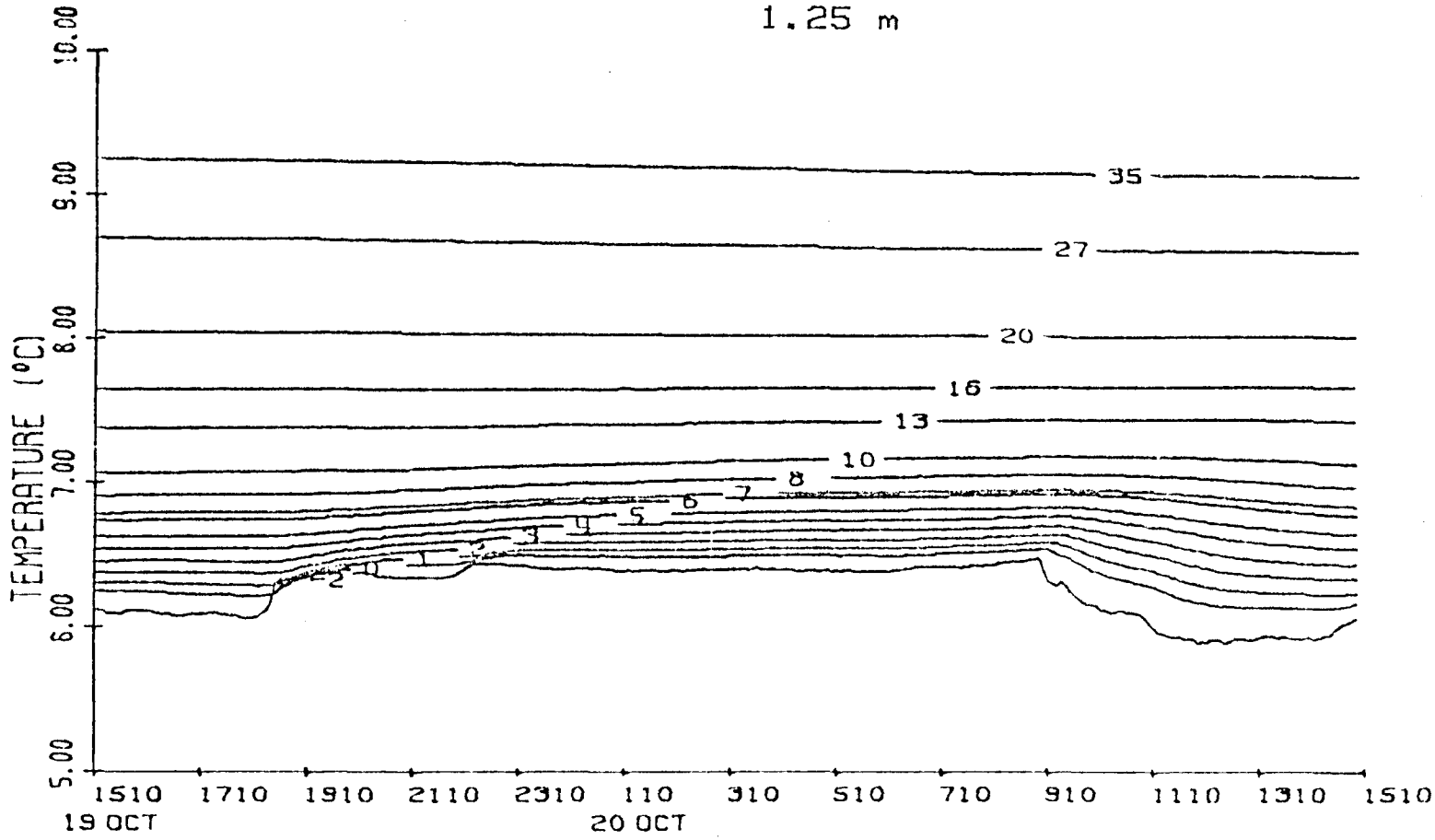
1.25 m
TEMPERATURE (°C)
10.00
9.00
8.00
7.00
6.00
5.00
35
27
20
16
13
10
8
7
6
5
4
3
2
1
0
1510
1710
1910
2110
2310
110
310
510
710
910
1110
1310
1510
19 OCT
20 OCT

Figure A.11b

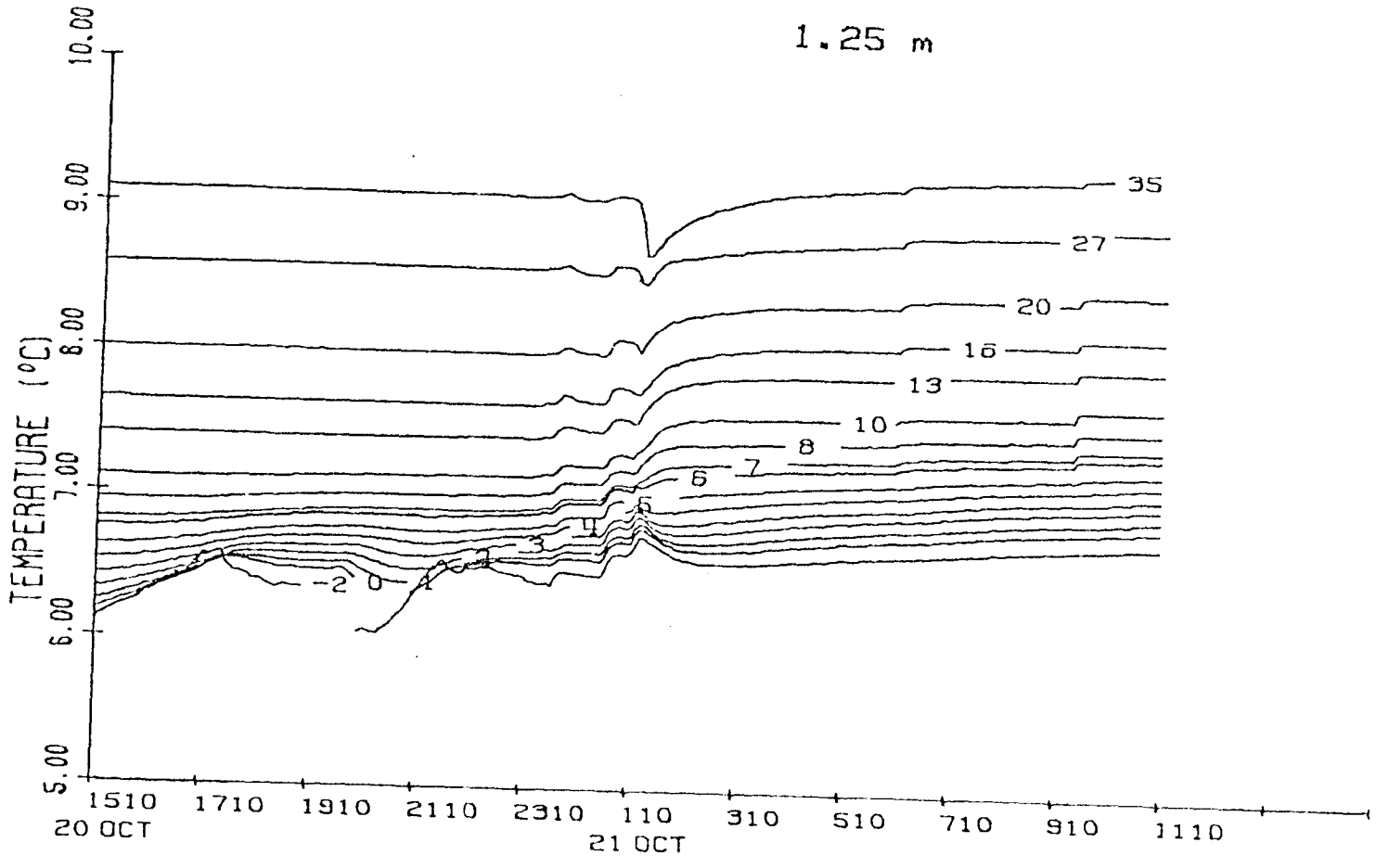
1.25 m
TEMPERATURE (°C)
10.00
9.00
8.00
7.00
6.00
5.00
35
27
20
16
13
10
8
7
6
5
4
3
2
-2
0
1510
1710
1910
2110
2310
110
310
510
710
910
1110
20 OCT
21 OCT

Figure A.11c

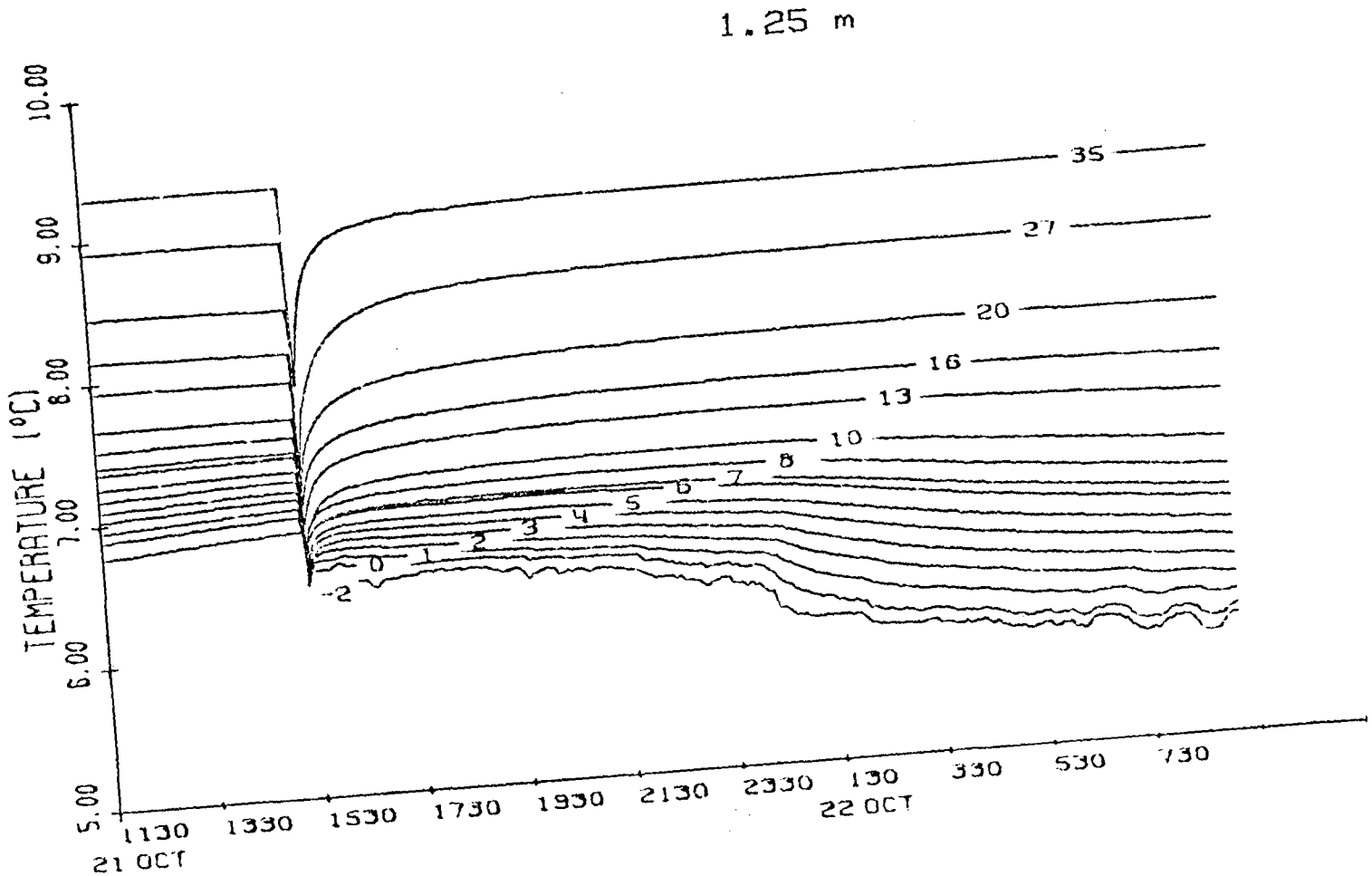
1.25 m
TEMPERATURE (°C)
10.00
9.00
8.00
7.00
6.00
5.00
35
27
20
16
13
10
8
7
6
5
4
3
2
1
0
-2
1130
1330
1530
1730
1930
2130
2330
130
330
530
730
21 OCT
22 OCT

Figure A.12

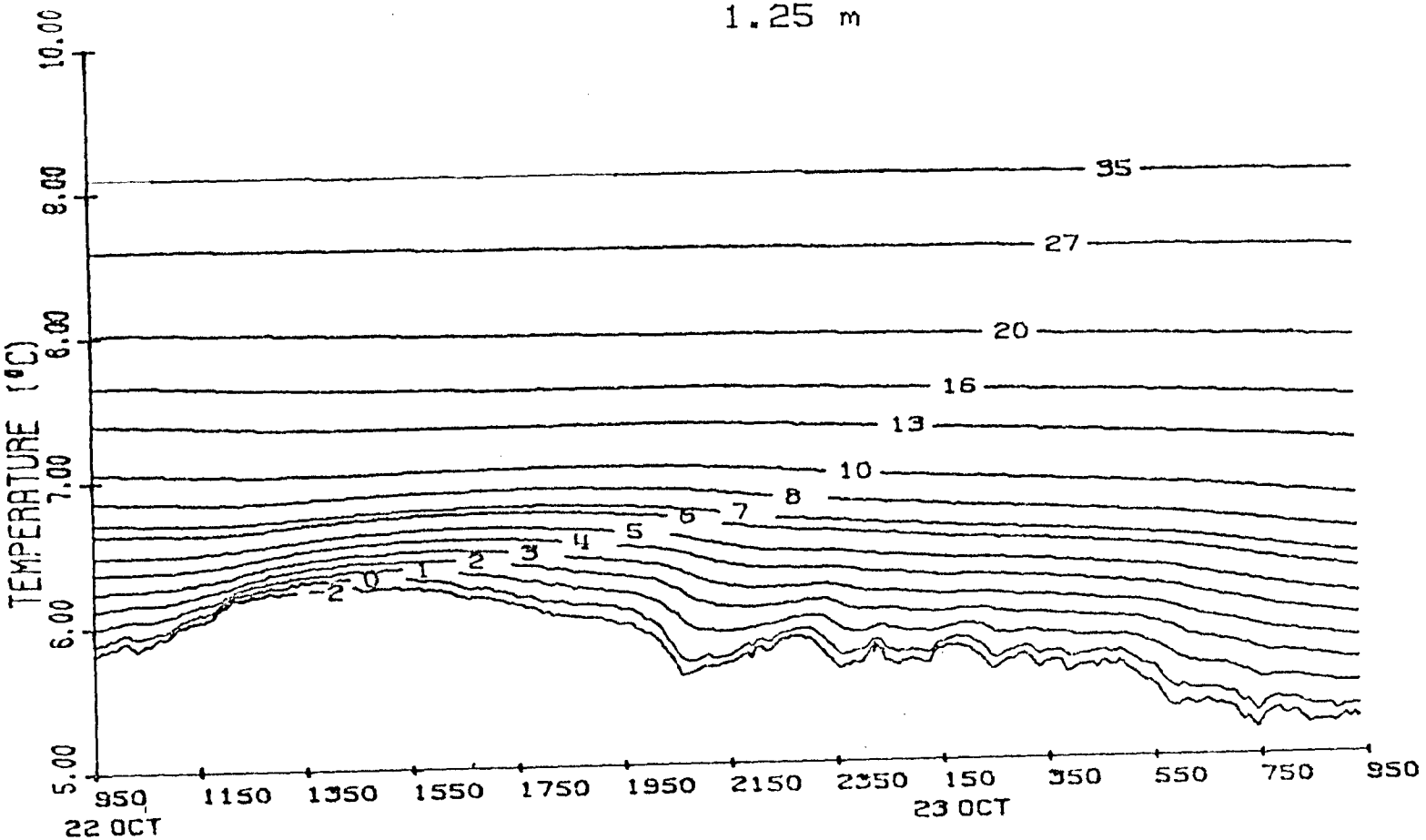
1.25 m
TEMPERATURE (°C)
10.00
8.00
8.00
7.00
6.00
5.00
35
27
20
16
13
10
8
7
6
5
4
3
2
1
0
-2
950
1150
1350
1550
1750
1950
2150
2350
150
350
550
750
950
22 OCT
23 OCT

Figure A.13a

Figure A.13b

1.25 m

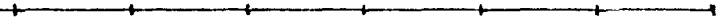

TEMPERATURE (°C)
4.50
5.50
6.50
7.50
8.50
9.50
23 OCT
15hS
17hS
19hS
21hS
23hS
24 OCT
1hS
3hS
5hS
7hS
9hS
11hS
13hS
-2
0
1
2
3
4
5
6
7
8
10
13
16
20
27
35
1.25 m

Figure A.14

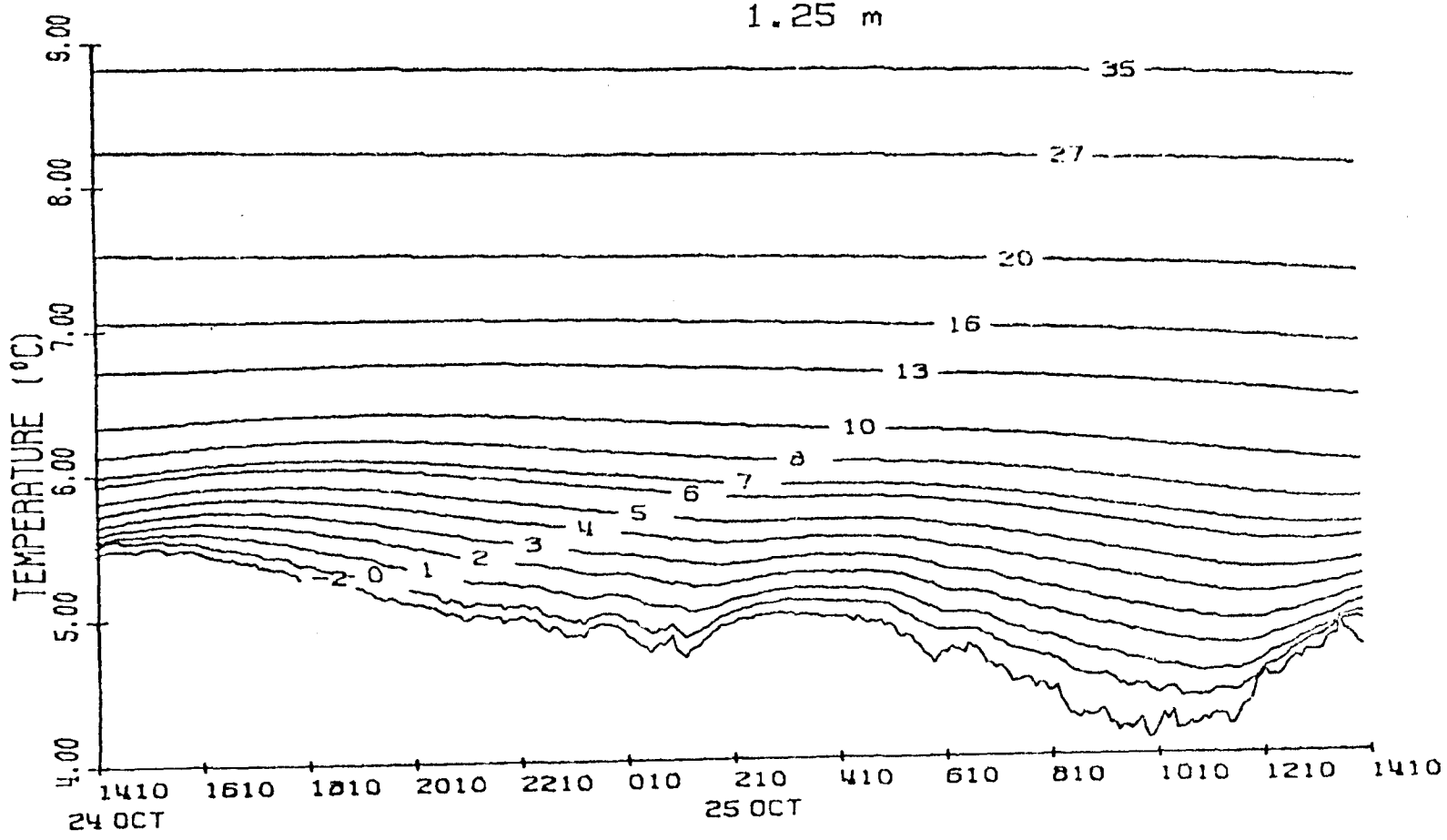
1.25 m
TEMPERATURE (°C)
9.00
8.00
7.00
6.00
5.00
4.00
35
27
20
16
13
10
8
7
6
5
4
3
2
1
0
-2
1410
1610
1810
2010
2210
010
210
410
610
810
1010
1210
1410
24 OCT
25 OCT

Figure A.15

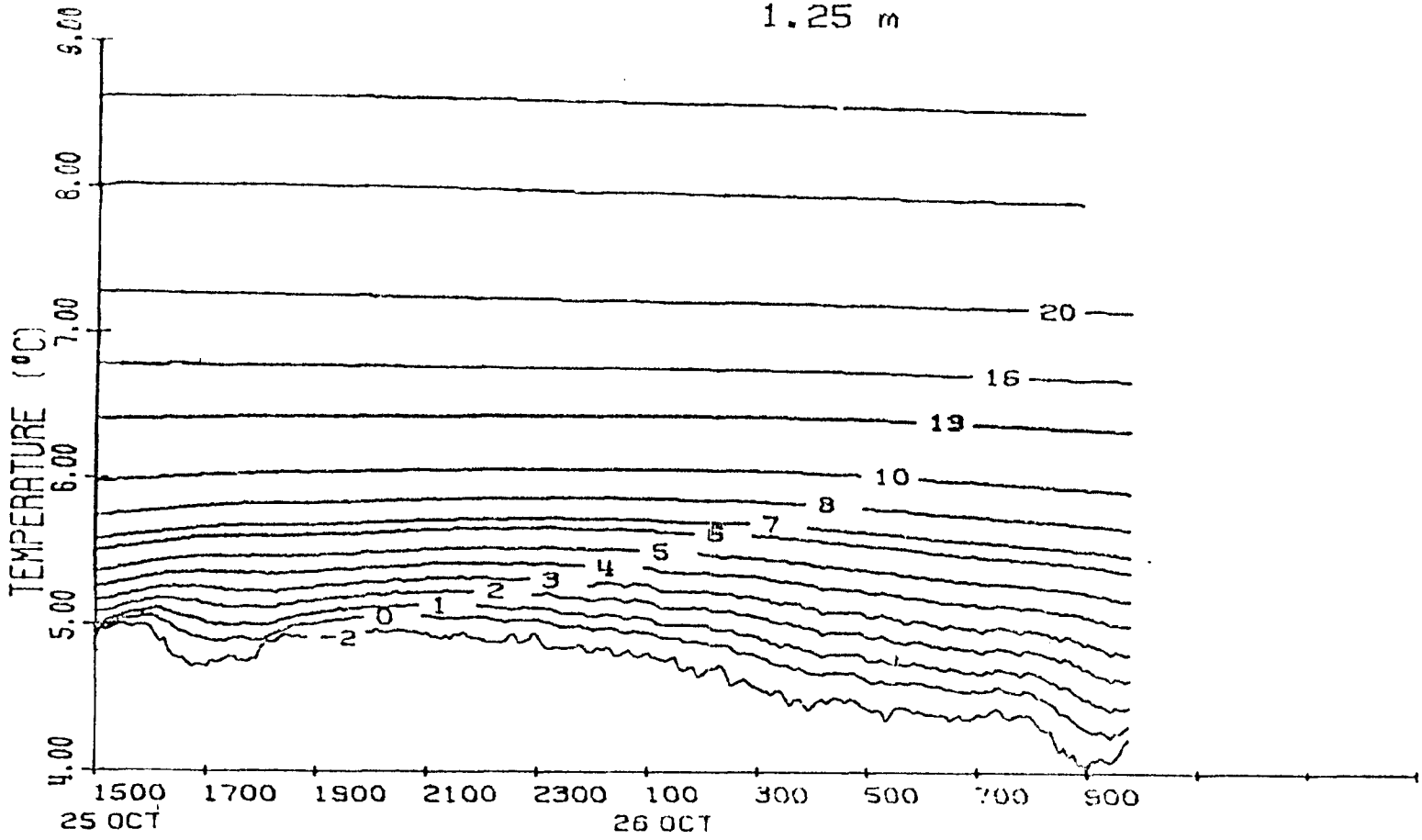
1.25 m
TEMPERATURE (°C)
9.00
8.00
7.00
6.00
5.00
4.00
20
16
13
10
8
7
6
5
4
3
2
1
0
-2
1500
1700
1900
2100
2300
100
300
500
700
900
25 OCT
26 OCT

Figure A.14

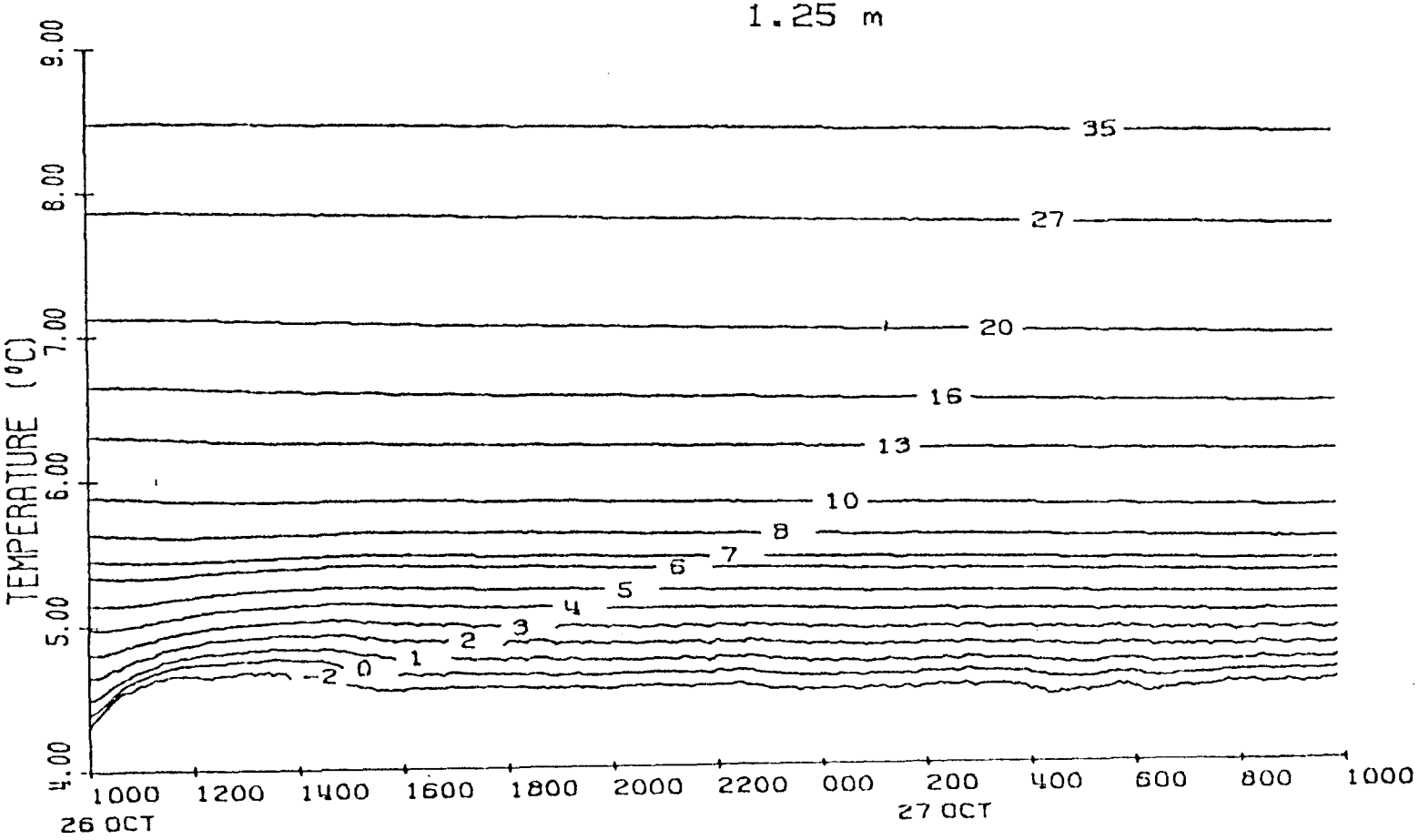
1.25 m
TEMPERATURE (°C)
9.00
8.00
7.00
6.00
5.00
4.00
35
27
20
16
13
10
8
7
6
5
4
3
2
1
0
-2
1000
1200
1400
1600
1800
2000
2200
000
200
400
600
800
1000
26 OCT
27 OCT

Figure A.17a

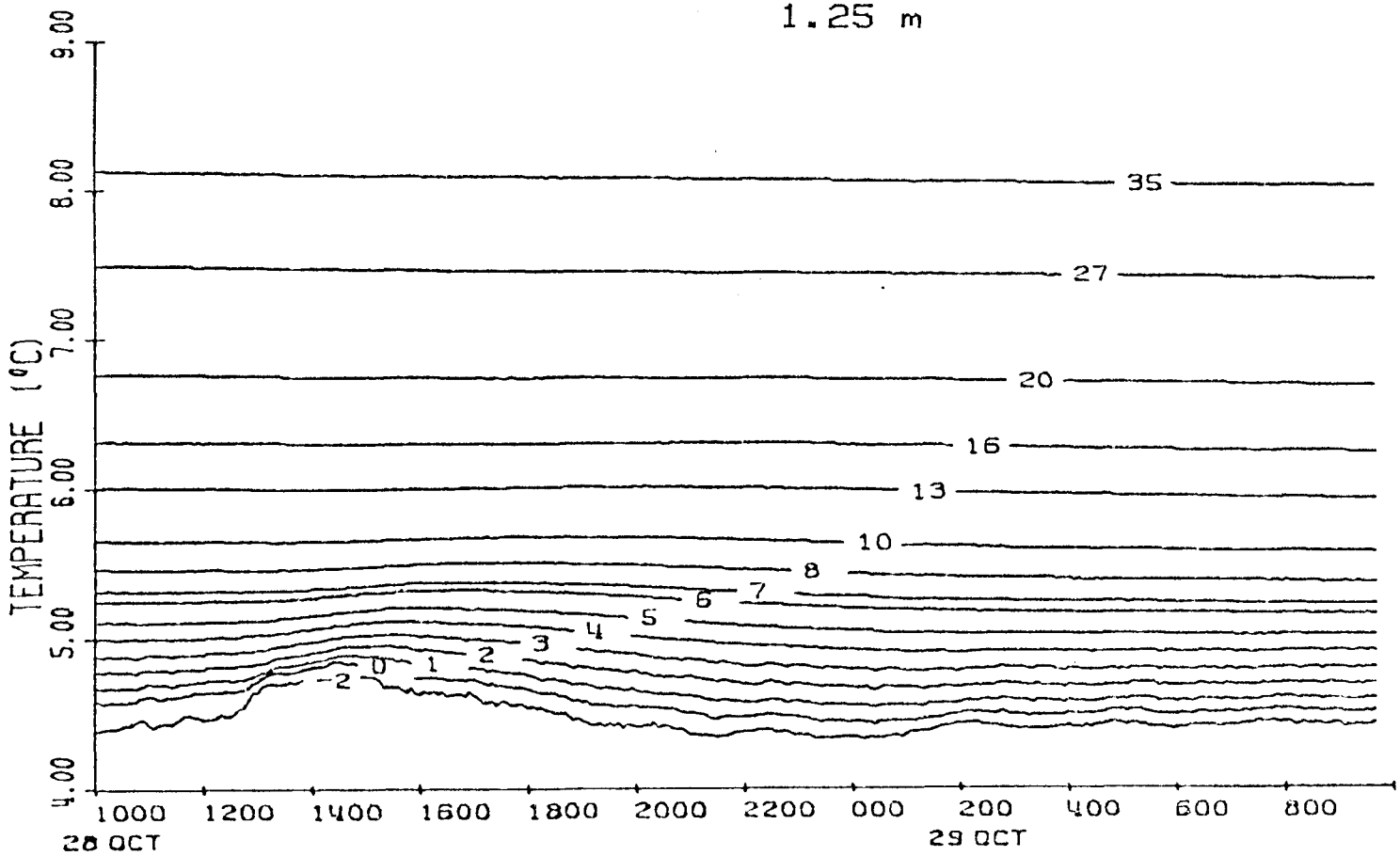
1.25 m
TEMPERATURE (°C)
9.00
8.00
7.00
6.00
5.00
4.00
35
27
20
16
13
10
8
7
6
5
4
3
2
1
0
-2
1000
1200
1400
1600
1800
2000
2200
000
200
400
600
800
28 OCT
29 OCT

Figure A.17c

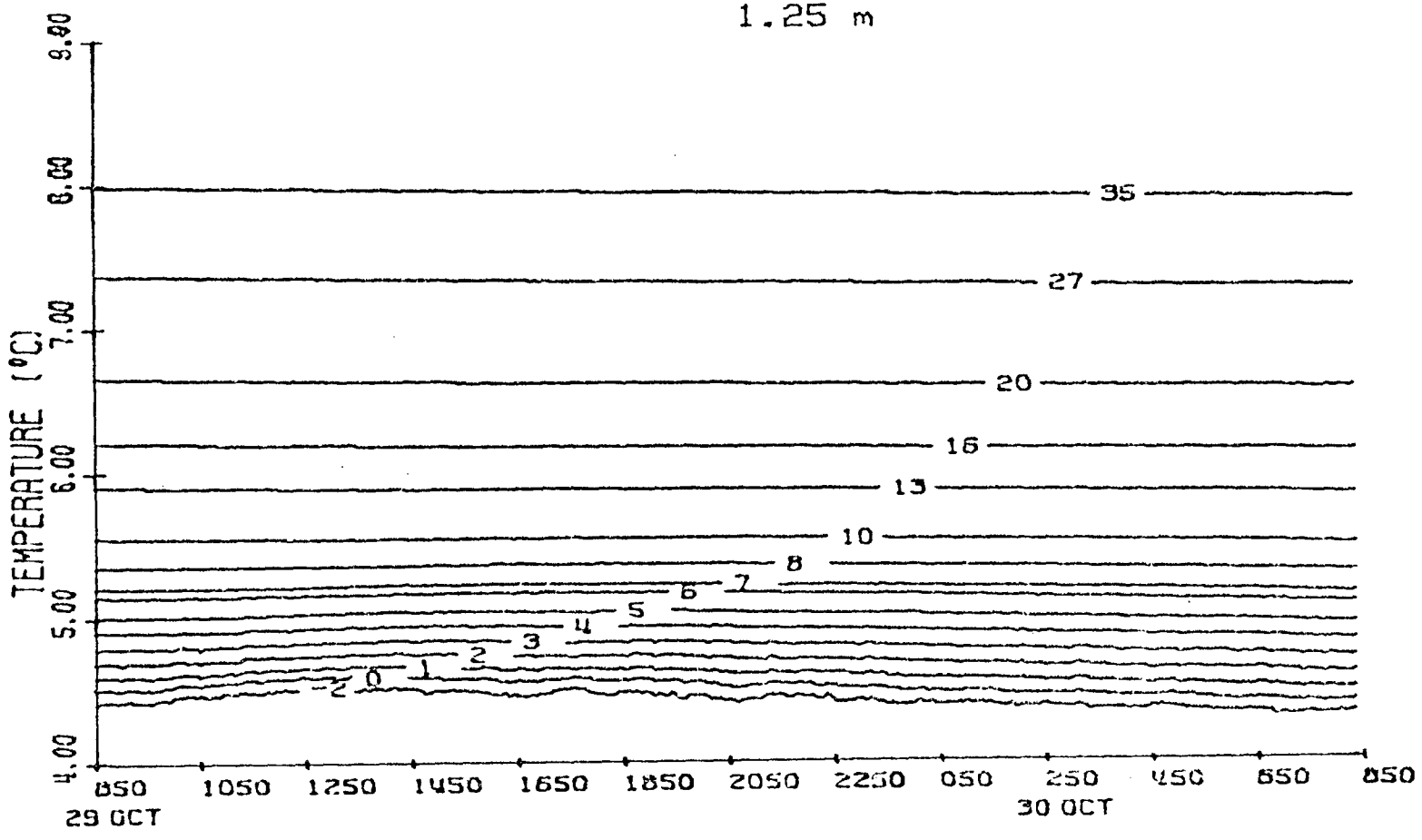
1.25 m
TEMPERATURE (°C)
9.00
8.00
7.00
6.00
5.00
4.00
35
27
20
16
13
10
8
7
6
5
4
3
2
1
0
-2
850
1050
1250
1450
1650
1850
2050
2250
050
250
450
650
850
29 OCT
30 OCT

Figure A.18a

Figure A.186

1.25 m

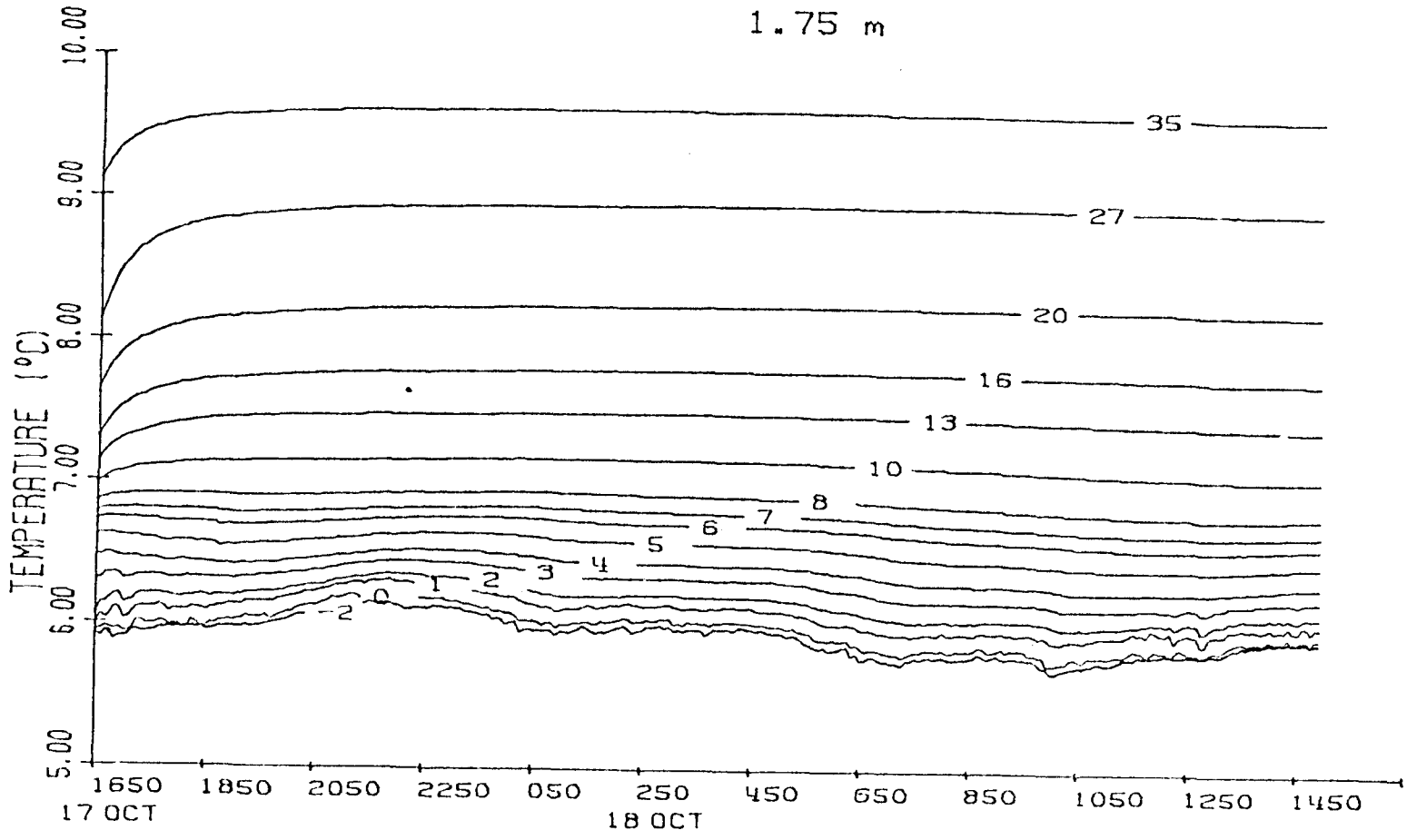
1.75 m
TEMPERATURE (°C)
10.00
9.00
8.00
7.00
6.00
5.00
35
27
20
16
13
10
8
7
6
5
4
3
2
1
0
-2
1650
1850
2050
2250
050
250
450
650
850
1050
1250
1450
17 OCT
18 OCT

Figure A.19

1.75 m
TEMPERATURE (°C)
5.50
6.50
7.50
8.50
9.50
10.50
18 OCT
19 OCT
1510
1710
1910
2110
2310
110
310
510
710
910
1110
1310
1510
0
1
2
3
4
5
6
7
8
9
10
13
16
20
27
35

Figure A.20a

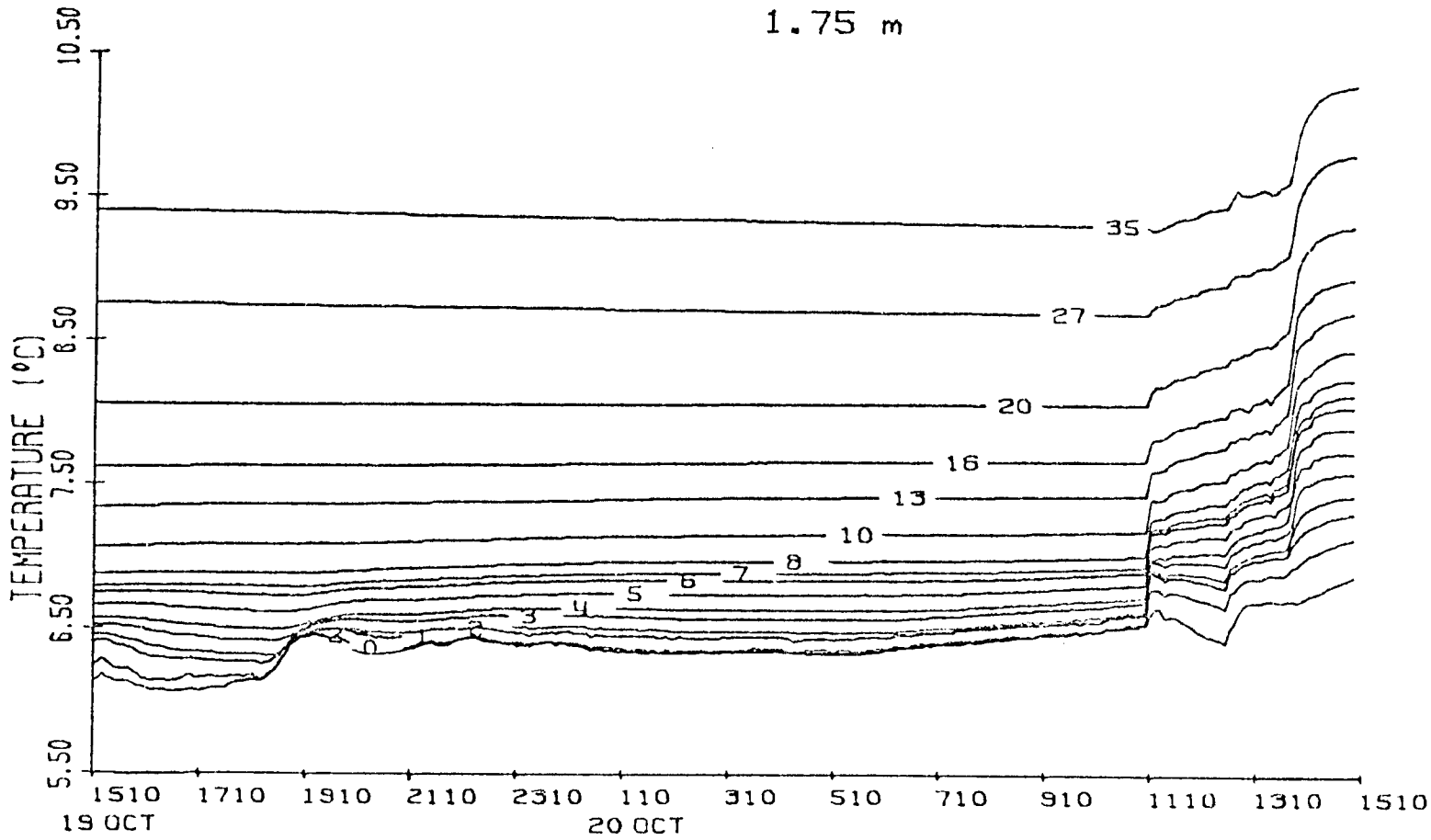
1.75 m
TEMPERATURE (°C)
10.50
9.50
8.50
7.50
6.50
5.50
35
27
20
16
13
10
8
7
6
5
4
3
2
1
0
1510
1710
1910
2110
2310
110
310
510
710
910
1110
1310
1510
19 OCT
20 OCT

Figure A.20b

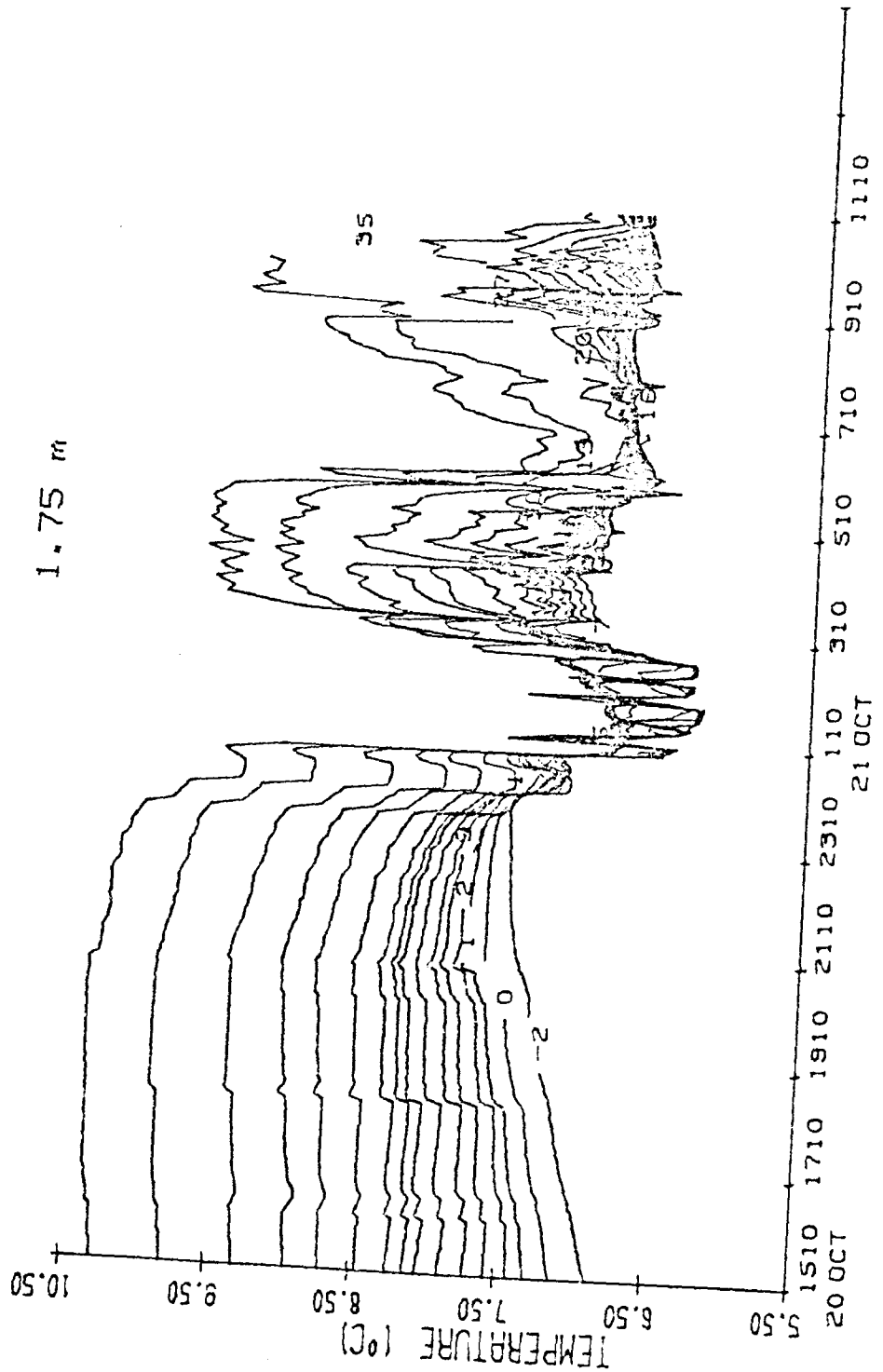
1.75 m
35
30
25
20
15
10
5
0
-2
TEMPERATURE (°C)
10.50
9.50
8.50
7.50
6.50
5.50
1510
1710
1910
2110
2310
110
310
510
710
910
1110
20 OCT
21 OCT

Figure A.20c

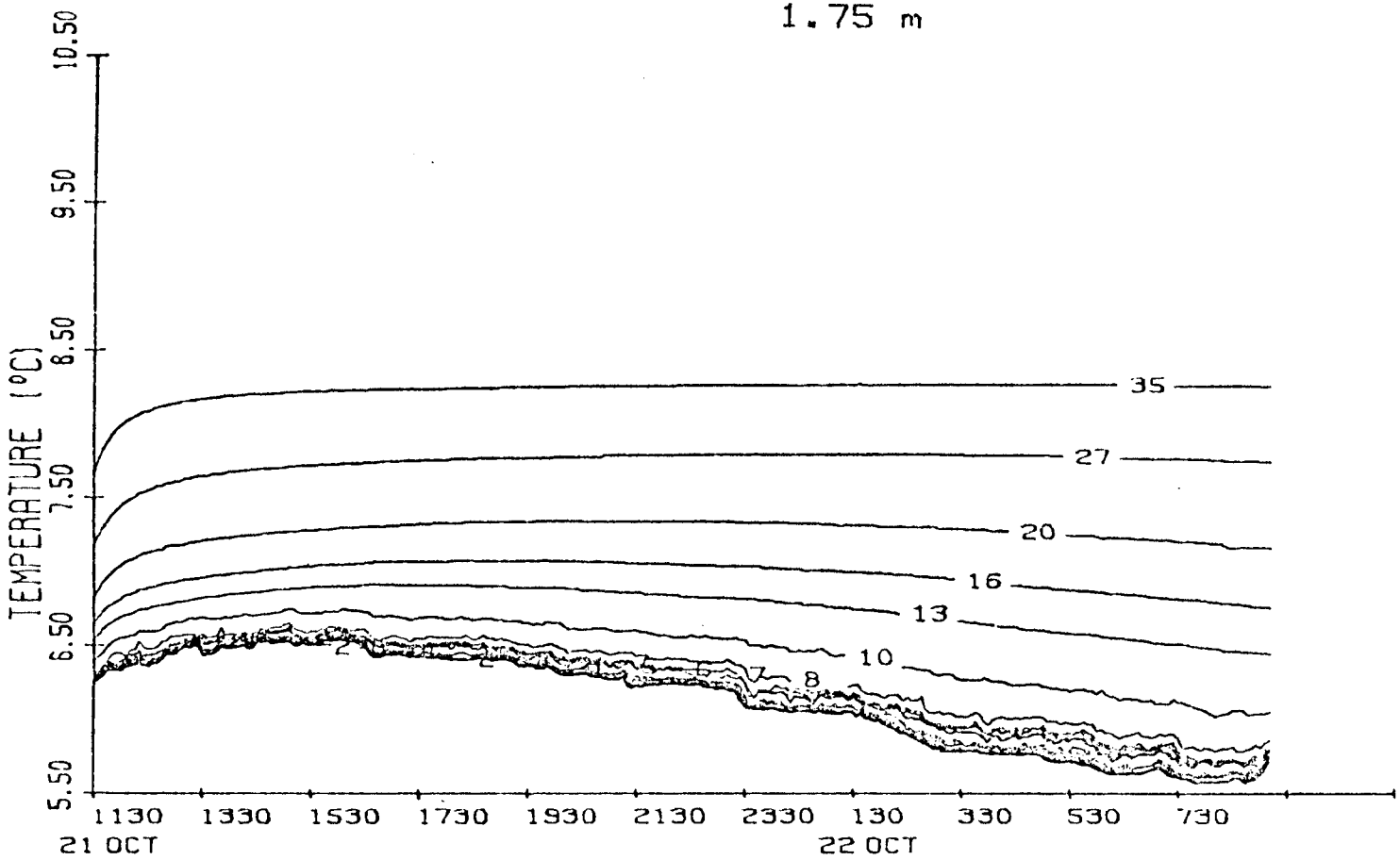
1.75 m
TEMPERATURE (°C)
10.50
9.50
8.50
7.50
6.50
5.50
35
27
20
16
13
10
1130
1330
1530
1730
1930
2130
2330
130
330
530
730
21 OCT
22 OCT

Figure A.21

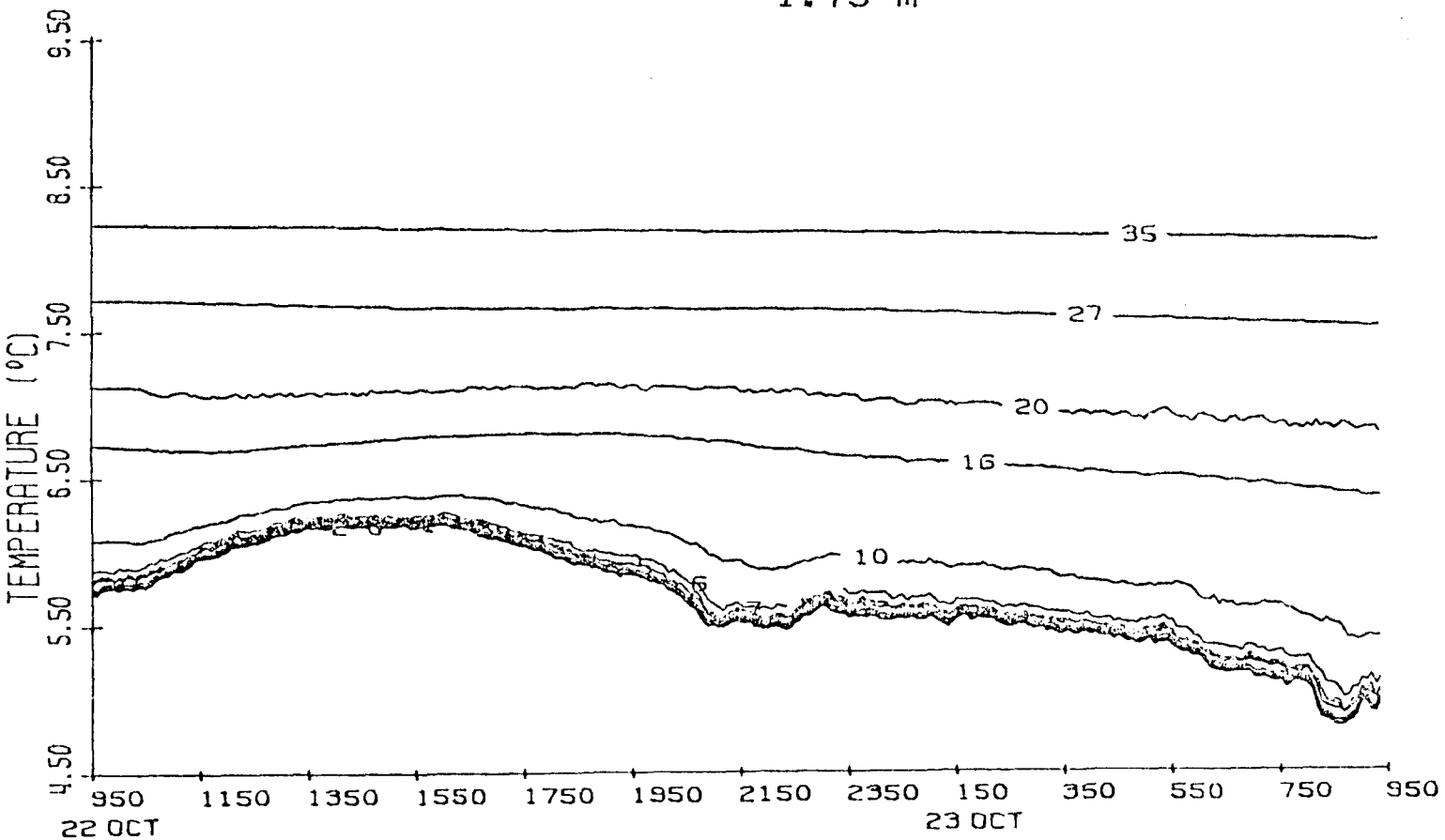
1.75 m
TEMPERATURE (°C)
9.50
8.50
7.50
6.50
5.50
4.50
35
27
20
16
10
950
1150
1350
1550
1750
1950
2150
2350
150
350
550
750
950
22 OCT
23 OCT

Figure A.22a

Figure A.225

1.75 m

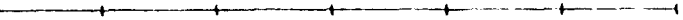

TEMPERATURE (°C)
4.50
5.50
6.50
7.50
8.50
9.50
23 OCT
15h5
17h5
19h5
21h5
23h5
24 OCT
1h5
3h5
5h5
7h5
9h5
11h5
13h5
-2
0
1
2
3
4
5
6
7
8
10
16
20
27
35
1.75 m

Figure A.23

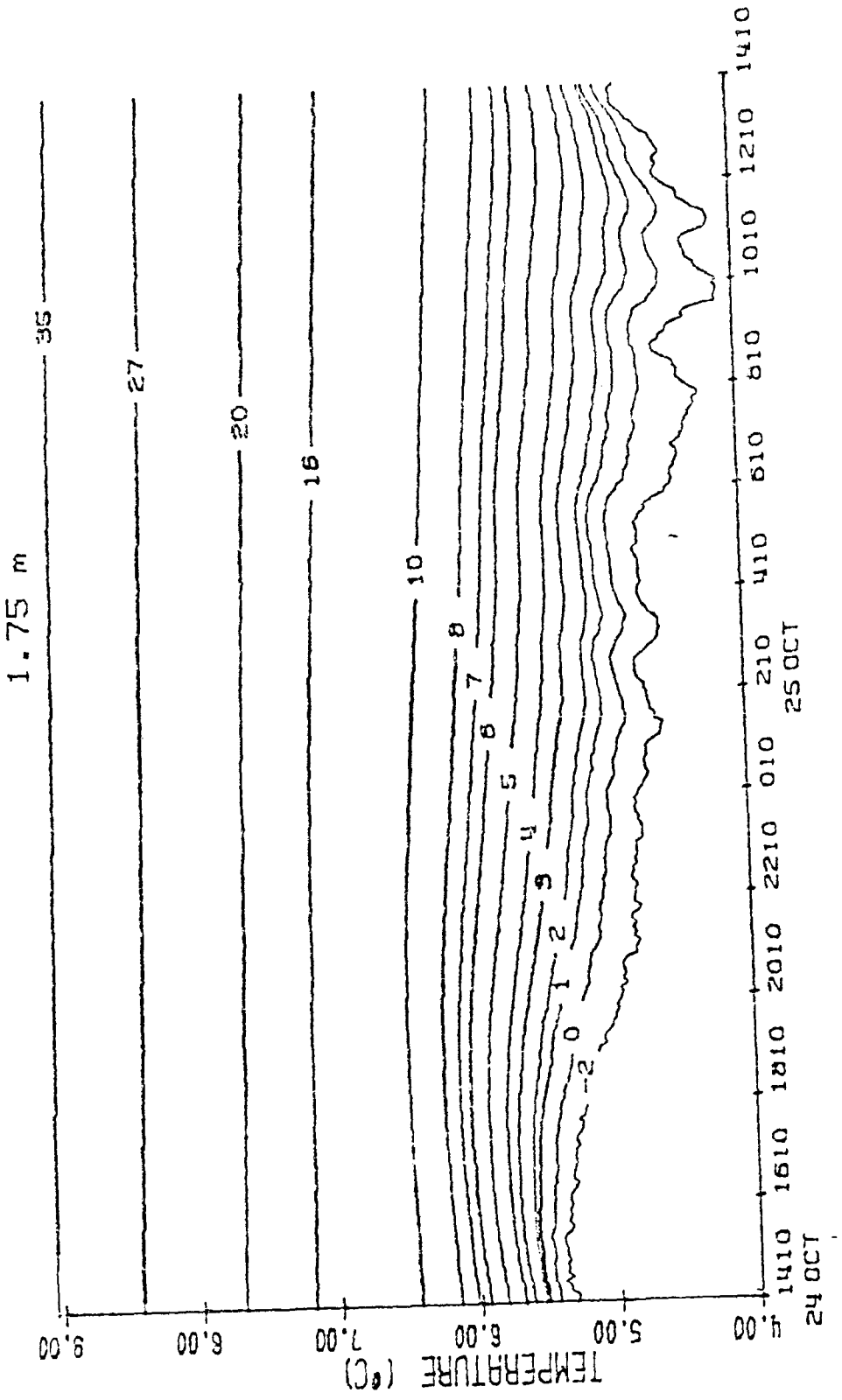
1.75 m
35
27
20
16
10
8
7
6
5
4
3
2
1
0
-2
1410
1610
1810
2010
2210
010
210
410
610
810
1010
1210
1410
24 OCT
25 OCT
5.00
6.00
7.00
8.00
9.00
TEMPERATURE (°C)

Figure A.24

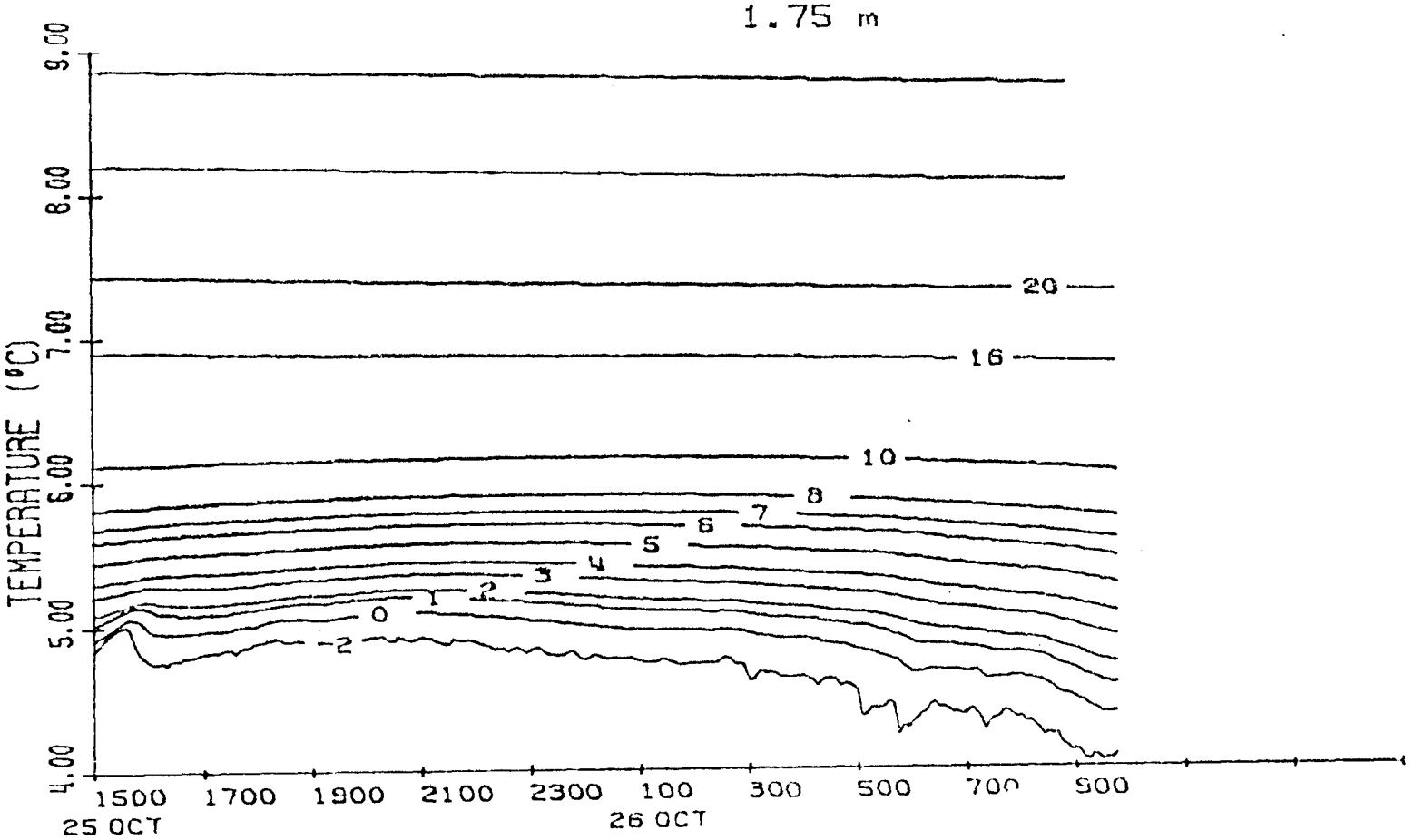
1.75 m
TEMPERATURE (°C)
9.00
8.00
7.00
6.00
5.00
4.00
20
16
10
8
7
6
5
4
3
2
1
0
-2
1500
1700
1900
2100
2300
100
300
500
700
900
25 OCT
26 OCT

Figure A.25

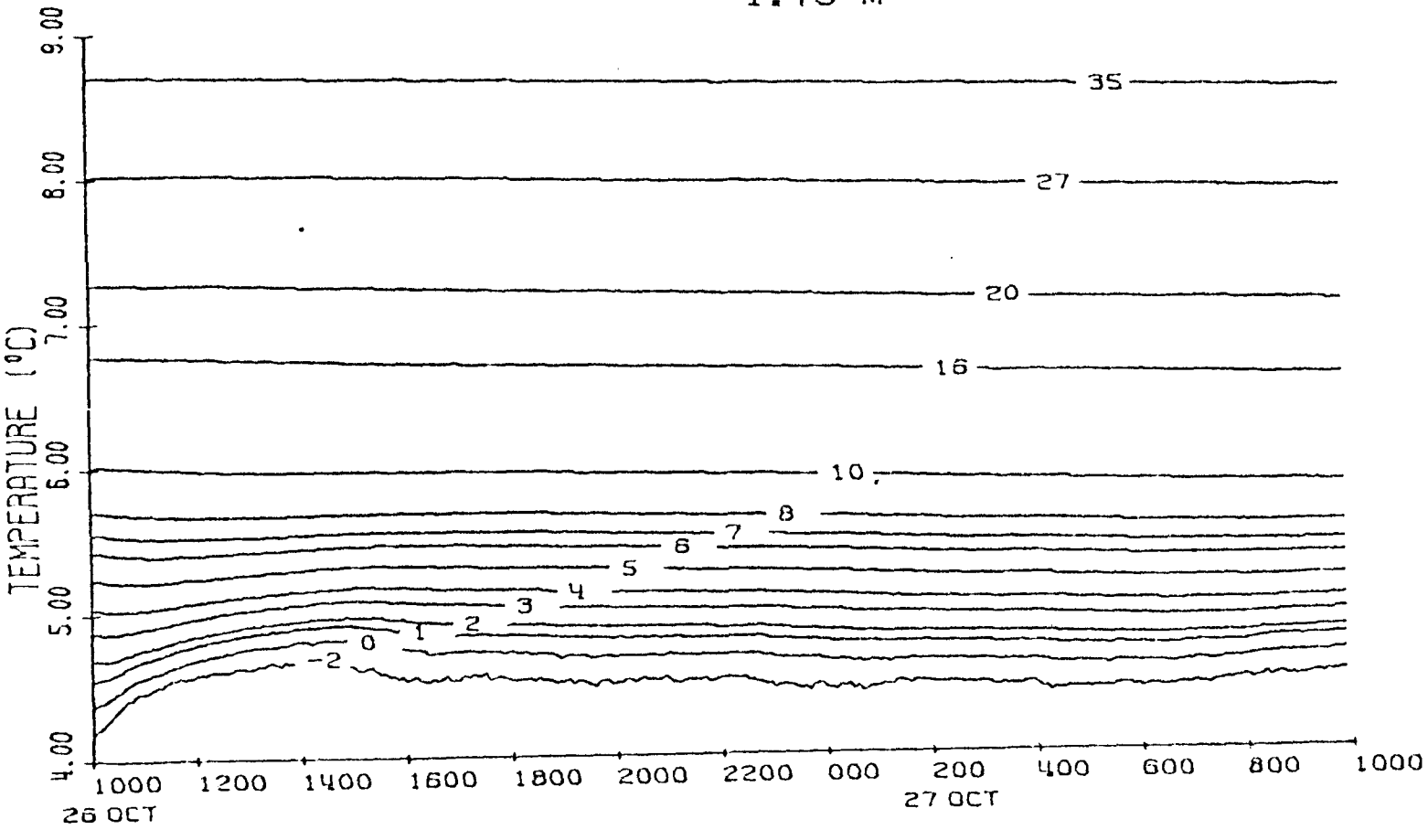
1.75 m
TEMPERATURE (°C)
9.00
8.00
7.00
6.00
5.00
4.00
35
27
20
16
10
8
7
6
5
4
3
2
1
0
-2
1000
1200
1400
1600
1800
2000
2200
000
200
400
600
800
1000
26 OCT
27 OCT

Figure A.26a

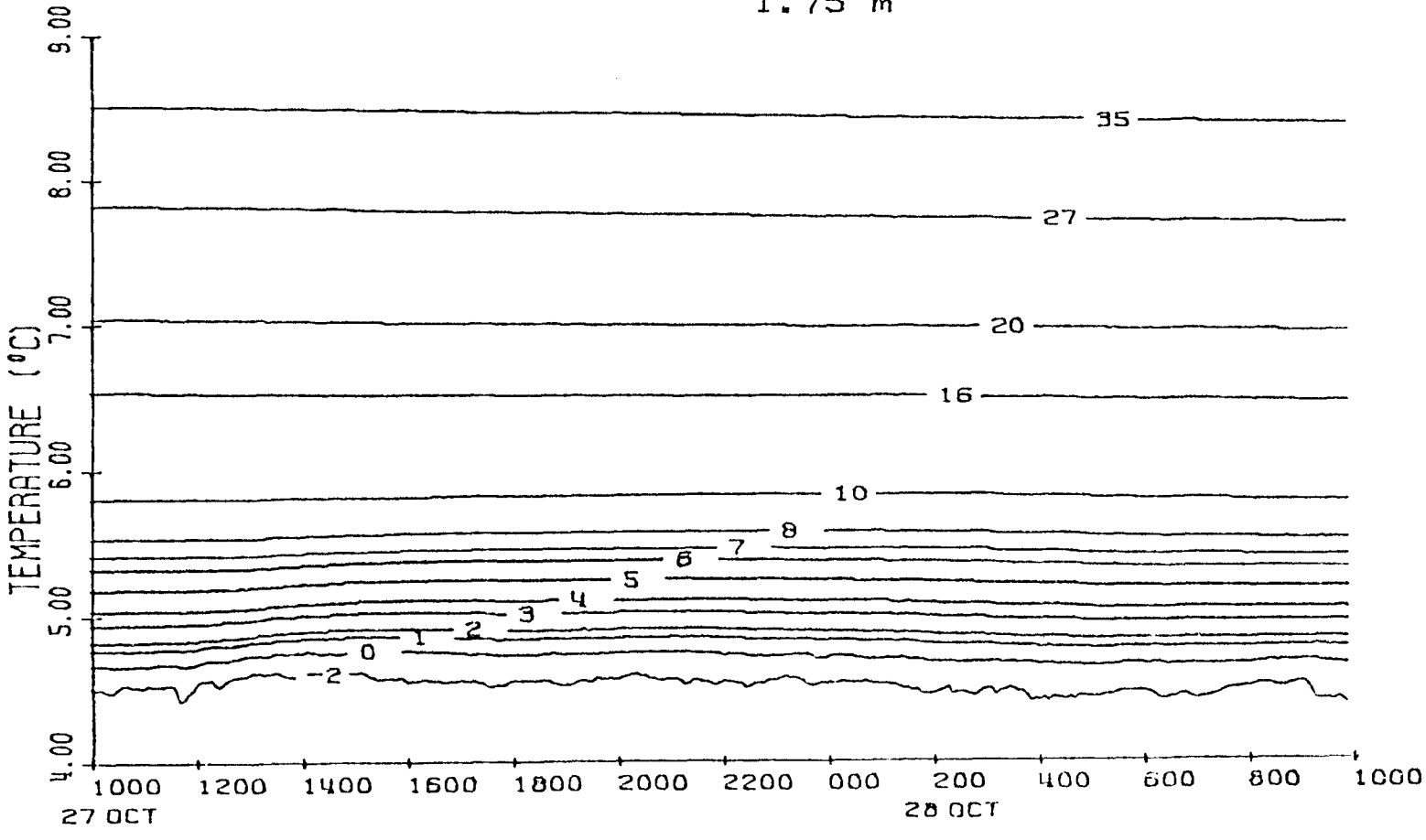
1.75 m
TEMPERATURE (°C)
9.00
8.00
7.00
6.00
5.00
4.00
35
27
20
16
10
8
7
6
5
4
3
2
1
0
-2
1000
1200
1400
1600
1800
2000
2200
000
200
400
600
800
1000
27 OCT
28 OCT

Figure A.265

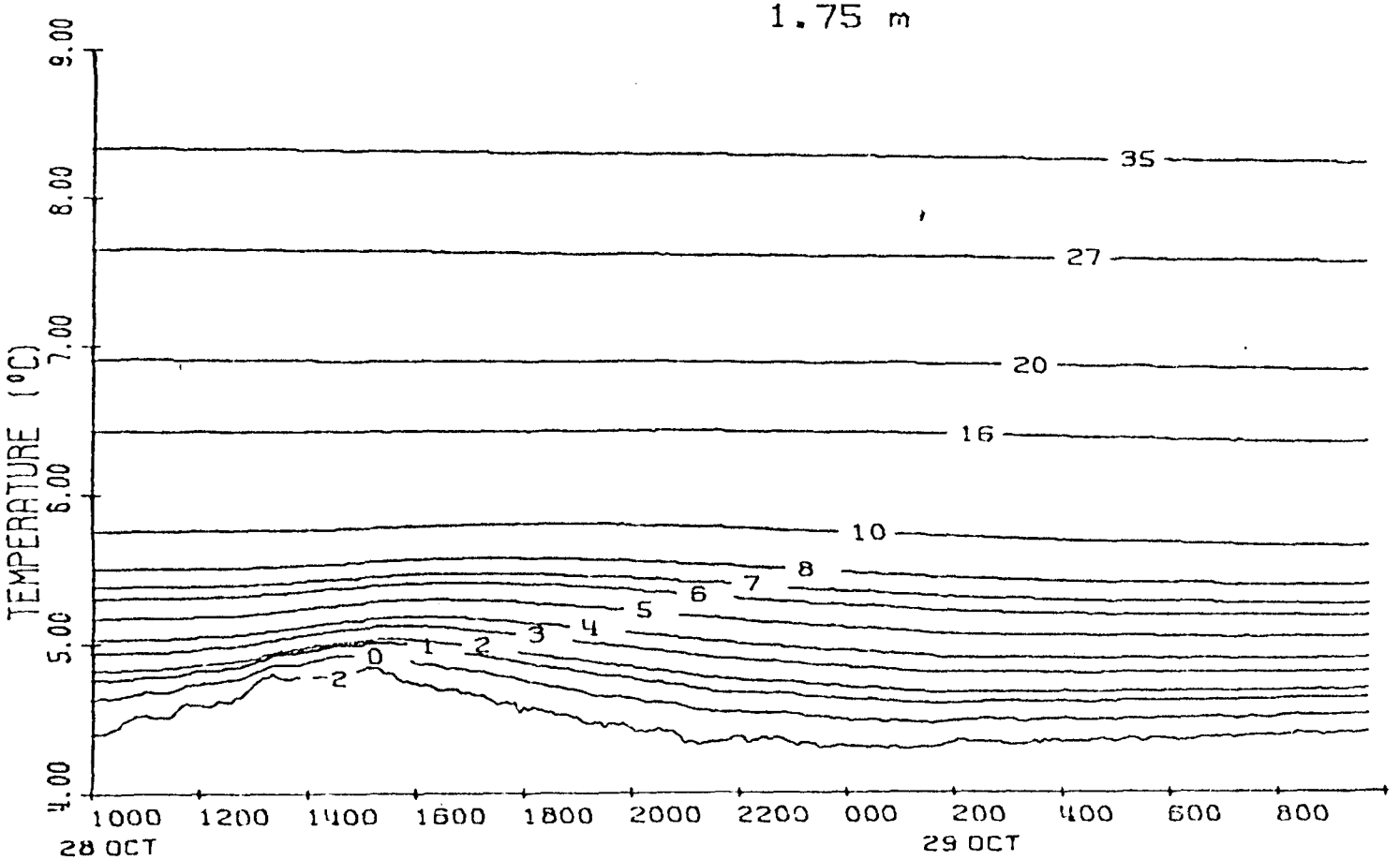
1.75 m
TEMPERATURE (°C)
9.00
8.00
7.00
6.00
5.00
4.00
35
27
20
16
10
8
7
6
5
4
3
2
1
0
-2
1000
1200
1400
1600
1800
2000
2200
000
200
400
600
800
28 OCT
29 OCT

Figure A.26c

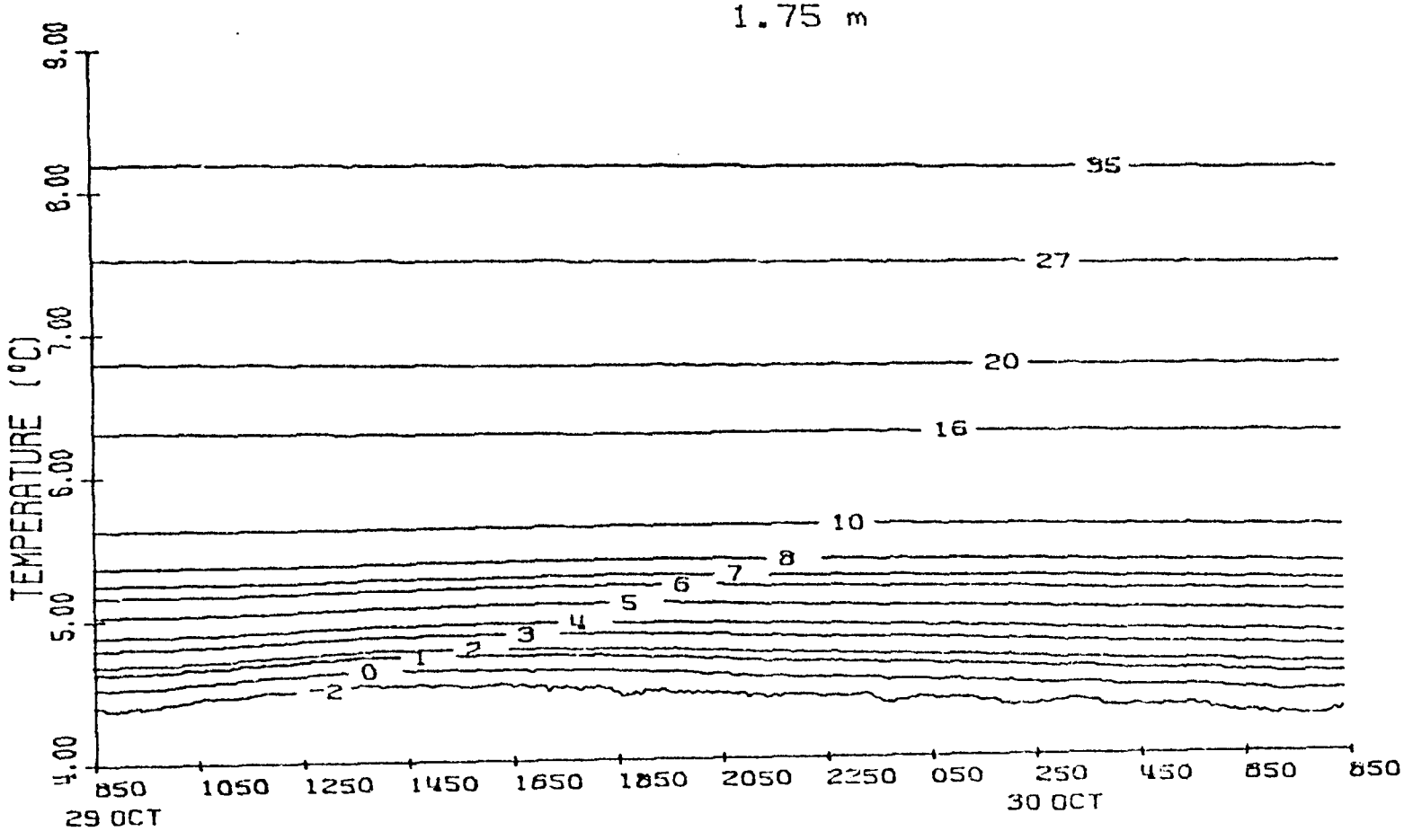
1.75 m
TEMPERATURE (°C)
9.00
8.00
7.00
6.00
5.00
4.00
95
27
20
16
10
8
7
6
5
4
3
2
1
0
-2
850
1050
1250
1450
1650
1850
2050
2250
050
250
450
650
850
29 OCT
30 OCT

Figure A.27a

Figure A.27b

1.75 m

APPENDIX B

I deployed a prototype thermistor probe in a tundra pond in Barrow, Alaska. This probe did not have any polyurethane foam in the interior. The pond was about 15 m in diameter and 50 cm deep in the deepest portion. The water column was 20 cm deep where the probe was inserted into the sediments. A permafrost layer at 35-45 cm (extrapolated from the linear temperature profile in Figure B.1) gave a lower boundary condition of 0 deg at this depth.

Temperature fluctuations occurred at thermistor depths 10-12 cm with a period of 2.4×10^3 s (40 min) and amplitude of 0.09 deg. At first I interpreted these fluctuations as being due to steady convection between the sediment surface and the permafrost layer. However, the modified Rayleigh number (based on a nonlinear temperature-density relationship [Wu *et al*, 1979]) was 3×10^{-4}. This value was based on the measured hydraulic conductivity of 10^{-4}, and was ten-thousand times too small for convection to be occurring in the sediments.

Water that had seeped into the interior of the probe had the same temperature gradient as that in the sediments. Because the frictional effects are much less for this water than for pore waters, the temperature fluctuations were more likely caused by water convecting in the interior of the probe. Indeed, the temperature fluctuations are similar to those observed in the interior of a water-filled pipe which is subjected to adverse temperature gradients (Azouni, 1981). Convection within the interior of a pipe filled with water

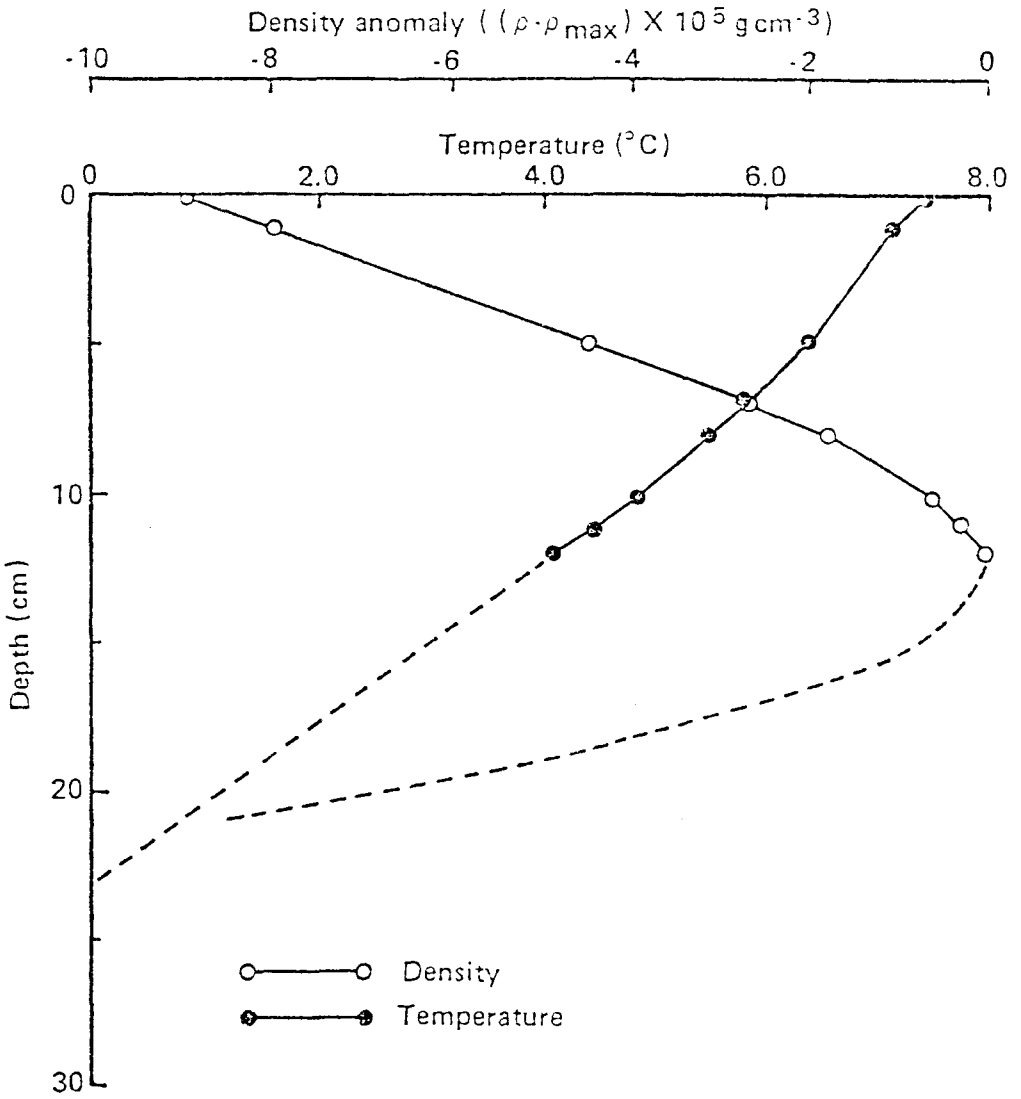

Figure B.1. Temperature and density anomaly for tundra pond. The dashed lines are extrapolated from the measured, linear temperature profile.

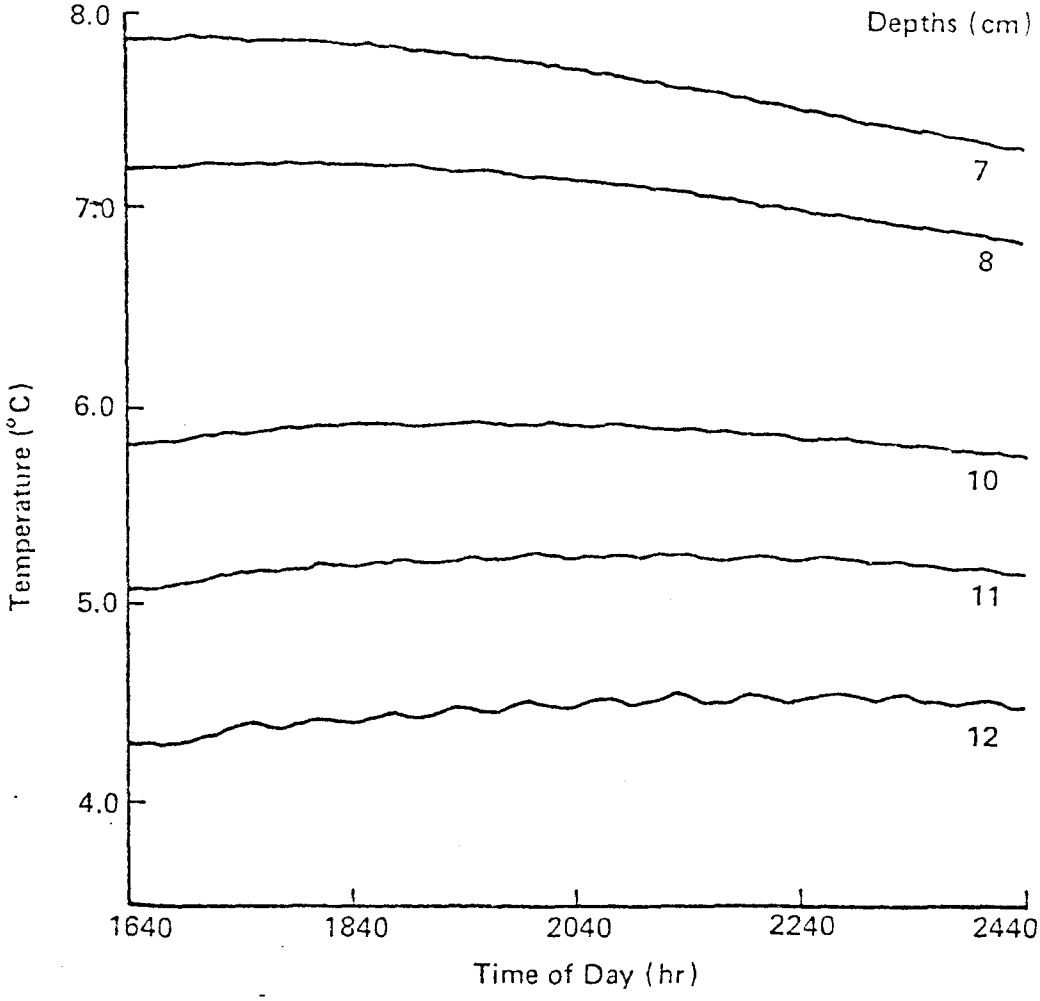

Figure 8.2. Temperature fluctuations at depths of 10-12 cm.

near the maximum density (4 deg) is governed by a Rayleigh number for viscous fluids (Azuoni, 1981). I calculated this number to be 10^5 which, according to Azouni, is much greater than lowest value at which oscillatory convection occurs in a pipe. The fluctuations are probably manifestations of convection within the probe. I have discounted the data from the tundra pond with the caveat to future investigators to fill your probes!

LITERATURE CITED

Anderson, R.N., M.A. Hobart, M.G. Langseth (1979) Geothermal convection through oceanic crust and sediments in the Indian Ocean. *Science*, 204, 828-832.

Azuoni, M.A. (1981) Oscillatory behaviour in convecting water. *Int. J. Heat Mass Transfer*, 24, 1983-1986.

Beck, J.V., (1963) Calculation of thermal diffusivity from temperature measurements. *J. Heat Transfer*, 85C, 182-182.

Berner, R. (1980) *Early Diagenesis: A Theoretical Approach*, Princeton University Press, 241 pp.

Bokuniewiscz, H. (1980) Groundwater seepage into Great South Bay, New York. *Estuar. and Coast. Mar. Sci.*, 10, 437-444.

Broecker, W. and T-H. Peng (1982) *Tracers in the Sea*. Lamont-Doherty Geological Observatory, Columbia University, 690 pp.

Brunskill, G.J., D. Povoledo, B.W. Graham and M.P. Stainton (1971) Chemistry of surface sediments of sixteen lakes in the Experimental Lakes Area, northwestern Ontario. *J. Fish. Res. Board Can.*, 18, 277-294.

Brunskill, G.J. and D.W. Schindler (1971) Geography and bathymetry of selected lake basins, Experimental Lakes Area, northwestern Ontario. *J. Fish. Res. Board Can.*, 28, 139-155.

Bryant, W.R., R.H. Bennett and C.E. Katherman (1981) Shear strength, consolidation, porosity, and permeability of oceanic sediments. In: *The Sea*, Vol. 7, C. Emiliani, editor, John Wiley and Sons, pp. 1555-1616.

Cairns, J.L. (1973) Propagation of thermal waves through sea floor sediment. *J. Geophy. Res.*, 78, 981-991.

Carslaw, H.S. and J.C. Jaeger (1959) *Conduction of Heat in Solids. 2nd Edition.* Clarendon Press, 510 pp.

Cheng, P. (1978) Heat transfer in geothermal systems. *Adv. Heat Transfer*, 14, 1-105.

Chhuon, B. and J.P. Caltagirone (1979) Stability of a horizontal porous layer with timewise periodic boundary conditions. *J. Heat Transfer*, 101, 244-248.

Clark, G.R. (1973) The Harrington Sound thermocline: observations

during the summer of 1972. (Unpublished manuscript.)

Combarnous, M.A. and S.A. Bories (1974) Hydrothermal convection in saturated porous media. *Adv. Hydrosci.*, 10, 232-309.

Deardorff, J.W., G.E. Willis and D.K. Lilly (1969) Laboratory investigation of non-steay penetrative convection. *J. Fluid Mech.*, 35, 7-31.

Draper, N.R. and H. Smith (1981) *Applied Regression Analysis. 2nd Edition.* John Wiley and Sons, 709 pp.

Dodimead, A.J., F. Favorite and T. Hirano (1962) Review of oceanography of the subartic Pacific region. Intern. North Pac. Fish. Comm. Bull. 13. 195 pp.

Elder, J.W. (1968) The unstable thermal interface. *J. Fluid Mech.*, 32, 69-96.

Farmer, D.M. (1975) Penetrative convection in the absense of mean shear. *Quart. J. R. Met. Soc.*, 101, 869-891.

Green, T. and R.L. Freehill (1969) Marginal stability in inhomogeneous porous media. *J. Appl. Phys.*, 40, 1759-1762.

Harrison, W.D. and T.E. Osterkamp (1978) Heat and mass transport processes in subsea permafrost. 1. An analysis of molecular diffusion and its consequences. *J. Geophys. Res.*, 18, 4707-4712.

Harrison, W.D., D.L. Musgrave and W.S. Reeburgh (1983) A wave induced transport process in marine sediments. *J. Geophys. Res.*, in press.

Hesslein, R.H. (1976) The fluxes of CH_4, ΣCO_2, and NH_3-N from sediments and their consequent distribution in a small lake. Ph.D. dissertation, Columbia Univ., New York, N.Y. 186 pp.

Hesslein, R.H. (1980) In situ measurements of pore water diffusion coefficients using tritiated water. *Can. J. Fish. Aquat. Sci.*, 37, 545-551.

Horne, R.N. and M.J. O'Sullivan (1974) Oscillatory convection in a porous medium heated from below. *J. Fluid Mech.*, 66, 339-352.

Jenkins, G.M. and D.G. Watts (1968) *Spectral Analysis and Its Applications.* Holden-Day, 525 pp.

Johannes, R.E. (1980) The ecological significance of the submarine discharge of groundwater. *Mar. Ecol. Prog. Ser.*, 3,365-373.

Kell, G.S. (1967) Precise representation of volume properties of water at one atmosphere. *J. Chem. Engng Data*, 12, 66-69.

Kennedy, K.G. (1974) The hydrology and hydrogeochemistry of a small Precambrian Shield watershed. M.Sc. thesis, Univ. Waterloo, Waterloo, Ont. 248 pp.

Kvernvold, O. and P.A. Tyvand (1979) Nonlinear thermal convection in anisotropic porous media. *J. Fluid Mech.*, 90, 609-624.

Lapwood, E.R. (1948) Convection of a fluid in a porous medium. *Proc. Camb. Phil. Soc.*, 44, 508-521.

Lerman, A. (1975) Maintenance of steady state in oceanic sediments. *Am. Jour. Sci.*, 275, 609-635.

Manheim, F.T. and F.L. Sayles (1974) Composition and origin of interstitial waters of marine sediments, based on deep sea drill cores. In: *The Sea*, Vol. 5, John Wiley and Sons, pp. 527-568.

McDuff, R.E. and J.M. Sieskes (1976) Calcium and magnesium profiles in DSDP interstitial waters: diffusion or reaction? *Earth Planet. Sci. Lett.*, 33, 1-10.

Matisoff, G. (1980) Time dependent transport in Chesapeake Bay sediments: Part 1. A time series study of temperature and chloride. *Am. Jour. Sci.*, 280, 1-25.

Newbury, R.W. and K.G. Beatty (1980) Water renewal efficiency of watershed and lake combinations in the ELA region of the Precambrian Shield. *Can. J. Fish. Aquat. Sci.*, 37, 335-341.

Nield, D.A. (1968) Onset of thermohaline convection in porous medium. *Wat. Resour. Res.*, 4, 553-560.

Poldervaart, A. (1955) Chemistry of the earth's crust. In: *Crust of the Earth*, A. Poldervaart, editor, Geol. Soc. Am. Spec. Pap. 62, pp.119-144.

Putnam, J.A. (1949) Loss of wave energy due to percolation in a permeable sea bottom. *Trans. Am. Geophys. Un.*, 30, 349-356.

Quay, P.D. (1977) An experimental study of turbulent diffusion in lakes. Ph.D. dissertation, Columbia Univ., New York, N.Y. 194 pp.

Roache, P.J. (1976) *Computational Fluid Dynamics*. Hermosa Publishers, 446 pp.

Riedl, R.J., N. Huang and R. Machan (1972) The subtidal pump: a mechanism of interstitial water exchange by wave action. *Mar. Biol.*, 13, 210-221.

Sayles, F.L. (1979) The composition and diagenesis of interstitial solutions I. Fluxes across the seawater-sediment interface in the Atlantic Ocean. *Geochim. et Cosmochim. Acta*, 41, 951-960.

Sayles, F.L. and W.L. Jenkins (1982) Advection of pore fluids through sediments in the equatorial East Pacific. *Science*, 217, 245-248.

Schindler, D.W. (1971) Light, temperature, and oxygen regimes of selected lakes in the Experimental Lakes Area, northwestern Ontario. *J. Fish. Res. Board Can.*, 28, 157-169.

Schindler, D.W., H. Kling, R.V. Schmidt, J. Prokopowich, V.E. Frost, R.A. Reid and M. Capel (1973) Eutrophication of lake 227 by addition of phosphate and nitrate: the second, third, and fourth years of enrichment 1970, 1971, and 1972. *J. Fish. Res. Board Can.*, 30, 1415-1440.

Schisler, I.P. and J.V. Beck (1979) Estimation of thermal parameters from transient temperature measurements containing correlated ARIMA errors. *Letters in Heat and Mass Transfer*, 6, 181-188.

Thorstensen, D.C. and F.T. Mackenzie (1974) Time variability of pore water chemistry in recent carbonate sediments, Devil's Hole, Harrington Sound Bermuda. *Geochim. Cosmochim. Acta*, 38, 1-19.

Townsend, A.A. (1964) Natural convection in water over an ice surface. *Quart. J. R. Met. Soc.*, 90, 248-259.

Townsend, A.A. (1966) Internal waves produced by a convective layer. *J. Fluid Mech.*, 24, 307-319.

Vanderborght, J-P., R. Wollast and G. Billen (1977) Kinetic models of diagenesis in disturbed sediments. Part 1. Mass transfer properties and silica diagenesis. *Limnol.*

Oceanogr., 22, 787-793.

Wu, R-S., K.C. Cheng and A. Craggs (1979) Convective instability in porous media with maximum density and throughflow effects by finite-difference and finite-element methods. *Numerical Heat Transfer*, 2 303-318.